CUKUROVA UNIVERSITY
INSTITUTE OF NATURAL AND APPLIED SCIENCES

MSc THESIS

Sevgi KIRAÇ

THE EFFECT OF VARIOUS-HEIGHT PLATES ON FLOW CHARACTERISTICS IN SIDE BY SIDE CIRCULAR CYLINDERS

DEPARTMENT OF MECHANICAL ENGINEERING

ADANA, 2010

INSTITUTE OF NATURAL AND APPLIED SCIENCES
UNIVERSITY OF CUKUROVA

THE EFFECT OF VARIOUS-HEIGHT PLATES ON FLOW CHARACTERISTICS IN SIDE BY SIDE CIRCULAR CYLINDERS

Sevgi KIRAÇ

M.Sc. THESIS

DEPARTMENT OF MECHANICAL ENGINEERING

We certified that the thesis titled above was reviewed and approved fort he award of degree of master of science by the board of jury on…………….

………………………………..	…………………………………..	…………………………….
Assoc.Prof. Dr. Hüseyin AKILLI	Assoc.Prof. Dr.Ahmet PINARBAŞI	Assist. Prof. Dr. Sami AKÖZ
Advisor	Member	Member

This M.Sc. Thesis is performend in Department of Mechanical Engineering of Institute of Natural and Applied Sciences of Cukurova Universty.

Registration Number

Prof. Dr. İlhami YEĞİNGİL
Director
The Institute of Natural and Applied Sciences

ABSTRACT

M.Sc. THESIS

THE EFFECT OF VARIOUS-HEIGHT PLATES ON FLOW CHARACTERISTICS IN SIDE BY SIDE CIRCULAR CYLINDERS

Sevgi KIRAÇ

DEPARTMENT OF MECHANICAL ENGINEERING
INSTITUTE OF NATURAL AND APPLIED SCIENCES
UNIVERSITY OF ÇUKUROVA

Advisor : Assoc. Prof. Dr. Hüseyin AKILLI
Year: 2010, Pages: 82
Jury : Assoc. Prof. Dr. Ahmet PINARBAŞI
: Assist. Prof. Dr. Sami AKÖZ

The main purpose of the present study is to investigate the flow behaviour around a vertical side-by-side two cylinders placed in shallow water was controlled by splitter plate inserted at various locations dowstream of the cylinder. Experiments were undertaken in a water channel in Fluid Mechanics Laboratory, Mechanical Engineering Department of Cukurova University. The splitter plate has a length which is ranged from 0 mm to 250 mm with 25 mm increments. The splitter plate has a heights which is 0 mm, 5 mm, 10 mm, 12.5 mm, 17.5 mm, 22.5 mm. And the cylinder has a fixed diameter which is equal to D=50 mm. The effect of plate thickness,T ,was examined using plate thicknesses, T/D=0,05. The gap between the base of the cylinder and the leading edge of the splitter plate was a fixed lenght which is equal to L=20 mm. Particle Image Velocimetry (PIV) was used to measure instantanoues velocity vector field in the wake region at Reynolds number based on cylinder diameter Re=5000. The mean velocity vector field, corresponding vorticity field and streamline topology and turbulence statistics were obtained from 350 instantanous images. Increasing splitter plate height controls the vortex shedding better. Moreover, the length increase of the splitter plate affects the control of vortex formation.

Keywords: Splitter plate, PIV, Vortex.

ÖZ

YÜKSEK LİSANS TEZİ

DEĞİŞİK YÜKSEKLİKTEKİ PLAKALARIN SIRALI SİLİNDİRLER ARKASINDAKİ AKIŞA ETKİSİ

Sevgi KIRAÇ

ÇUKUROVA ÜNİVERSİTESİ
FEN BİLİMLERİ ENSTİTÜSÜ
MAKİNA MÜHENDİSLİĞİ ANABİLİM DALI

Danışman : Doç. Dr. Hüseyin AKILLI
Yıl: 2010, Sayfa: 82
Jüri : Doç. Dr. Ahmet PINARBAŞI
: Yrd. Doç. Dr. Sami AKÖZ

Bu tezin amacı, sığ suda silindirler arkasına plaka yerleştirilerek, oluşan vortex kontrol altına alınmaya çalışılmıştır. Deneyler Çukurova Üniversitesi akışkanlar mekaniği laboratuarında su kanalı kullanılarak yapılmıştır. Silindirler arasına yerleştirilen plakanın boyu 0 mm ile 250mm arasında 25mm' lik artımlar ile değişmektedir. Silindirler arasına yerleştirilen plakanın yüksekliği 0mm, 5mm, 10mm, 12.5mm, 17.5mm, 22.5mm olarak değişmektedir. Silindirin çapı 50mm de sabit kalmıştır. Plakanın kalınlık etkisi, T ile ifade edilmiş olup, plaka kalınlığı için T/D : 0,05 değeri elde edilmiştir. Plaka ile silindirler arasındaki boşluk eşit olup 5 mm'dir. Bu çalışma Reynolds sayısı Re=5000'de, Parçacık görüntülemeli hız ölçüm tekniği kullanılarak anlık ve ortalama hız vektörleri, akım çizgisi, türbülans isatistik değerleri toplam 350 anlık imageler ile elde edilmiştir. Plaka yüksekliği arttıkça akışın yapısı daha etkin bir şekilde kontrol altına alınmaktadır. Ayrıca, plakanın uzunluğunun artmasının girdap oluşumunda önemli bir parametre olduğu da belirlenmiştir.

Anahtar Kelimeler: Plaka, PIV, Girdap.

TEŞEKKÜR

Yapılan çalışmaların her aşamasında, desteğini ve yakın ilgisini benden esirgemeyen değerli hocam Doç. Dr. Hüseyin AKILLI'ya en derin saygılarımı ve minnettarlığımı ifade etmek isterim.

Deneylerin yapımında ki yardımlardan dolayı ve çalışmanın her aşamasında bilgilerinden yararlandığım Dr. Sedat Yayla'ya ve Proje Assist. Engin Pınar'a teşekkür ederim.

Deneylerin yapımında ki yardımlardan dolayı ve çalışmanın her aşamasında bilgilerinden yararlandığım Ar. Gör. Göktürk ÖZKAN ve Proje Assist. Tuğçe AYDİL'e teşekkür ederim.

Çukurova Üniversitesi Mühendislik Mimarlık Fakültesi Makine Mühendisliği Bölümünde eğitim gördüğüm süre içerisinde beraber çalıştığım tüm akademik ve idari görevlilere ayrıca teşekkür ediyorum.

Bu çalışma süresi boyunca benden manevi desteğini esirgemeyen ailem ve sevgili eşim Tayfun KIRAÇ'a sonsuz teşekkür ederim.

Bu çalışmanın ülkemize faydalı olmasını diliyorum.

NOMENCLATURE

b	: Body width (mm)
D	: Diameter of cylinder (mm)
d	: Plate width (mm)
G	: Distance between the base of cylinder and the leading edge of plate.
h	: Water depth (mm)
hb	: Distance between the bottom of the plate and platform (mm)
hL	: Elevation of laser sheet
hp	: Height of plate (mm)
hw	: Height of water level (mm)
L	: Length of the plate (mm)
Lf	: The formation length (mm)
Re	: Reynolds number based
u	: Free stream velocity (mm/sec)
u,v	: Component of velocity V in x and y axis system (mm/sec)
u_{rms}	: Root-mean-square of u velocity component (mm^2/sec^2)
u'v'	: Reynolds stress correlation (mm^2/sec^2)
<V>	: Time-averaged total velocity vector (mm/sec)
v_{rms}	: Root-mean-square of v velocity component (mm^2/sec^2)
W	: Width of water channel (mm)
<ω >	: Time-averaged vorticity (1/sec)

TABLE OF CONTENTS **PAGE**

LIST OF FIGURES **PAGE**

1. INTRODUCTION

Various areas of engineering and science have studied on vortex shedding behind a circular cylinder because of its practical importance.These areas include mechanical and engineering, power and process industries for türbine blades and heat exchanger tubes, civil engineering for bridges, offshore structures and radio telescopes and undersea technology. Lots of scientists such as Von Karman, Roshko, Tritton and Berger have carried out extensive studies on the phenomena of vortex shedding.

A shallow water flow is defined as the situation where the horizontal length scale of the flow is significantly larger than its depth. Many wake flows could be characterized as shallow flow in nature such as flows in nature and in engineering practise, e.g. wide rivers, lakes, estuaries, shallow coastal waters, mountains or the stratified atmosphere. For example, the tanker Argo merchant stranded on the Nontucket Shoals produced large eddies in the wake region which has a size of about 609.6 m, when the depth of the same location is only about 15.24 m.

1.1. Flow Over a Circular Cylinder

When a body is placed into the flow, the flow separates from the body as result of pressure gradient increment. This can cause periodic shedding of vortices from the body. When the vortex shedding occurs behind a cylinder, drag on the cylinder increases and the body suffers from the periodic force in the normal direction to the main stream. This force makes the life of the structure shorten. On the other hand, the vortex shedding enhances mixing behind the cylinder.

The vortex shedding significantly depends on the Reynolds numbers based on the cylinder diameter. At low Reynolds numbers, two steady vortices are formed on the rear side of the cylinder and remain attached to it. At higher Reynolds numbers, the flow unstable and Von Karman Vortex Street appears in the wake past the cylinder. Schematic flow over a circular cylinder is shown at Figure1.1.

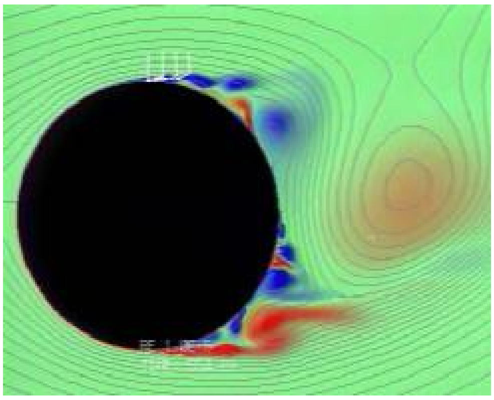

Figure1.1. Flow over a circular cylinder

1.1.1. Flow Separation

The existence of the fluid viscocity retardeds the fluid particles very close to the solid. Since there is no slip boundary condition, the flow velocity is zero at the surface.If the pressure decreases in the direction of the flow, the pressure gradient is called to be favorable. In this case, the pressure force can help the fluid movement and the flow doesn't slow down.On the other and, while the pressure is increasing in the direction of the flow, opposite the pressure gradient condition as so it is called exist. In this position, the presence of a strong viscous force, the fluid particle have to move against the increasing pressure force.As a result, the fluid particles could be sopped , causing the neighboring particles to move away from the surface. This is called the boundary layer separation.

1.1.2. Wake

The pressure is maximum at the stagnation point and slowly decreases along the front half of the cylinder. This is favorable pressure region as expected. Yet, if the pressure starts to rise in the rear half of the cylinder, the flow will separate from the surface and a turbulent region behind the cylinder will be created; the cylinder called the "wake". Figure 1.2 shows the wake flow region.

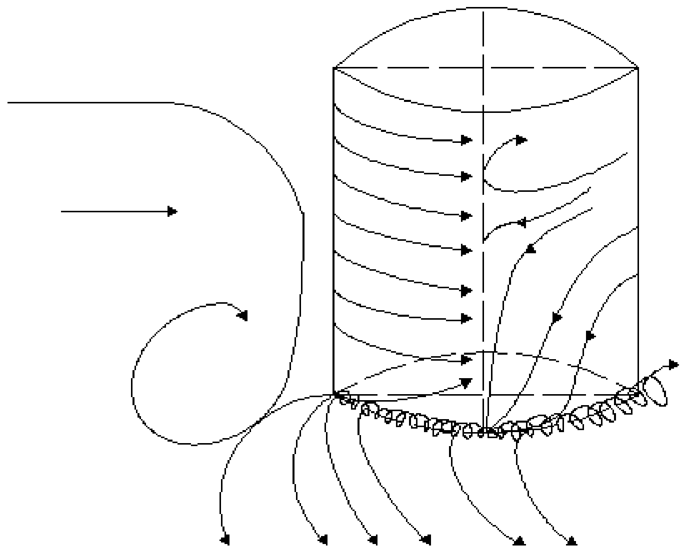

Figure 1.2. Wake structure behind cylinder

1.1.3. Vortex Shedding

The boundary layer leaves from the surface forms a free shear layer. This shear layer will eventually roll into a discrete vortex and detach from the surface. This is called “vortex shedding”. Another type of flow instability emerges as the shear layer vortices shed from both the top and bottom surfaces interact with one another. They shed alternatively from the cylinder and generates a regular vortex pattern which is called as “The Karman Vortex Street”. The vortex shedding occurs at a discrete frequency and is a function of the Reynolds number. Figure 1.3. Schematic Karman Vortex Street.

Figure 1.3. Karman Vortex Street

1.1.4. Flow Patterns

Depending on the Reynolds, experimental observations show various type of flow pattern described below.

Reynold number is less than 1 (Re<<1)

In this condition, the flow is completely dominated by viscosity and the fluid follows a smooth, laminar profile around the cylinder.

Reynold number is between 1 and 4 (1<Re<4)

In this condition, the symmetry disappears and the flow is disturbed in a much longer distance behind the cylinder.

Reynold number is between 4 and 40 (4<Re<40)

Separation starts on the back of the cylinder and a symmetric pair of vortices is formed close to the cylinder. The length of the vortices in the along flow direction increases linearly with Reynolds number, reaching a length of three cylinder diameters. Re-circulations appear in the wake behind the cylinder.

Reynold number is between 40 and 400(40<Re<400)

Up to critical Reynolds, about 40, oscillations are so strong that one of the two vortices break away from the cylinder. This is strouhal instability. The second vortex is shed while the first one is shaped again. The vortices appear and are shed alternatively at a constant frequency. About Reynolds 200, the structure of Von Karman Vortex Street becomes.

Reynolds is upper than 400 (400<Re)

Turbulence develop and Von Karman Vortex Street disappears.

Reynold number is between 300 and $1.5x10^5$(300 <Re < $1.5x10^5$ sub critical flow)

The laminar boundary layers separate from the cylinder and the vortex shedding is strong and periodic.

Reynolds is between $1.5x10^5$ and $3.5x10^5$($1.5x10^5$<Re< $3.5x10^5$ transitional flow)

The vortex street transitions to turbulent in the range, which is know as the transitional range.

Reynolds is lower than $3.5x10^6$ (Re > 3.5x106 supercritical flow)

Flow could be called as supercritical flow, periodic vortex shedding is re-established with a turbulent boundary layer.

1.2. Flow Control

Many control methods of vortex shedding have been developed as shown in Figure 1.4.

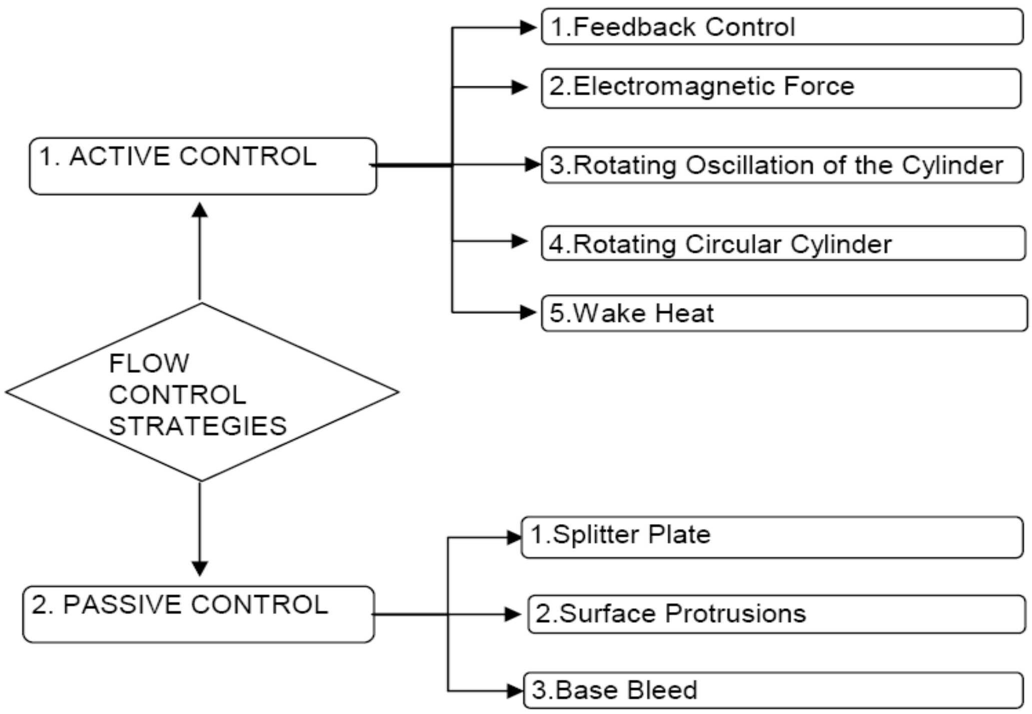

Figure 1.4. Schematic flow control strategies.

1.2.1. Active Flow Control

The aim of active control is to exploit the instability of the wake, which is the cause of the vortex formation, to indirectly modify the mean wake velocity profile and drag. There are two primary advantages to active flow control from passive techniques. First active flow control technology leverages and controls a natural stability of the flow to attain a large effect using small localized energy input. Secondly, active control can be used to control complex, dynamical processes like turbulence production in turbulent boundary layers to reduce skin friction and hence viscous drag where the reduction is proportional to the surface area covered by the actuators.

This is in contrast to the passive control where the mean flow is directly altered to suppress the instability, and consequently the vortex shedding.

1.2.1.1. Feedback Control

Feedback control method has been studied by many researchers in the past two decades. Feedback control method has applied practical to various problems in thermal and fluid engineering. It is consisted of a hot-film probe, a phase shifter, amplifiers and a dynamic shaker. The hot-film probe was located in one of the shear flows of the wake, so as to produce strong signals of the vortex shedding. The signals from the feedback probe were phase-shifted and amplified to drive the shaker which was connected to the cylinder to generate perturbations in the wake. A monitor hot-film probe was also located in the wake to assess the control effect on vortex shedding. Signals from both the feedback and the monitor probes were converted into frequency spectra by a computer.

1.2.1.2. Electro-Magnetic Control

The main advantage of electromagnetic control strategy for electrically conducting fluids is that the Lorentz force acts as a volume force inside the fluid, and it may be tuned to act only in specific region of the flow. Many techniques using electric and magnetic fields have been developed in weakly conducting fluids since 1960s.

At this method: the cylinder body is covered with electrodes and the permanent magnets side by side in the order positive electrode, N-pole magnet, negative electrode, S-pole magnet, a sequence which is repeated once more ending with a positive electrode in the axial direction of the circular cylinder. So, the Lorentz force occurs(acts) in the circumferential direction of the cylinder. If you want, you can change the Lorentz force's direction by altering the poles of the each electrode.

The Lorentz force is applied locally on the cylinder surface in the region of 70–130. It is found that both continuous and pulsed Lorentz forces have a significant effect on the flow behaviors around and behind the cylinder as well as on the drag and lift forces acting on the cylinder.

Both Weier et. al.(1998), Kim and Lee's (2001) investigations show that the flow around a circular cylinder can effectively be controlled using the Lorentz force. The Lorentz force can suppress the vortex shedding and delay flow seperation. Figure 1.5 shows schematic diagram of the circular cylinder for electromagnetic flow control.

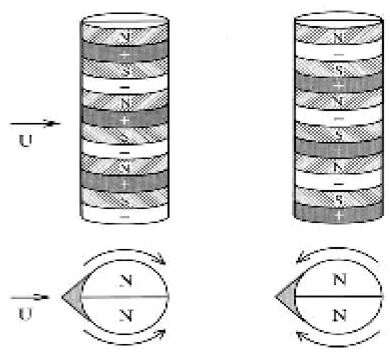

Figure 1.5 Schematic of electromagnetic flow control

1.2.1.3. Rotary Oscillation Of The Cylinder

The method uses small amplitude transverse cylinder oscillations with displacement of a few percent of the cylinder diameter.

The degree of flow control that can be achieved by utilizing rotating control cylinders depends on a variety of parameters. Some of them are the relative sizes of the main and control cylinders, their relative arrangements, and the rotation rates of the two control cylinders.

1.2.1.4. Rotating Circular Cylinder

The flow is controlled by a rotating circular cylinder which is placed in the flow field. At this control method, the forcing frequency and natural shedding frequency are observed: The forcing frequency is lower than the natural shedding frequency an initial clockwise vortex is formed on the lower half of the cylinder when the cylinder is rotated in the counter-clockwise direction and a counter-clockwise vortex is formed on the upper half when the clockwise rotation starts. This leads to a non-synchronized vortex formation mode which can not lead to the suppression of Karman vortex shedding.

Nonetheless, this does not imply that the mean drag coefficient monotonously decreases as the forcing frequency is increased.

1.2.1.5. Wake Heating

It has been noted in the past that Karman vortex shedding can be suppressed by heat addition to the near wake. The connection of this effect to local stability properties was investigated. The primary effect of heating was a reduce the density of the near wake, which in turn decreased local absolute growth rates.

1.2.2. Passive Flow Control

Passive control techniques are easier and simplier than the active control techniques and they are widely used for flow control applications.

A considerable amount of research has been performed using passive methods of flow control, which modify a flow without external energy expenditure. Passive techniques include geometric shaping to manipulate the pressure gradient, the use of fixed mechanical vortex generators for separation control, and placement of longitudinal grooves or riblets on a surface to reduce drag.

1.2.2.1. Splitter Plate

Controlling vortex shedding by splitter plate is one of the most successful methods. The use of splitter plates to control bluff bodies vortex shedding provides an important change in flow structure behind the cylinder.

The vortex shedding behind a circular cylinder completely disappears when the length of the splitter plate is larger than a critical length, and this critical length is found to be proportional to the Reynolds number.

The Strouhal number of the vortex shedding is rapidly decreasing with the increased plate length until the plate length (L) is nearly the same as the cylinder diameter (D) as shown in Figure 1.6

The net drag is significantly reduced by the splitter plate, and there exists an optimum length of the plate for minimum drag at a given Reynolds number.

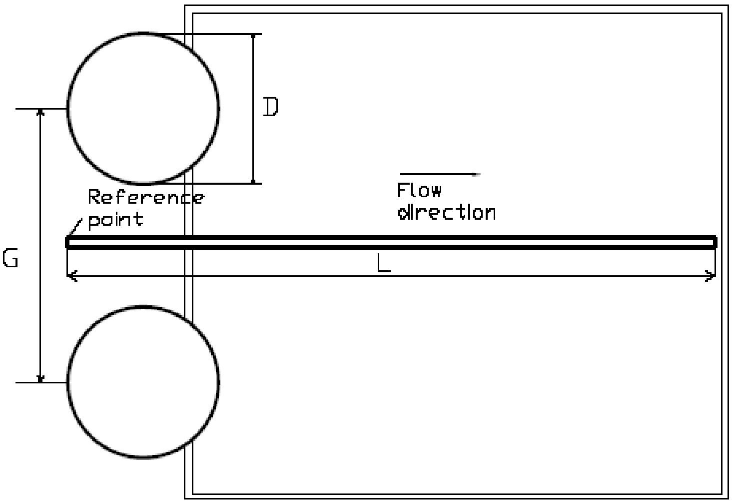

Figure 1.6. Splitter plate flow configuration

1.2.2.2. Surface Protrusions

One effective method for controlling the flow around a body is to install protrusions on the body's surface. The protrusions modify the wake structure by changing seperation lines or direction of surface flow. O-rings are installed as surface protrusions for controlling the flow around a cylinder. The test cylinders are supported at both sides using identical load-cells: one for measuring force and the other a dummy for balancing.

The circular cylinder is wrapped helically by three small wires (d=0.075D) with pitches of 5D and 10D.

The surface protrusions decrease the vortex shedding frequency and also drag coefficient. For the P=5D model, vortex shedding are suppressed when Re=25000. The wake of the P=10D model remains suppressed for all Reynolds number. At Figure 1.7 a horizontal circular cylinder fitted with o-rings are shown.

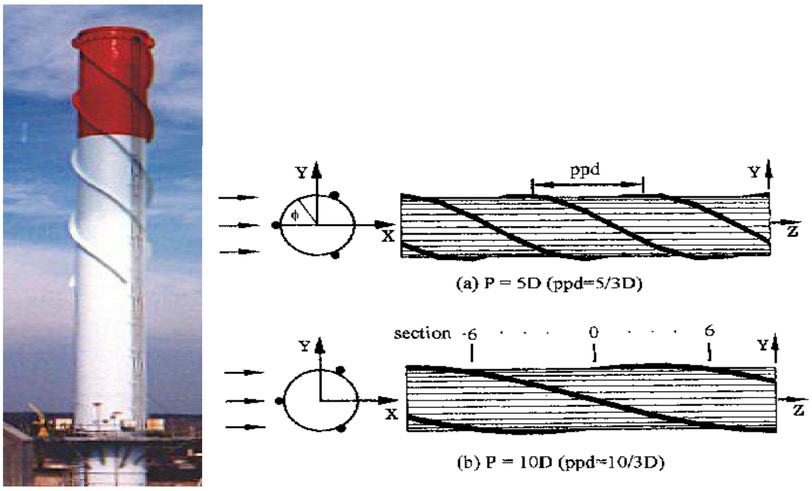

Figure 1.7. Surface Protrusions schematic of diagrams of models

1.2.2.3. Base Bleed

Another well-known method for the suppression of vortex shedding from bluff bodies consists in bleeding fluid from the blunt base. The aim is to suppress vortex shedding completely at some supercritical Reynolds number by base bleed.

1.3. Shallow Water

Most of the previous experiments were conducted in test sections of large depths compared to the width of the wake. However, many turbulent shear flows exist in shallow environments where the horizontal length scale is significantly large compared to the depth of the flow field (Burger and Wille, 1972; Ingram and Chu, 1987; and Wolanski et al., 1984). For example, the tanker Argo Merchant stranded on the Nantucket shoals produced turbulent eddies in the wake region, which has a size of about 609.6 m, while the depth of flow at the same location is only about 15.24 m [figure 1.8.Van Dyke, 1982].

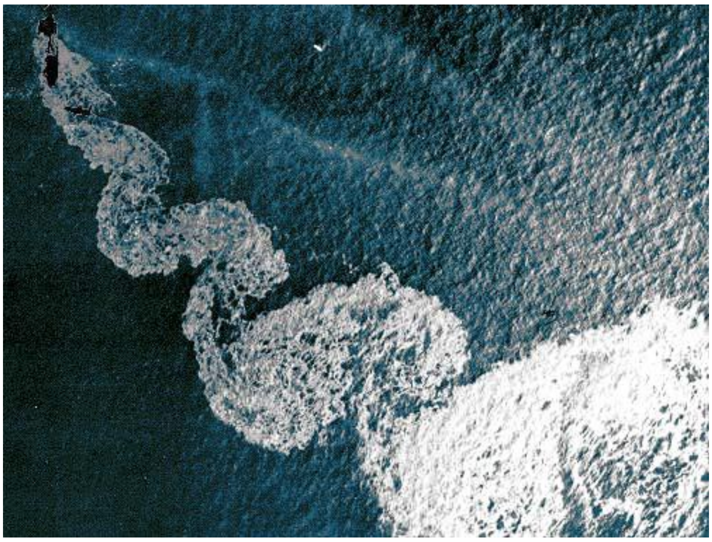

Figure 1.8. Aerial photograph of turbulent motion in wake of Stranded Tanker Argo Merchant on Nantucket Shoals (from an album of fluid motion, 1982).

In this study, it is aimed to control of the circular cylinder wakes by using splitter plates. Also, the aim was to visualize the effects of conditional sheet plate parameters on vortex sheeding characteristics around a cyrindirical pad of 50 mm diameter by experimental approaches. At the beginning of the iterational experiment period, we were thinking that, the length of the tail plate would be the dominant parameter by means of the vortex street, as [Kwon and Choi, 1996]

As a conclusion, length of the splitter plate is accepted to be the dominant variable which is varied in the size range of 0 mm to 250 mm with 25 mm of increments, the height of the splitter plate and of the cylinder and leading edge of the splitter plate which are varied in the size range of 10 mm in experiment in which the varying resultant values of the vortex, vorticity and velocity vectors is precisely recorded.

2. LITERATURE SURVEY

In order to works on wake flow is mainly concentrated on understanding of flow instability phenomena and control of vortex shedding. Basically, active and passive control methods are used. The vortex shedding enhances mixing behind the cylinder. By controlling vortex shedding, unsteady forces acting on the bluff bodies and their vibrations are reduced. Therefore, controlling the vortex shedding is very useful in practical situations.

2.1. Shallow Water

A great number of investigations on the circular cylinder vortex flows have been done so far.

Akıllı and Rockwell (2002) investigated the near wake of a vertical, circular cylinder in shallow water using a combination of visulation marker and particle image velocimetry tecnique (PIV). They have located laser sheet parellel to the bed of the water channel at different heights to investigate the flow characteristics at the bed and at the various locations above it. At the bed, the time averaged streamline topology downsream of the base of the cylinder takes on a form known as an owl face of the first kind, which was originally defined for a completely different exterior flow. Immediately adjacent to the base of the cylinder, an additional system of saddle points is located at either end of a nodal line. At locations above bed, one of the two principle saddle points of the owl face of the first kind disappears and the principle foci are transformed from a stable to an unstable state.

LI Wei, WU Jian and LI Guo-ya (2005**)** researched in the gap-ratio range of $0.0 \leq G \leq 7.0$, a particle image velocimetry PIV is applied to conduct a systematic experimental research of the flow around a horizontal circular cylinder in the cross-flow of shallow water. The findings of this paper are of guiding significance for engineering issues with similar flowing features. This study indicates that the flow in the wake flow zone behind the circular cylinder is local unsteady flow, the main feature of which is the generation and development of vortex in shear layer. The research in this paper indicates that the Strouhal number for the vortex shedding of the flow around a circular cylinder is independent of magnitude with the gap-ratios between the circular cylinder and the bottom wall, and when $0.5 \leq G \leq 6.0$, the wake flows around a horizontal circular cylinder in the cross-flow of shallow water have similar flowing structures.

An experimental study of Akıllı, Atar and Karakuş (2004) investigeted on the around two and three side-by-side circular cylinders of equal diameter in shallow water was investigated experimentally using the particle image velocimetry (PIV) technique, over a transverse gap ratio in the range of *G/D* = 1.0-3.0 with an increment of 0.25. Here, the experiments were conducted in a closed-loop water channel with Reynolds number 5000 based on the cyl-inder diameter. For the two side-by-side cylinder case, it was found that the flow structure behind the cylinders is asymmetrical at small gap ratios as a result of jet-like flow between the cylinders In the case of three cylinders, both an asymmetrical flow structure at small gap ratio (*G/D* = 1.25) and a symmetrical flow structure at intermediate gap ratios ($1.5 < G/D < 2.0$) were observed. Bistable wake regions were obtained for the asymmetrical cases. The Reynolds stress $(u'v)$ downstream of the upper cylinder was significantly attenuated for *G/D* = 1.25 where the jet-like flow is more effective for both two and three circular cylinder arrangements.

An experimental study of Akıllı, Atar and Karakuş (2004) found bistable nature of the flow was observed especially for the gap ratio of *G/D* = 1.25, both for two and three side-by-side cylinders arrangements. Without changing any experimental conditions, the jet-like flow has been changed direction and switched from one side to the other. For example, wider wake region occurred down-stream of upper cylinder most of the time for two-cyl-inder case, but, sometimes wider wake occurred downstream of the lower cylinder. Similar phenomenon was observed for three-cylinder case. However, this bistable nature of the flow was not observed for the gap ratios bigger than 1.5.

Eventually, negative Reynolds stress concentrations have been barely could be detected downstream of the cylinder which has been a wider wake flow region at the gap ratio of *G/D* = 1.25 for both two and three cylinders arrangements. Another important point found that the peak concentrations of Reynolds stress occurred very close to the saddle points (Akıllı, Atar and Karakuş (2004)).

2.2. Control of Vortex Shedding Behind a Circular Cylinder by Using Splitter Plate

The method of splitter plate is one of the most successful methods among passive control techniques.

Akıllı, Şahin and Tümen (2005) researched flow behavior around a vertical circular cylinder placed in shallow water was controlled by a splitter plate inserted at various locations downstream of the cylinder. Here, splitter plates with a length of 50 mm, which is equal to the diameter of the cylinder ***(D)***, were used during the experiments. Gap distance between the base of the cylinder and the leading edge of the splitter plate ranged from 0 to *2D*. Velocity vector field, corresponding vorticity contours and streamline topology and Reynolds stress concentrations were used to explain the characteristics of the flow. The splitter plates having different thicknesses present the same influence on the flow characteristics. Also, the gap between the base of the cylinder and the leading edge of the splitter plate was increased successively from 0 to 100 mm with 12.5 mm increments. Particle Image Velocimetry (PIV) has used to measure the instantaneous velocity vector field in the wake region at Reynolds number ***Re*** = 5000 based on the cylinder diameter. The mean velocity vector field, corresponding vorticity field and streamline topology and turbulence statistics have obtained using 200 instantaneous images. The water height has kept constant at 25 mm during the experiments.

An experimental study of Akıllı, Şahin and Tümen (2005) found the splitter plate has a substantial effect on the suppression of the vortex shedding for the gap ratio ***(G/D)*** between 0 and *1.75D*. For *G/D* = 1.75, the normalized Reynolds stress has a peak value of 0.0158, which is approximately 8.5 times smaller than the concentrations occurring for the bare cylinder.

Eventually, when the splitter plate was located at *2D* location, no effect of the plate was observed.

In this study Akıllı, Şahin and Gözmen (2007) researched the effect of splitter plates having various height and lengths on the control of vortex shedding behind a circular cylinder placed in shallow water layer was investigated experimentally using Particle Image Velocimetry Technique (PIV). The cylinder having outer diameter of 50mm was used for all experiments. The plate thickness was chosen constant as 4mm. On the other hand, the length of the plate was ranged from 25mm to 100mm with 25mm increments. The heights of plate were 6.25mm, 12.5mm and 18.75mm. The gap between the base of cylinder and the leading edge of the splitter plate was ranged from 0 to 100mm with 12.5mm increments. All experiments were carried out in shallow water having 25mm height. Particle Image Velocimetry (PIV) technique was used to measure instantaneous velocity vector field in the wake region at Reynolds number based on cylinder diameter Re=6300. Time-averaged velocity vector field, corresponding vorticity contours, streamline topology and turbulent statistics were obtained by 300 instantaneous images.

In this study Akıllı, Şahin and Gözmen (2007) founded increasing splitter plate height controls the vortex shedding better. Moreover, the distance between the base of the cylinder and the leading edge of the splitter plate affects the control of vortex formation. The splitter plate lengths of 75 mm and 100 mm have full effect on control of vortex shedding. For the cases which the splitter plate is placed on to the platform except the case of the splitter plate height of 6.25 mm, the splitter plates have important effect on the suppression of vortex shedding. For the cases which the splitter is not located on the platform, the maximum control of the vortex shedding is obtained for hb/hw=0.25 cases and minimum effect on the suppression of vortex shedding is hb/hw=0.75 cases.

Bearman (1964) investigated the effect of splitter plates as measures to stabilize the wake and reduce the drag of two-dimensional bluff bodies. Flow visualization and hot wire measurements showed that the vortex formation location was shifted downstream and the strength of the vortices was reduced. Both effects increased the base pressure and thus reduced the pressure drag. Measuring the base pressure, a drag reduction of up to 50% was found. If the base bleed rate in the base bleed experiments was high enough, the vortex street disappeared completely.

2.3. Flow Control Methods

Many researchers have studied on flow control methods to prevent the flow's negative impression.

An experimental study of GUO Xiao-hui, LIN Jian-zhong, TU Cheng-xu, WANG Hao-li (2008) investigated of flow by the combined effects of the rotation and the Reynolds number on the flow past two rotating circular cylinders in a side-by-side-arrangement at a range of $425 < Re < 1130$,$0 < \mathbf{a} < 4$ (**a** is the rotational speed) at one gap spacing of $T/d = 1.11$ (T and d are the distance between the centers of two cylinders and the cylinder diameter, respectively) and measurements were performed using Particle Image Velocimetry (PIV) to analyze the modification. A new Immersed-Lattice Boltzmann Method (ILBM) scheme was used to study the effect of the gap spacing on the flow. In this case, show that the vortex shedding is suppressed as rotational speed increases. The flow reaches a steady state when the vortex shedding for both cylinders is completely suppressed at critical rotational speed. As the rotational speed further increases, the separation phenomenon in the boundary layers disappears at the attachment rotational speed. The critical rotational speed and attachment rotational speed become small as Reynolds number increases. The absolute rotational speed of cylinders should be large at same critical rotational speed and attachment rotational speed in the case of large Reynolds number. As a result, it is very different in the mechanism of vortex shedding suppression for the flows around two rotating cylinders and single rotating cylinder. The results show that the rotational speed has an important effect on the vortex shedding, separation of boundary layers on the cylinders and state in the wake flow.

Lim and Lee (2004) investigated the flow characteristics of the wakes behind circular cylinders fitted with orings. The drag force,wake velocity and turbulence intensity were measured for Reynolds numbers in the range $Re_d = 7.8 \times 10^3 \sim 1.2 \times 10^5$ for various combinations of o-ring diameter and pitch distance between adjacent o-rings. The results were summarized as follows: The cylinder fitted with o-rings of diameter d=0.0167D in a pitch interval of 0.165D showed a maximum drag reduction of about 9% at $Re_d = 1.2 \times 10^5$, compared with the smooth cylinder.

However, installation of o-rings with diameters longer than d= 0,067D reduces the drag only slightly.

3. MATERIAL and METHOD

3.1. Experimental Arrangement

Experiments were undertaken in a water channel in Fluid Mechanics the Laboratory, Mechanical Engineering Department of Cukurova University.

Increasing technological developments, especially in electric and electronic engineering, provide new measuring techniques. All measurement techniques have some advantages and disadvantages associated with the specific method. It is increasingly important not only to measure the mean values at a point in space, but also to measure and characterize turbulent and instantaneous values in the investigated flow field. Particle Image Velocimetry, PIV, is a non-intrusive technique used to measure an instantaneous two dimensional velocity vector field under investigated area. The velocity is determined by measuring the displacement of particles in a flow field that is illuminated by a laser sheet.

3.1.1. Water Channel

Both PIV and dye visualization experiments were performed in a large-scale water channel located in the Fluid Mechanics Laboratory at Cukurova University. The water channel (see Figure 3.1) test section which has the following dimensions: a length of 8000 mm, width of 1000 mm, and a depth of 750 mm was constructed of transparent Plexiglas with upstream and downstream fiberglass reservoirs. The water channel also has honeycomb screen arrangement, which is located at the entrance of contraction. These reservoirs and honeycomb screen arrangements are used to maintain the turbulence intensity in the section below 0.1 %. The water flow speed was controlled by an axial flow pump. Pump rotation speed was controlled by an ABB controller unit. This system was built for PIV experiments for steady and unsteady flows. Schematic view of the water channel is shown in Figure 3.2.

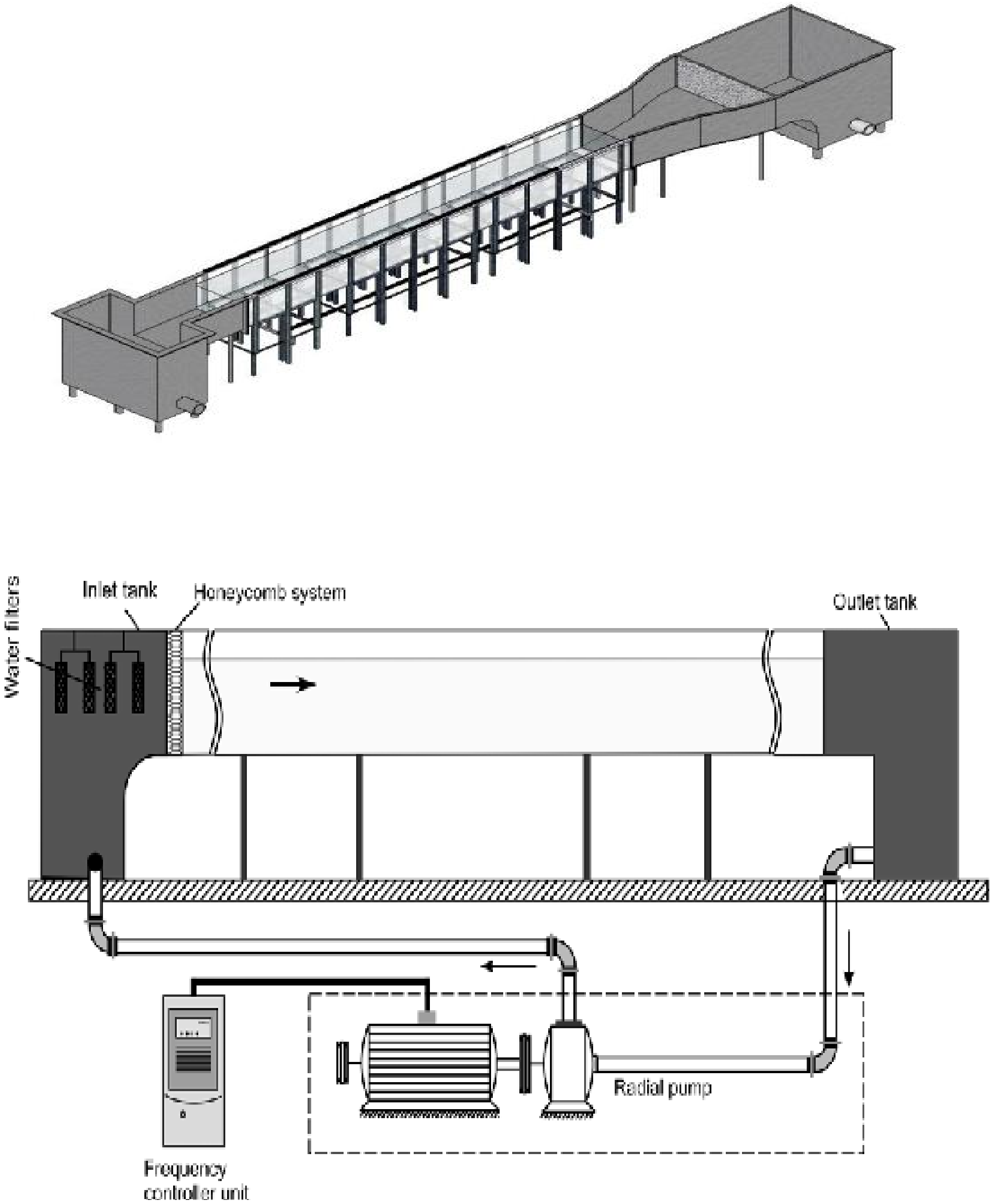

Figure 3.1. The water channel

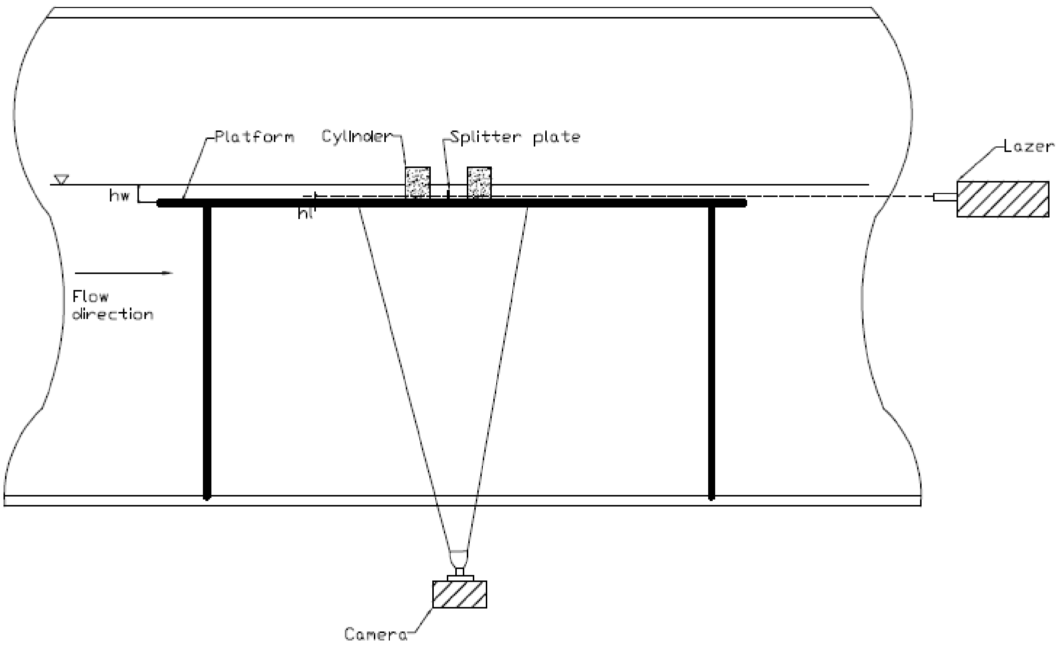

Figure 3.2. Schematic view of the water channel

3.1.2. Experimental Model

The water level was (h_w) maintained at the depth of 25 mm. Experiments were carried out at a free-stream velocity yielding Reynolds number based on the cylinder diameter of Re = 5000.

The cylinder which was used during the experiments was made of plexiglas material and its diameter was D=50 mm and the length of used plate was 250 mm, and their widths were taken as 2,5 mm. Plates were also made from Plexiglas material. During this experimental study, both the effects of height of the plate and the gap between plate and the bottom were investigated. In order to understand the effect of plate height, six different heights were used. These heights were 0 mm, 5 mm, 10mm, 12.5 mm, 17.5 mm and 22.5 mm. In order the understand the effect of the distance between the plate and the bottom of the table, six different heights, 0 mm, 5 mm, 10 mm, 12.5 mm, 17.5 mm and 22.5 mm. The cylinder and plates were located at 10mm from the leading edge of the table. According to the investigation of

Kırkgöz and Ardıçlıoğlu (1997), this entrance length, water depth and flow velocity provide a fully developed turbulent boundary layer at the location of the cylinder.

Total of 198 experiments were carried out by using total of 1 plate. The distance between the base of the cylinder and the leading edge of plates were changed between 0 mm and 250 mm in intervals 25 mm. All experiments were done as two sets. The first set includes 350 instantaneous images.

By using the PIV tecnique, instantaneous velocity vectors can be measured in a region illuminated by a two-dimensional laser sheet. Velocity vector measurements have been carried out using dantec PIV system. The flow field illumination was provided by two Nd: Yag pulsed laser sources of a wavelength of 532 nm, each with a maximum energy output of 120 mJ. Dantec Flow Map Processor, that controlled the timing of the data acquisition, was used to synchronize the image taking and laser unit. The thickness of the laser sheet illuminating the flow field was approximately 1 mm. The water was seeded with the neutrally buoyant spherical particles of 12µm in diameter. The movement of the particles was recorded by using a CCD camera with a resolution of 1024 x 1024 pixels. The camera was equipped with a 55 mm focal-length lens. Dantec flow grabber digital PIV software employing frame- to- frame cross-correlation technique was employed to calculate the raw displacement vector field from the particle image velocity data. In the image processing, 32x32 pixels rectangular effective interrogation windows were used. During the interrogation process, an overlap of 50% was employed in order to satisfy Nyquist criterion. In the post-processing step, interpolation between surrounding vectors was used in order to remove erroneous vectors and replace. Displacement of vector field could be measured and by using this, velocity vectors of the flow could be calculated. The vorticity patterns of the wake flow can be calculated from the velocity field using a finite difference scheme. Streamlines and circulation can be obtained by post processing of the velocity data. The overall field of view was 160 x 160 mm^2 (3.2x3.2 cylinder diameters). Patterns of instantaneous particle images (total of 300 images for a continues series) were taken at a rate of 15 Hz, thereby spanning 13.4 s. Averaged patterns of the flow structure were calculated from these total number of instantaneous images. The time delay between pulses ranged from 1.5 to 2ms. A software developed in-house were then used to compete the velocity vector field, streamline topology and other turbulent statics. In terms of uncertainty of velocity measurement using the PIV technique, the digital PIV approach carried out during the experiments in similar to that employed by Westerweel (1993) who concluded that an uncertainly in velocity is less than 2%.

3.2. Principle of Particle Image Velocimetry Technique

Particle Image Velocimetry (PIV) is a whole-flow-field technique providing instantaneous velocity vector measurements in a cross-section of a flow. Two velocity components are measured, but use of a stereoscopic approach permits all three velocity components to be recorded, resulting in instantaneous 3D velocity vectors for the whole area. The use of modern digital cameras and dedicated computing hardware, results in real-time velocity maps.

PIV technology have some advantage and disadvantage then other velocimetry technique. These are respectively;

Advantages:

Thousands of measurements per image
Measurements are simultaneous
Few fundamental limitations
Non-intrusive

Disadvantages

Very expensive
Poor temporal resolution
Elaborate set-up

3.2.1. Principles of Particle Image Velocimetry (PIV)

In Particle Image Velocimetry (PIV), the velocity vectors are derived from sub-sections of the target area of the particle-seeded flow by measuring the movement of particles between two light pulses:

Speed =Distance / Time

$V=\Delta x / \Delta t$

For the PIV technique the property actually measured is the distance between two images of particles that travels in the flow field within a known time interval. These particles are added to the flow and known as seeding. The type of seeding particle is chosen to follow the flow, and in order to detect their movement, an area of the flow field is illuminated by a laser light-sheet. The light-sheet, which is generated by a laser and a system of optical components, is not continuous/permanent, but pulsed to produce a stroboscopic effect, freezing the movement of the seeding particles. The time between the light pulses is the denominator in the equation above. To detect the position of the illuminated seeding particles, a CCD-camera (CCD = Charge Coupled Device) is positioned at right angles to the laser light-sheet, and particle positions will appear as light specks on a dark background on each camera frame. The pulsing light-sheet and the camera are synchronized so that particle positions at the instant of light pulse number 1 are registered on frame 1 of the camera, and particle positions from pulse number 2 are on frame 2. (Older generations of CCD cameras couldn’t switch frames fast enough, so both the first and the second pulse of the light sheet was recorded on the same camera frame). The camera images are divided into square regions called interrogation areas or interrogation regions, and for each of these interrogation areas the image from the first and the second pulse of the light-sheet are correlated to produce an average particle displacement vector. Doing the same process for all interrogation regions produce a vector map of average particle displacements. Dividing with the known time between the two images captured the displacement vectors are converted into a map of so-called raw velocity vectors. Then validation algorithms can be applied to the raw vector maps, so that outliers, the term for erroneous vectors, can be detected and removed. In the FlowMap PIV system, for reasons of experimental reproducibility, the raw vector map is archived and a new validated vector map is output, and further analysis can produce streamlines, vorticity and so on.

From the basic principles the following main topics of PIV emerge:

• Seeding
• Illumination
• Cameras
• Synchronization
• Correlation
• Validation and further analysis

3.2.1.1. Seeding

Recording both light pulses in the same image frame to track the movements of the particles gives a clear visual sense of the flow structure. In air flows, the seeding particles are typically oil drops in the range 1 µm to 5 µm. For water applications, the seeding is typically polystyrene, polyamide or hollow glass spheres in the range 5 µm to 100 µm. Any particle that follows the flow satisfactorily and scatters enough light to be captured by the camera can be used. The number of particles in the flow is of some importance in obtaining a good signal peak in the cross-correlation. As a rule of thumb, 10 to 25 particle images should be seen in each interrogation area. Figure3.3. shows seeding particles image.

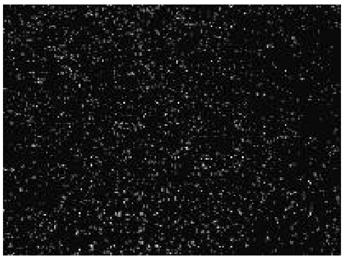

Figure 3.3. Seeding particle

3.2.1.2. Illumination

Illumination provide sufficient energy density for obtaining images of seeding particles in the flow. The laser is integrated in the traverse and the laser and beam path are completely shielded from surroundings under normal operating conditions. Advantage is that the displacement field is obtained on a regular grid. A typical size of these interrogation areas is 32x32 pixels, which means that one gets about 7300 vectors from an image with a resolution of 1600×1186 pixels.

For the illumination, it is preferable to use a laser, since the laser beam is easy to form into a sheet by a cylindrical lens. A pulsed laser is to prefer, since one obtains a high light energy during a very short time interval (typically 5 ns for a YAG-laser), which means that the particle images will be practically frozen even for high velocities (> 100 m/s). The repetition rate of a YAG-laser is typically 10-30 Hz, which is too low except for very low velocities (< 1 cm/s). One therefore needs two lasers to get full freedom in terms of time separation between the pulses. Special PIV YAG-lasers are available that combine two laser cavities with a common beam outlet.

3.2.1.3. Cameras (Image Capturing)

The PIV camera, together with Computer-controlled Synchronizer and Image Capture and Analysis Software provides state of the art capabilities for PIV image capture and analysis. In crosscorrelation mode, the Synchronizer provides the pulse delay that positions the first laser pulse at the very end of the first video frame and the second laser pulse towards the beginning of the second frame. The Insight software signals the camera to capture a pair of frames when the laser is pulsed. The pulse separation can be as low as 0.2 microsecond and adjusted to measure velocities ranging from mm/sec to supersonic speeds.

A very important issue for obtaining accurate PIV measurements is the appropriate seeding of the flow with tracer particles. To closely follow the flow the particles should be as small as possible, but on the other hand they may not be too small, because then very small particles will not scatter enough light, and hence produce too weak images

3.2.1.4. Synchronisation

To capture a flow field image with Particle Image Velocimetry, the laser pulse and camera must be triggered with the correct sequence and timing for the flow conditions under investigation. Computer-controlled LASER PULSE Synchronizer performs this task, tying PIV imaging and image capture components together as an integrated and automated system.

3.2.1.5. Correlation (Image Evaluation)

The position of the highest peak in the correlation plane indicates the mean displacement of the particles in a particular interrogation window. The displacement vectors of all interrogation windows are finally transformed into a complete instantaneous velocity map. Figure 3.4. shows principles of cross-correlation.

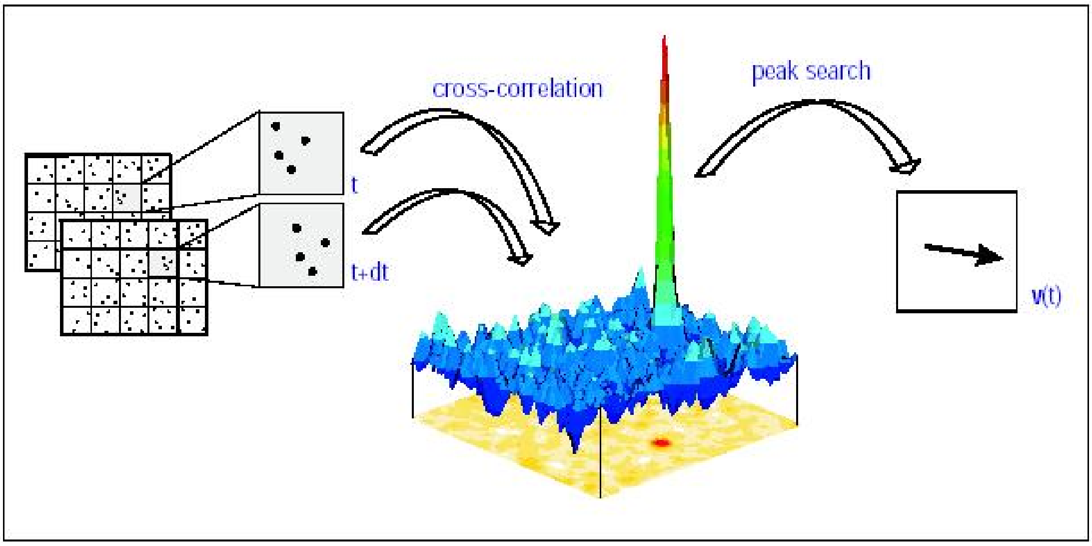

Figure 3.4. Principles of cross-correlation

3.2.1.6. Validation and further analysis (Image Post-Processing)

Images were received from CCD camera that has resolution 1024×1024 at a rate of 15 frames per second. The time delay changes from 2 ms and 3 ms between frames depending on the flow conditions and camera location. Digital image was analyzed using FLOWMAP software. The image was recorded on a CDD array. A frame grabber in the computer read the camera image from CCD camera and stored it as the digital image file format (TIFF) in the RAM. This digital image was processed and analyzed using the FLOWMAP software. During each continuous run, a total 390 images were taken. In order to determine the velocity field, a cross-correlation technique, with 32×32-interrogation window, was employed, with an overlap of % 50.

The resulting vector field obtained from INSIGHT software and the corresponding boundaries of objects were then viewed using in-house program V3 (Robinson, 1992) to determine incorrect vectors from interrogation. These types of vectors can result when an incorrect particle correlation is made near boundaries or within shadow regions, when the particle images are too widely spaced for interrogation window side specified, or the power of laser sheet is poor (Jefferies, 1996 and Çetiner, 1998).

Vector validation software called CLEANVEC was used to remove incorrect vectors. The software CLEANVEC contains four statistical filters designed for incorrect vectors removal:

- Absolute range filter
- RMS tolerance filter
- Magnitude difference filter
- Quality filter

Finally, the magnitude difference tool removes unnecessary vectors based on the difference in magnitude between a vector and its neighborhood median. This is the local-median test defined by Westerweel (1994). This filter is the most effective among the available filters, as indicate by Westerweel (1994). However, it should be handled carefully, because it may lead to an excessive vector in a certain type of flows.

3.2.2.7 Time-Averaging of PIV Images

Time-averaging of PIV images were performed using following formulation. Time-averaged horizontal component of velocity:

$$\langle u \rangle = \frac{1}{N}\sum_{n=1}^{N} u_n(x,y) \qquad (3.1)$$

Time-averaged transverse component of velocity:

$$\langle v \rangle = \frac{1}{N}\sum_{n=1}^{N} v_n(x,y) \qquad (3.2)$$

Time-averaged vorticity:

$$\langle \omega \rangle = \frac{1}{N}\sum_{n=1}^{N} \omega_n(x,y) \qquad (3.3)$$

Root-mean-square of u component fluctuation:

$$u_{rms} = \left\{ \frac{1}{N}\sum_{n=1}^{N} \left[u_n(x,y) - \langle u(x,y) \rangle \right]^2 \right\}^{1/2} \qquad (3.4)$$

Root-mean-square of v component fluctuation:

$$v_{rms} = \left\{ \frac{1}{N}\sum_{n=1}^{N} \left[v_n(x,y) - \langle v(x,y) \rangle \right]^2 \right\}^{1/2} \qquad (3.5)$$

Averaged value of Reynolds stress correlation:

$$\langle u'v' \rangle = \frac{1}{N}\sum_{n=1}^{N}\left[u_n(x,y) - \langle u(x,y)\rangle\right]\left[v_n(x,y) - \langle v(x,y)\rangle\right] \quad (3.6)$$

Where N is the total number of instantaneous images used for the time-averaged values and n refers to the instantaneous images.

4. RESULTS and DISCUSSION

4 1. General Information

In the present experimental study, the effect of splitter plates having various height and lengths on the control of vortex shedding behind side-by-side two cylinders placed in shallow water layer was investigated experimentally using Particle Image Velocimetry Technique (PIV) is shown. The splitter plate has a length which is ranged from 0 mm to 250 mm with 25 mm increments. The istance between the bottom of the splitter plate and the table surface which are 0 mm, 5 mm, 10 mm, 12.5 mm, 17.5 mm, 22.5 mm. Moreover, The cylinder having outer diameter of 50 mm was made of plexiglass all experiments and the plate thickness is chosen constant as 2,5 mm. The effect of plate thickness, T, was examined using plate thicknesses, T/D=0,05. The gap between the base of the cylinder and the leading edge of the splitter plate is a fixed height which is equal to 20 mm. Particle Image Velocimetry (PIV) is used to measure instantanoues velocity vector field in the wake region at Reynolds number based on cylinder diameter Re=5000. The mean velocity vector field, corresponding vorticity field, streamline topology and Reynolds stress are obtained from 350 instantanous images. Experimental results of wake flow structures of circular cylinders were investigated for side by side cylinders at gap ratios G/D (ratio of the spacing between the sphere centers to diameter), which is 1.25. Increasing the distance between the bottom of the splitter plate and the table surface controls the vortex shedding better. Moreover, the length increase of the splitter plate affects the control of vortex formation. Experiments was realized in the water depth of 25 mm. The velocity of the flow was adjusted by an electronic pump controller unit in terms of the frequency control unit.

A camera and a laser source were used for experiments. For the PIV experiments, a camera, a laser source, a synchronizer and a computer with the user interface program was used. Images was acquired using a CCD camera with a resolution of 1186×1600 pixels. The camera was equipped with a 55 mm lens. Plan view of the test section, position of the cylinders and splitter plates as well as the coordinate system is shown in figure 4.1.

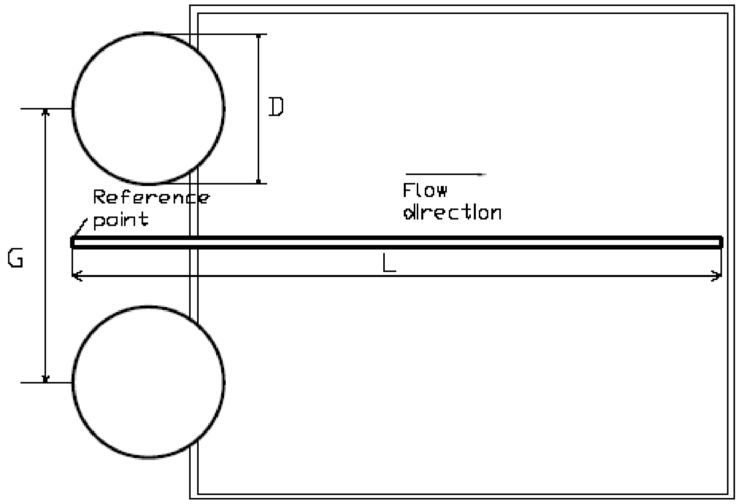

Figure 4.1. Plan view of the experiment area

4.2. Flow Behind Bare Cylinder

Figure 4.2 presents the flow of the velocity vector field (<v>), corresponding vorticity contours (<ω>), the streamline topology (<ψ>) and Reynolds stress contours (<u'v'>) for circular cylinder in shallow water obtained from PIV experiments. The time averaged data were obtained from 350 instantaneous images.

When flow past a circular cylinder in shallow water, bluff-body alternate vortex formation is observed and a defined vortex street (Large- scale Karman vortex street) can be observed. This value is in harmony with studies in the literature. Figure 4.2 shows no suppression of vortex shedding and the flow direction is from left to right.

Velocity vector (<v>) map shows that low velocity region which represents the wake region just behind the cylinder. The velocity vectors exterior to the bubble type wake region are much greater than those of in the wake region. Significant reverse flow occurs within this bubble type wake region. The length of the wake region is approximately one cylinder diameter. The wake has a symmetrical structure. The near wake is relatively narrow and symmetrically. Here dashed lines represent negative vorticity (clockwise direction) and solid lines show positive vorticity (counter- clockwise direction). Both vorticity layers extend in streamwise direction. Condensed vorticity contours are also an indication of the presence of the shear layer.

In terms of vorticity contours(<ω>) of the bare cylinder, the vorticity stays condenced near the cylinder and the central region of each layer is deflected towards the plane of symmetry. Both vorticity layers extend in streamwise direction. Condensed vorticity contours are also an indication of the presence of the shear layer.

Also the patterns of streamlines (<ψ>) are shown in this figure. This case indicates that two well-defined foci and a saddle point are observed from streamline topology. The saddle point occurs approximately at one cylinder diameter downstream of the base of the cylinder. The wake region and the shear layer occur at this region, too.

Also the patterns of Reynolds stress (<u'v'>) are shown in this figure. There are strong concentration contours. This figure indicates that high concentrations are centered at a distance of about one cylinder diameter downstream of the base of the cylinder. Reynolds stress concentrations, pronounced concentrations of Reynolds stress occur adjacent to the base of the cylinder. As the flow goes downstream, the Reynolds stress concentration of the wake behind the cylinder increases initially. Besides the well-defined Reynolds stress pattern due to fluctuations in the shear layers, a weaker Reynolds stress region very close to the base of the cylinder occurs as a result of the entrainment of free-stream flow into this wake region.

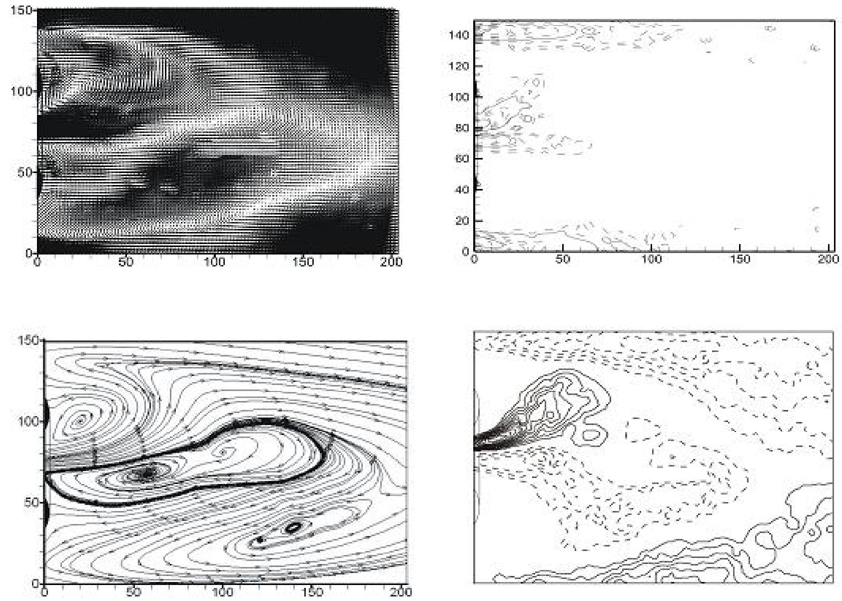

Figure 4.2 Flow Behind Bare Cylinder

4.3. Flow Control around Side-By-Side Cylinders Using Splitter Plates

Among the passive control techniques, the splitter plate has been one of the most successful devices for control of the vortex shedding. In this section, the effects of splitter plates on the flow characteristics of circular cylinders arranged side-by-side are investigated experimentally. Splitter plates, having 2 mm thickness, are made of transparent Plexiglas material to provide optical access for PIV measurements. Experiments were only carried out for the gap ratio of G/D=1.25. The splitter plates were kept in position along the axis which devices for the gap between cylinders into equal parts. Moreover, the centers of the splitter plate and cylinders were located at the same line into equal parts.

4.3.1. Splitter Plate with 250 mm Length(x=5D)

Patterns of velocity vector field, <v>, vorticity contours, <ω>, streamline, <ψ>, and normalized Reynolds shear stress correlations, <u'v'> at the elevation are given in figure 4.30 as a function of splitter plate length. The effect of the plate on the control of flow structure for the plate length of (x=5D) 250 mm and the distance between the bottom of the splitter plate and the table surface 0 mm, 5 mm, 10 mm, 12.5 mm, 17.5 mm and 22.5 mm are depicted.

The velocity vector field clearly indicates that the deflection of the jet flow is completely prevented by the presence of splitter plate. The wake region of the cylinders does not effect each other. Pair of vorticity having small scale at the vicinity of both sides of the splitter plate is result of existing of the vorticity contours.

Peak concentrations of Reynolds shear stress have bigger values at the distance between the bottom of the splitter plate and the table surface of the plate 12.5 mm and 15 mm than the distance of the plate 0 mm .

Increasing the distance between the bottom of the splitter plate and the table surface, the control of flow increases at the **Figure 4.30, 4.31, 4.32, 4.33, 4.34 and 4.35.** When the distance between the bottom of the splitter plate and the table surface increases, the vorticity contours reduce, on the other hand, streamline elongates. The location of the peak concentration slightly moves downstream. Moreover, deflected jet flow between cylinders plays an important role on the flow topology for all splitter plate lengths. Maximum Reynolds stress concentrations generally occur along the shear layers in figure 4.35.

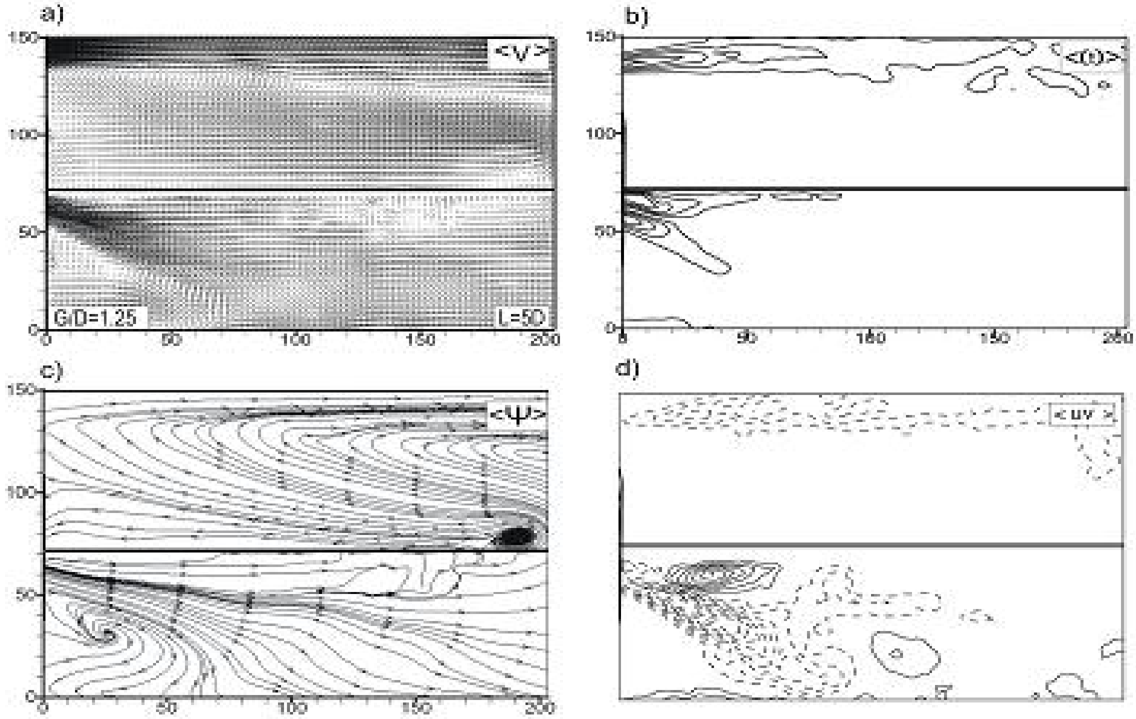

Figure 4.30. Flow characteristic which the case of plate having x=5D length and 0 point height

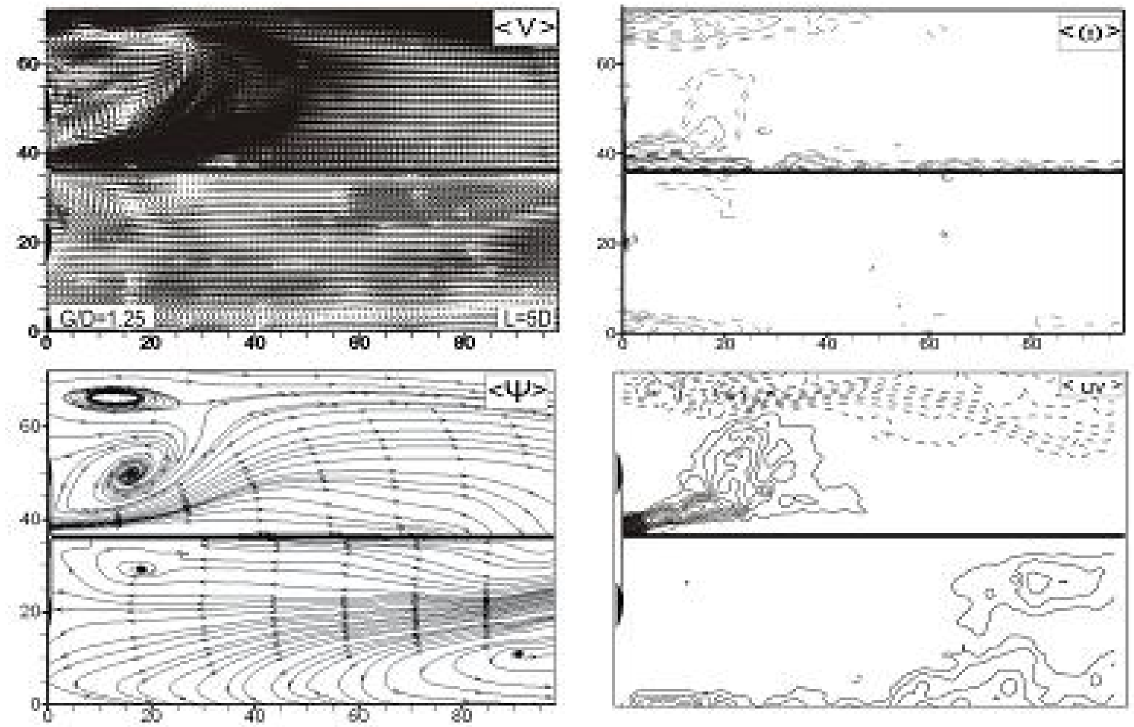

Figure 4.31. Flow characteristic which the case of plate having x=5D length and 5 mm height

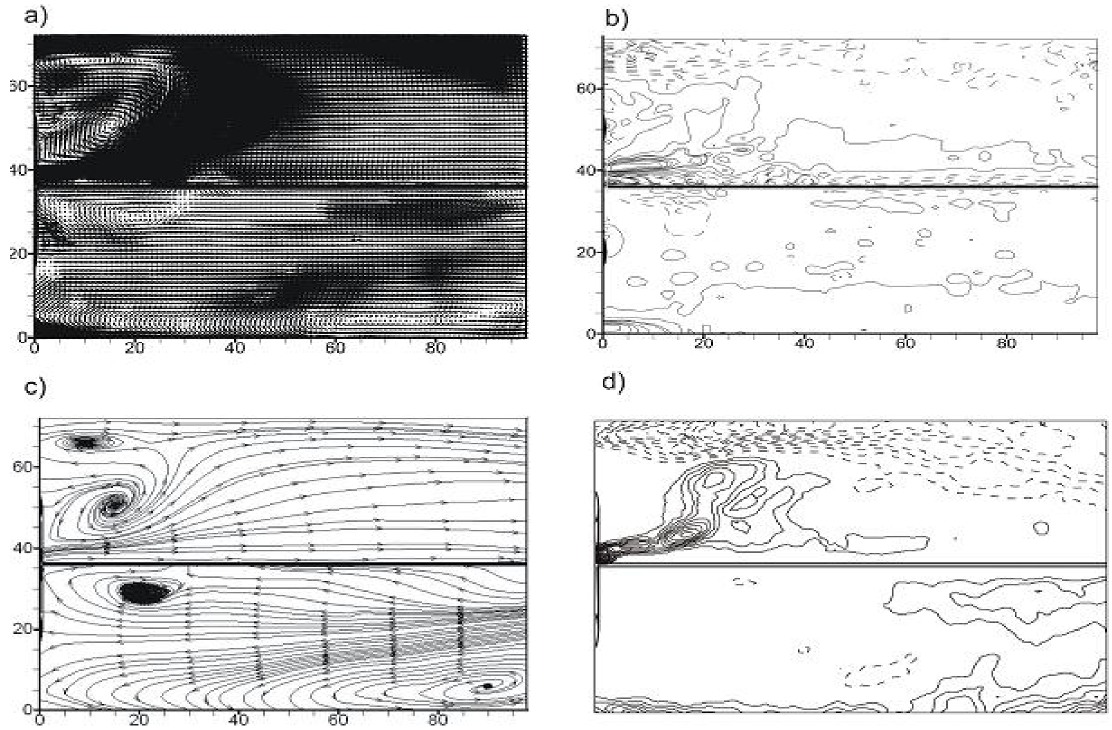

Figure 4.32. Flow characteristic which the case of plate having x=5D length and 10 mm height

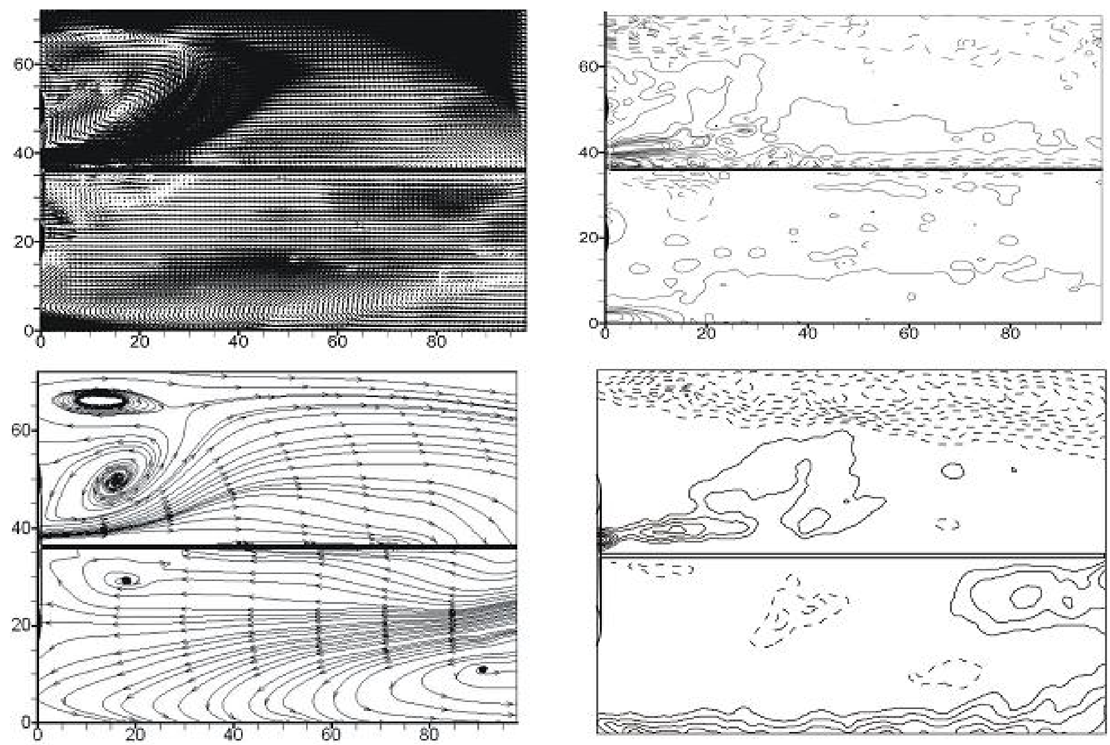

Figure 4.33. Flow characteristic which the case of plate having x=5D length and 12.5 mm height

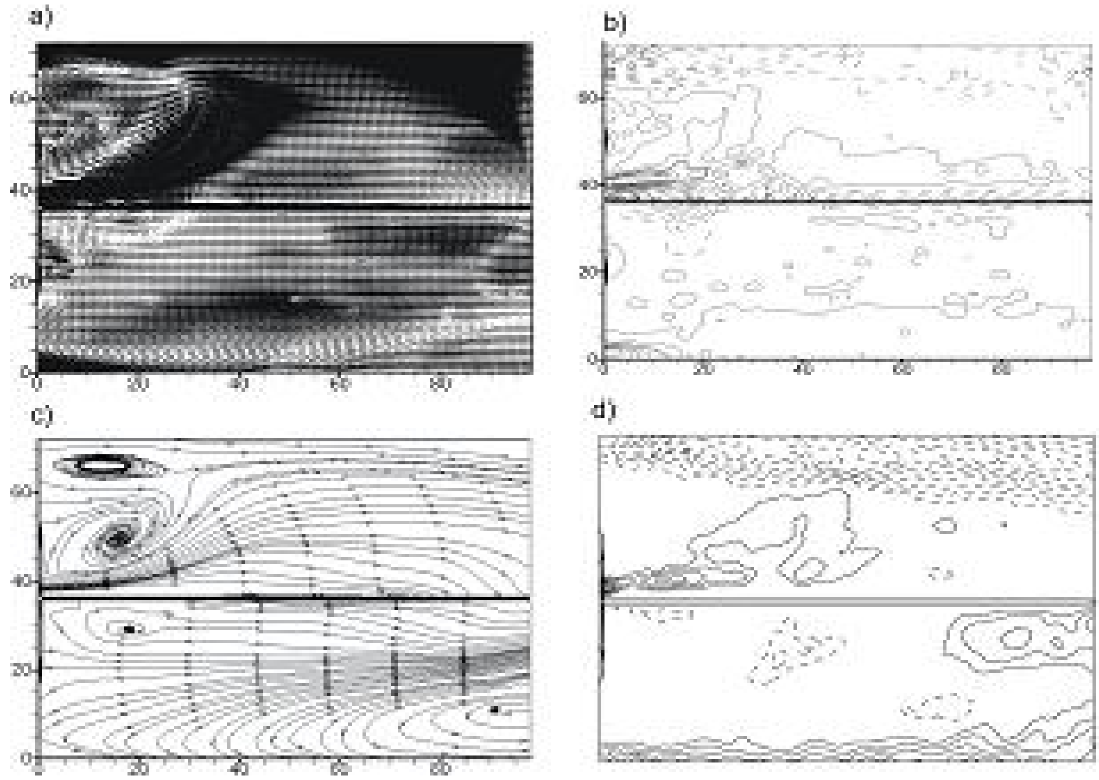

Figure 4.34. Flow characteristic which the case of plate having x=5D length and 17.5 mm height

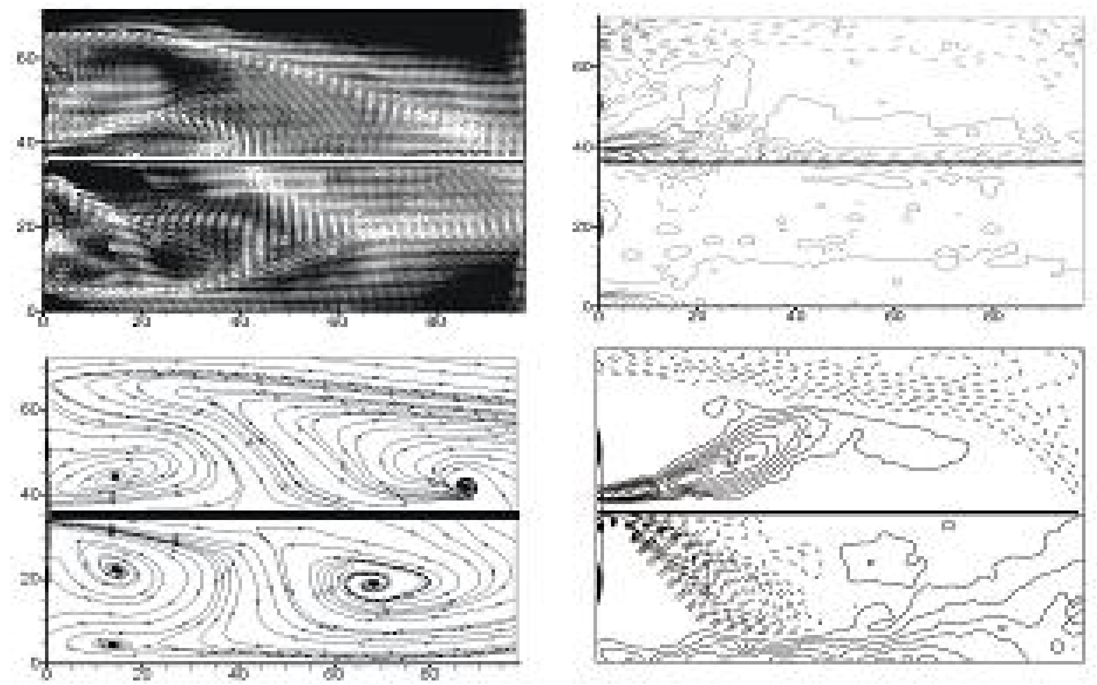

Figure 4.35. Flow characteristic which the case of plate having x=5D length and 22.5 mm height

4.3.2. Splitter Plate with 225mm Length(x=4.5D)

The velocity vector field, <v>, vorticity contours,<ω> , streamline,<ψ>, and Reynolds stress concentrations,<u'v'>, for the length 225 mm (x=4.5D), for the distance between the bottom of the splitter plate and the table surface 0 mm, 5 mm, 10 mm, 12.5 mm, 17.5 mm and 22.5 mm are depicted.

The vorticity contours are horizontal and they are little smaller than no-plate case. After the edge of the plate, the stronger Reynolds stress concentrations occur in **Figures 4.39, 4.40 and 4.41.**

In general, increasing the distance between the bottom of the splitter plate and the table surface causes to the elongation of streamline at the streamwise direction. The location of the peak concentration moves slightly downstream. A pair of vorticity contour appears both sides of the splitter plate. Increasing the distance between the bottom of the splitter plate and the table surface causes to decrease the peak concentration of Reynolds stress considerably and controls the vortex shedding better than the cases shown in **Figures 4.36, 4.37, 4.38, 4.39, 4.40 and 4.41**. Maximum Reynolds stress concentrations generally occur along the shear layers.

By increasing the distance between the bottom of the splitter plate and the table, the control of flow increases in **Figures 4.36, 4.37, 4.38, 4.39, 4.40 and 4.41.** When the distance between the bottom of the splitter plate and the table surface increases, the Reynolds shear stres elongates, on the other hand, wake flow region reduces.

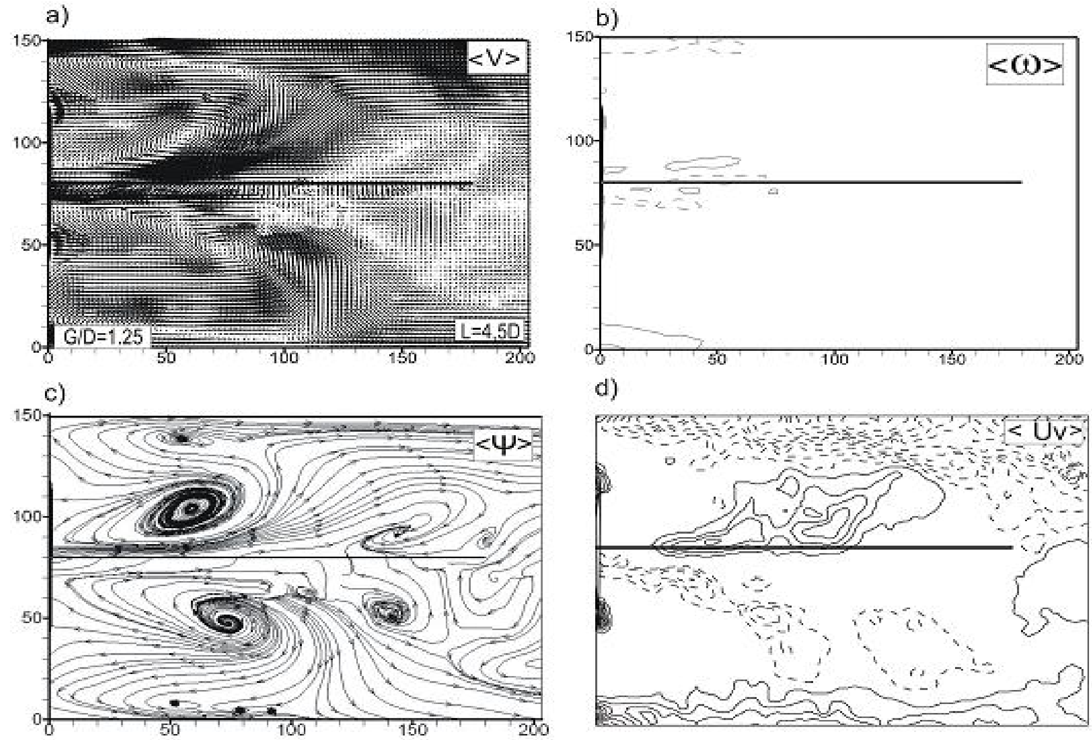

Figure 4.36. Flow characteristic which the case of plate having x=4.5D length and 0 point height

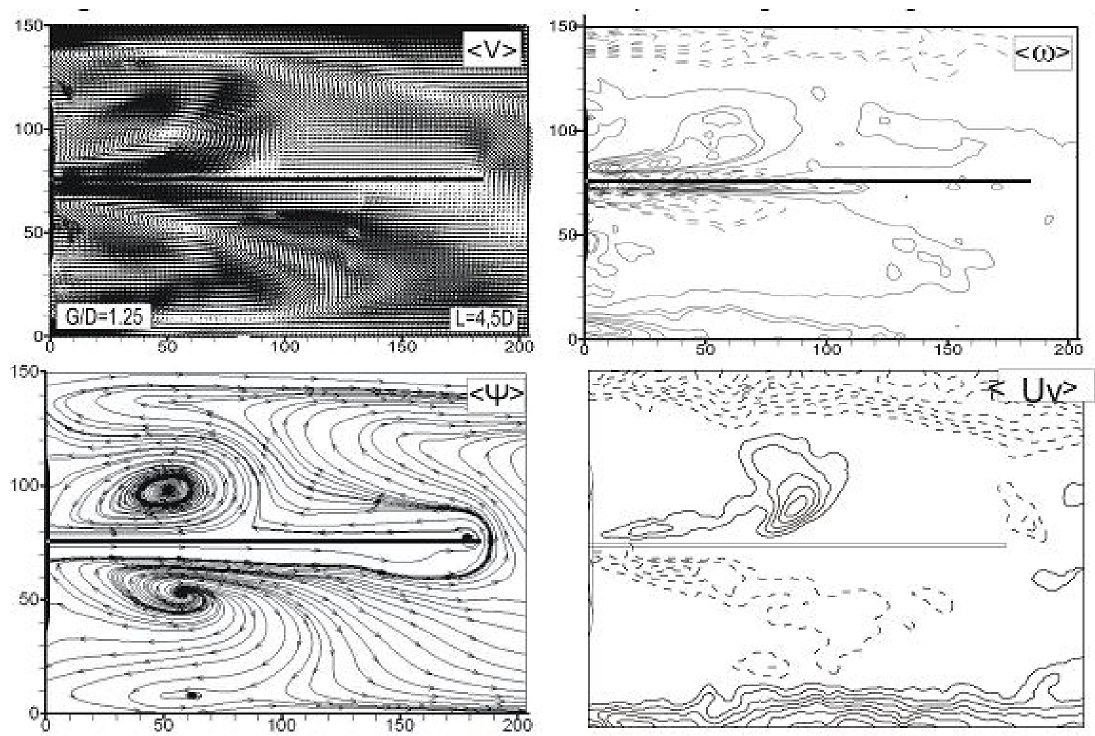

Figure 4.37. Flow characteristic which the case of plate having x=4.5D length and 5 mm height

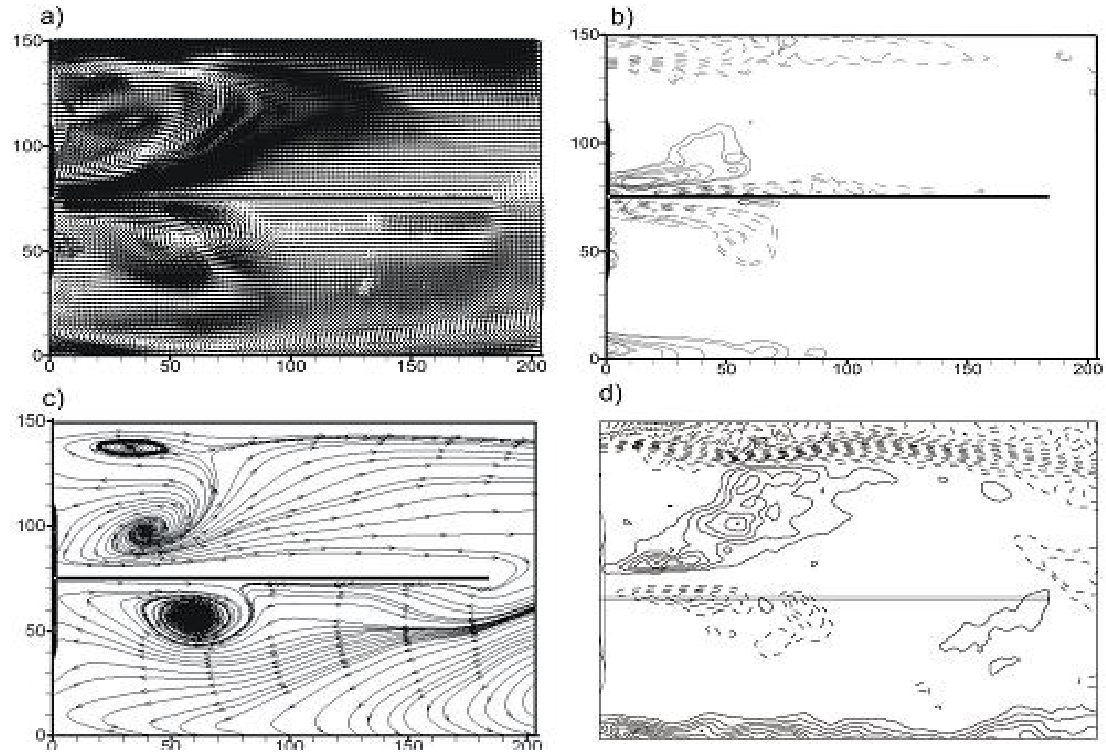

Figure 4.38. Flow characteristic which the case of plate having x=4.5D length and 10 mm height

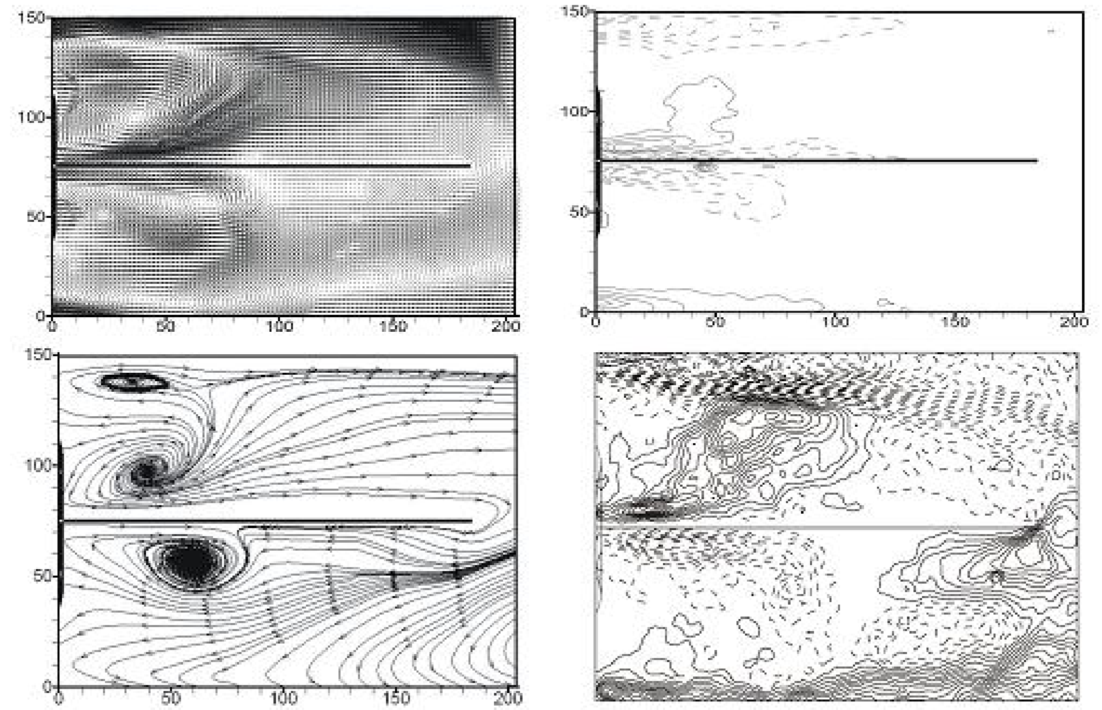

Figure 4.39. Flow characteristic which the case of plate having x=4.5D length and 12.5 mm height

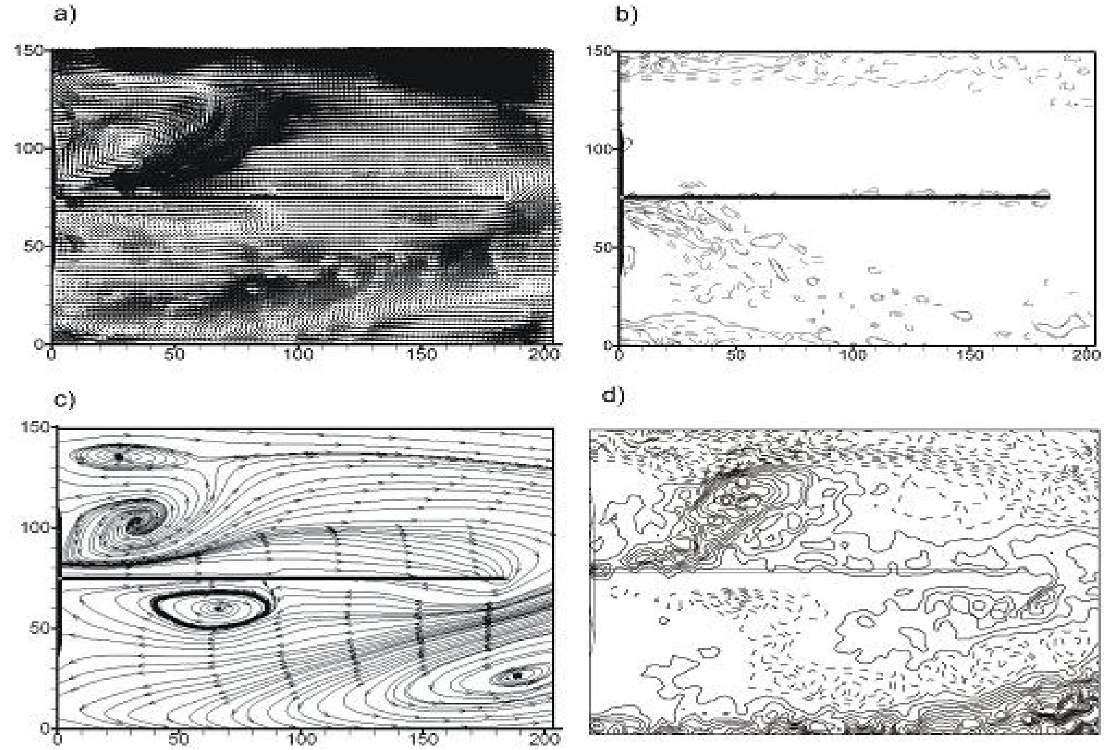

Figure 4.40. Flow characteristic which the case of plate having x=4.5D length and 17.5 mm height

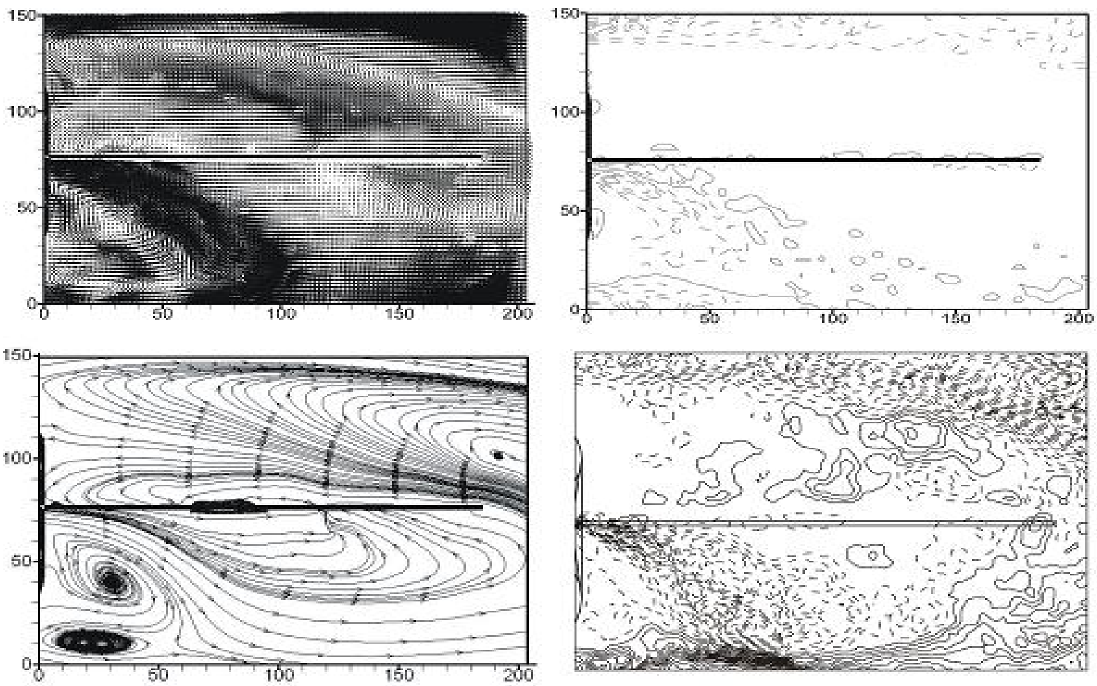

Figure 4.41. Flow characteristic which the case of plate having x=4.5D length and 22.5 mm height

4.3.3. Splitter Plate with 200 mm Length(x=4D)

The velocity vector field, (a), <v>, vorticity contours,(b), <ω>, streamline,(c), <ψ>, and normalized Reynolds stress contours,(d), <u'v'>, were shown in Figures between 4.42 and 4.47. The figures between 4.42 and 4.47 where the splitter plate has 200 mm length have very little effect on the flow characteristics.

Peak concentration increases slightly compared to the peak value of Reynolds shear stress obtained for x=4D case.

For the case in Figure 4.42, the splitter plate has no influence on the flow structure.

In general, decreasing splitter plate length (from x=5D up to x=4D) causes elongation of vorticity contours on streamwise direction and decreases the peak concentration of the Reynolds stress. A pair of vorticity contour appears on both sides of the splitter plate.

Increasing the distance between the bottom of the splitter plate and the table surface, the flow control increased in **Figures 4.42, 4.43, 4.44, 4.45, 4.46 and 4.47.** With respect to the obtained results, as the distance between the bottom of the splitter plate and the table surface increases, it is seen that streamline elongates. Also, as the distance between the bottom of the splitter plate and the table surface increases, it is seen that wake flow region and Reynolds shear stress increase in Figure 4.47. It is seen that vorticity contours were symmetrical at heights of 17.5 mm and 22.5 mm, negative vorticity contours elongate in Figure 4.43.

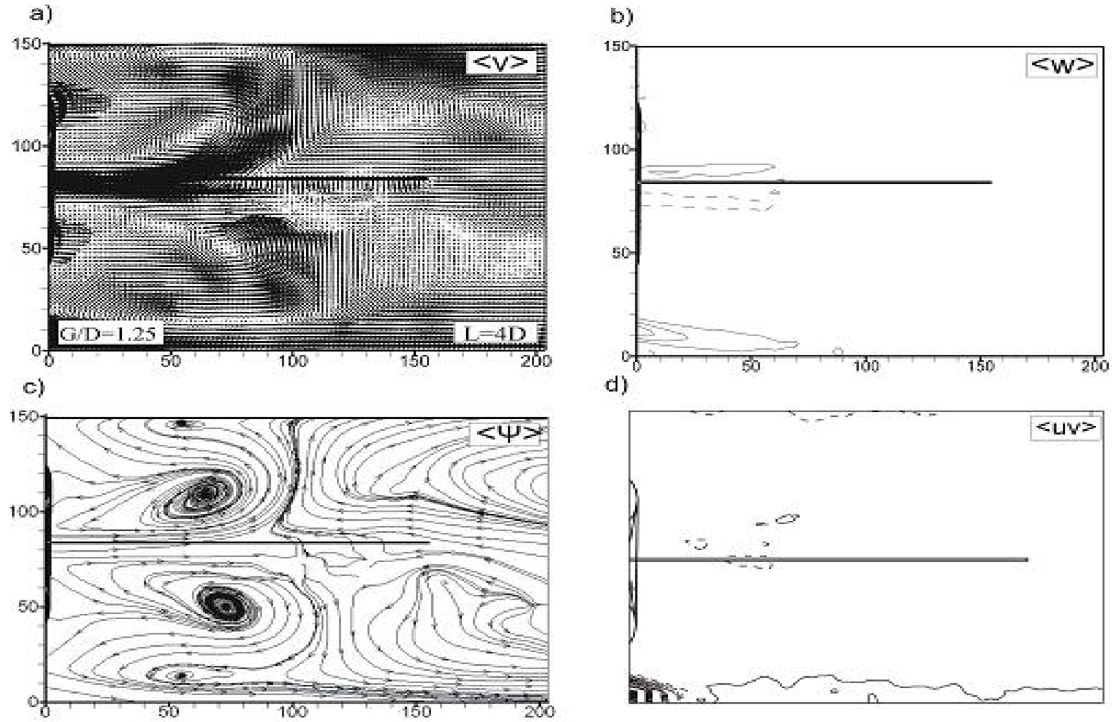

Figure 4.42. Flow characteristic which the case of plate having x=4D length and 0 point height

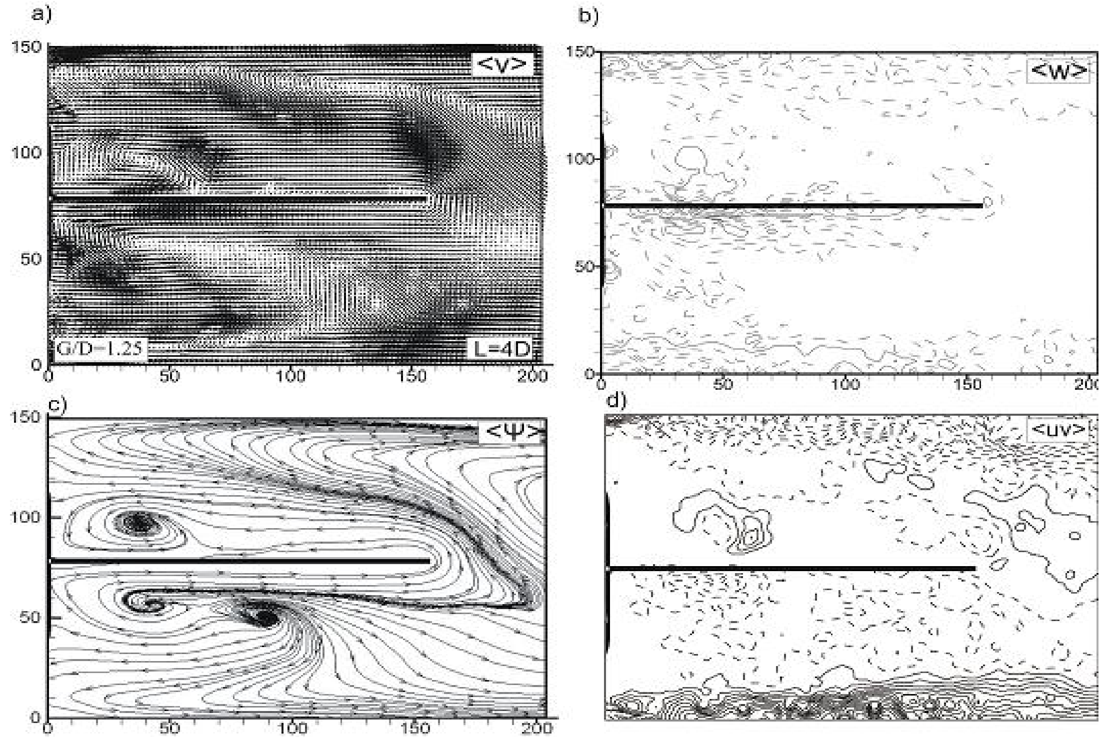

Figure 4.43. Flow characteristic which the case of plate having x=4D length and 5 mm height

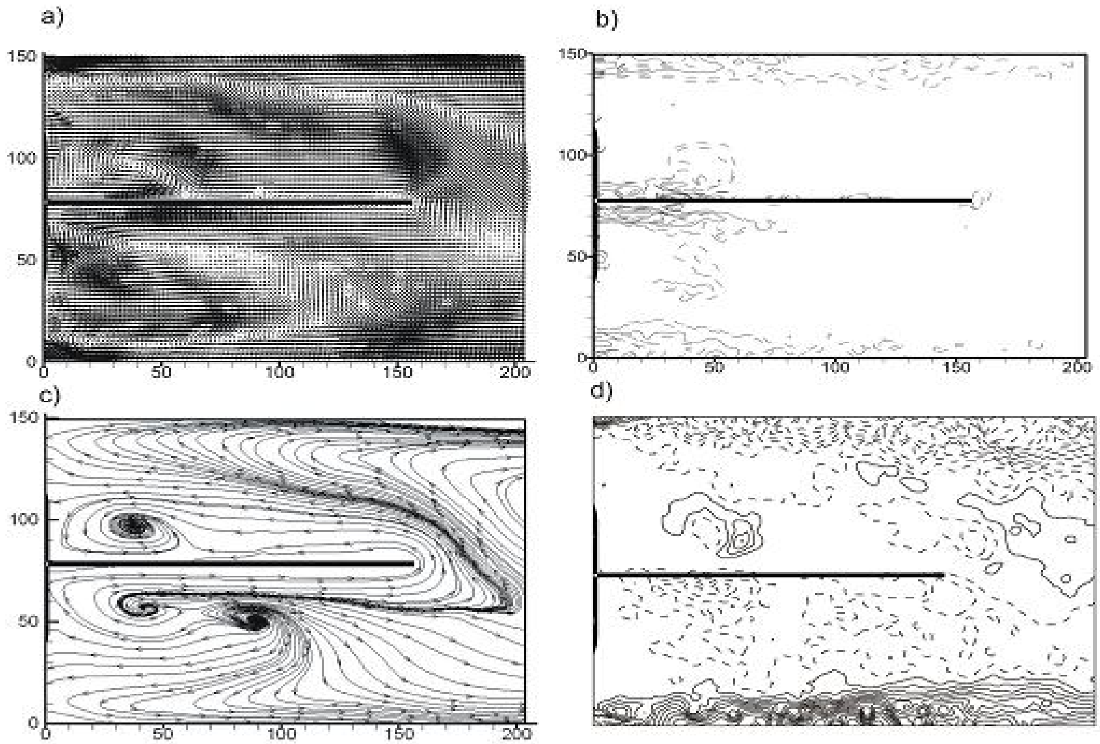

Figure 4.44. Flow characteristic which the case of plate having x=4D length and 10 mm height

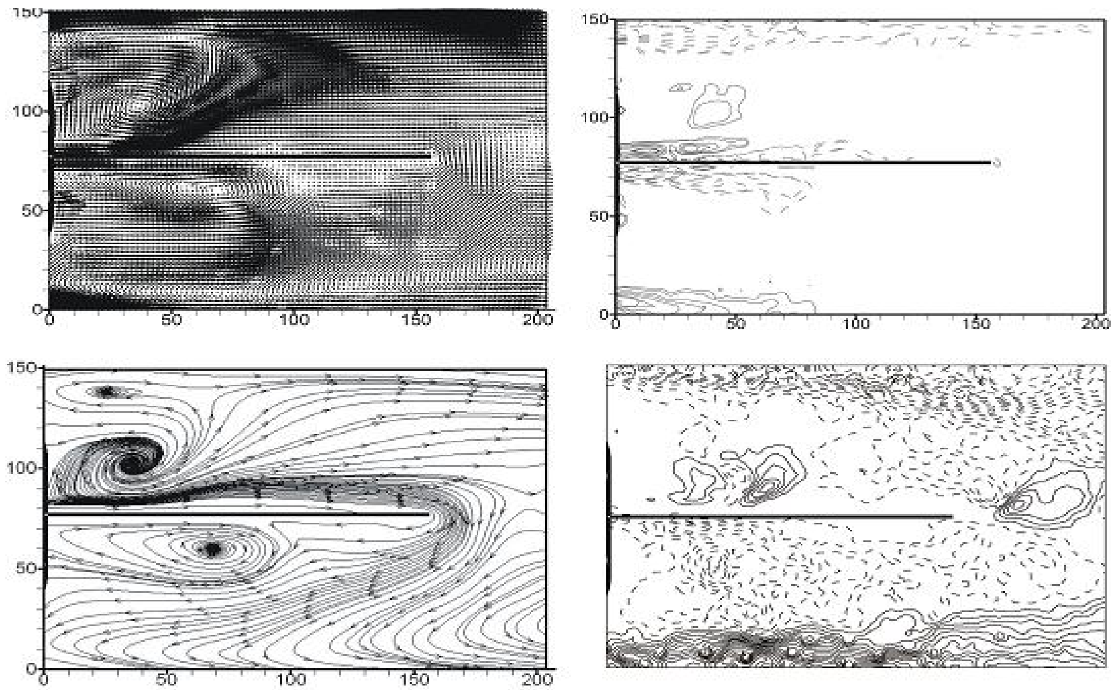

Figure 4.45. Flow characteristic which the case of plate having x=4D length and 12.5 mm height

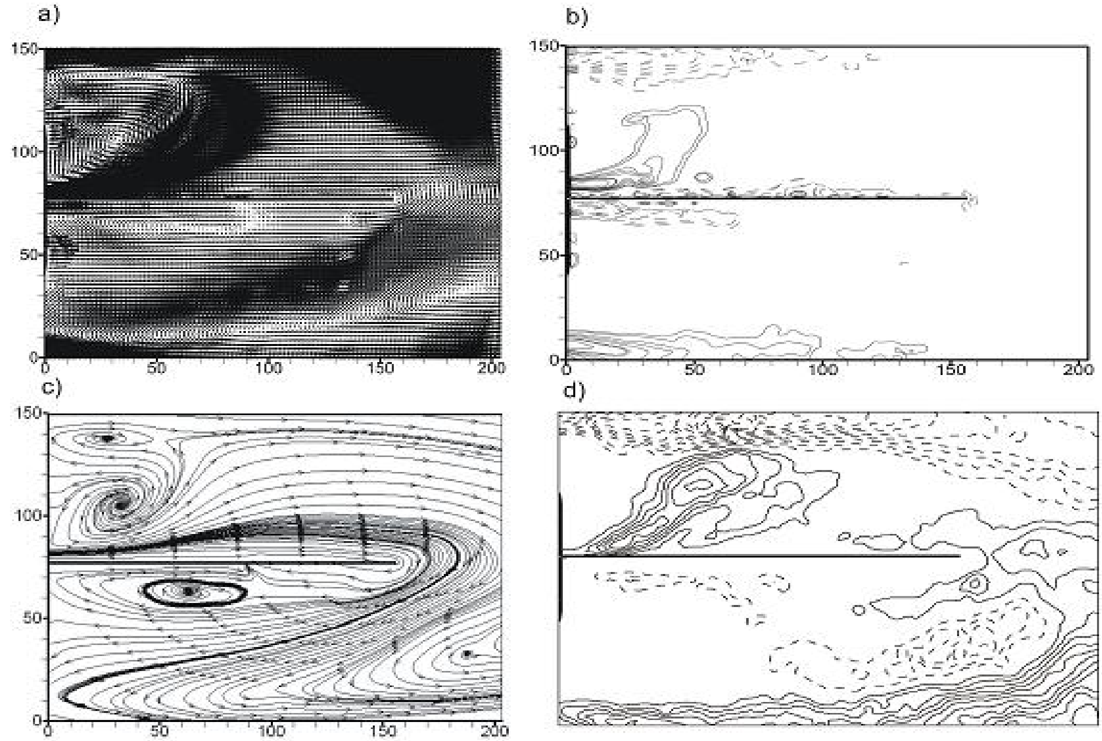

Figure 4.46. Flow characteristic which the case of plate having x=4D length and 17.5 mm height

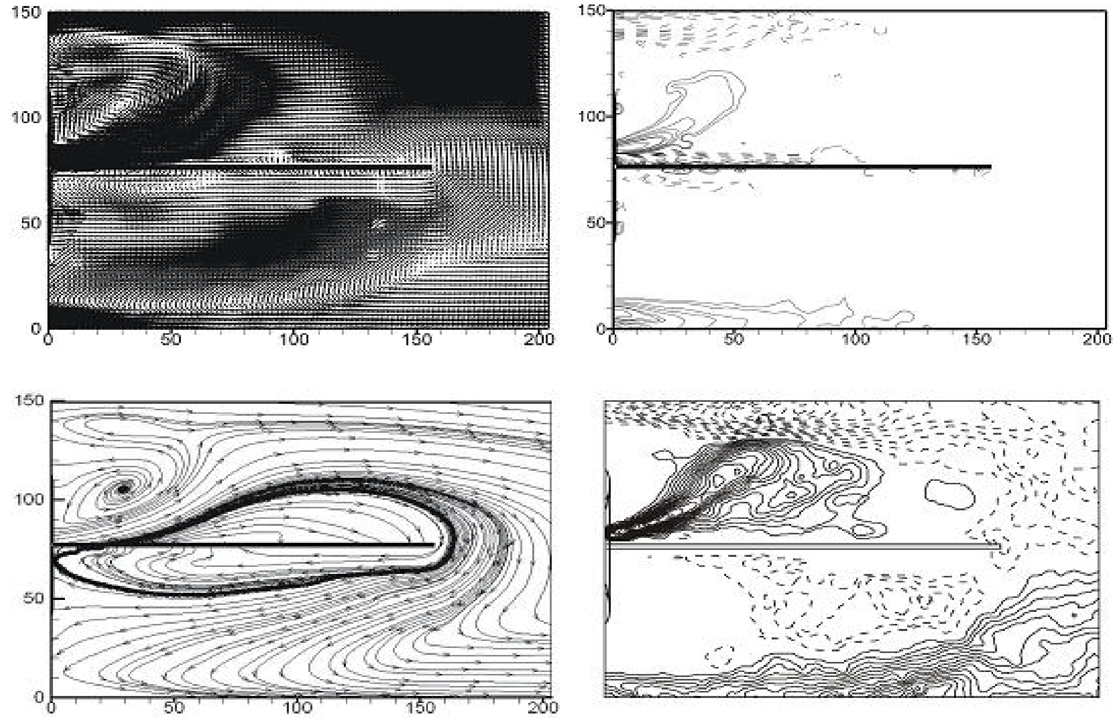

Figure 4.47. Flow characteristic which the case of plate having x=4D length and 22.5 mm height

4.3.4. Splitter Plate with 175 mm Length(x=3.5D)

The velocity vector field,(a), <v>, vorticity contours,(b), <ω>, streamline,(c),<ψ>, and normalized Reynolds stress contours,(d), <u'v'>, were shown between the Figures 4.48 and 4.53. The figures between 4.48 and 4.53 shown that splitter plate having 175 mm length has very little effect on the flow characteristics.

The vorticity contours and Reynolds shear stress concentrations show strong similarities compared with the results obtained for no splitter plate case. Briefly, it can be concluded that splitter plate which has the length of 175mm, has very little effect on the flow structure.

Peak concentration decreases slightly compared to the peak value of Reynolds shear stress obtained for x=3.5D case.

Compared to the results obtained in Figure 4.48, the intensity of the Reynolds stress decreases slightly. It is seen that vorticity contours are symmetrical in Figures 4.48, 4.49, 4.50 and 4.51,on the other hand, positive vorticity contours elongate in Figures 4.52 and 4.53. When the distance between the bottom of the splitter plate and the table surface increases, it is seen that wake flow region elongates in Figures 4.48, 4.49, 4.50 and 4.51. Also it is seen that wake flow region elongates in Figures 4.52 and 4.53. Further increase in the splitter plate length causes a increase in the peak concentration of the Reynolds stress.

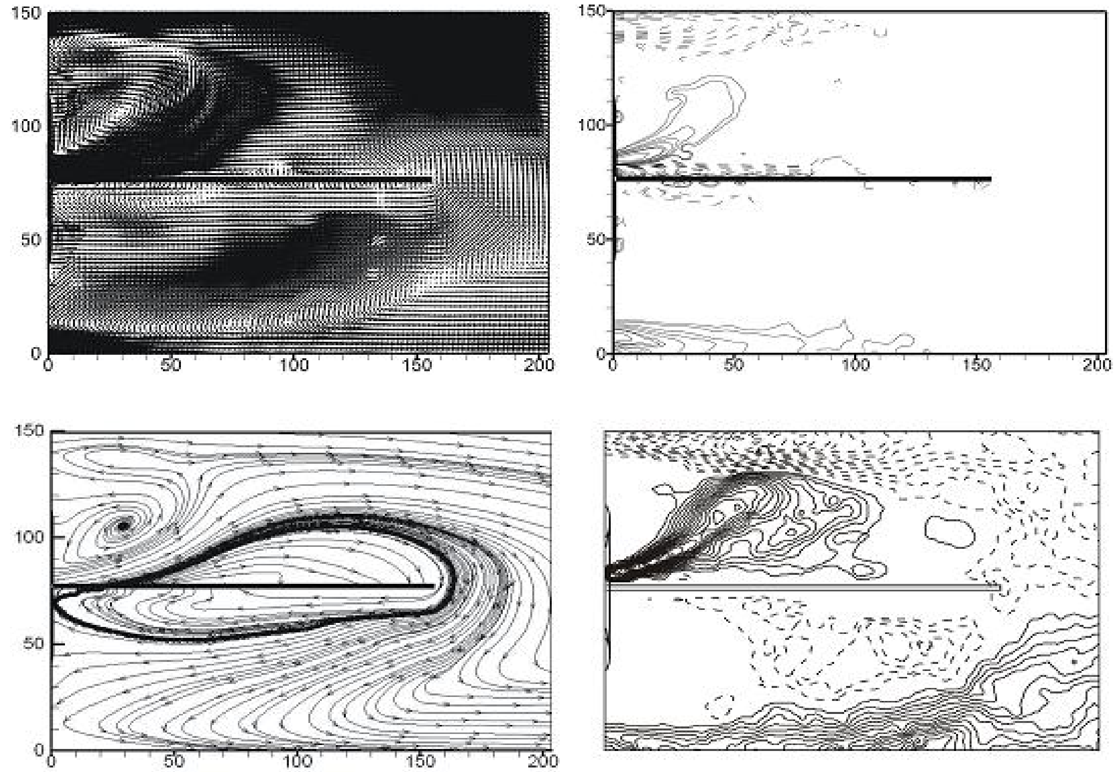

Figure 4.48. Flow characteristic which the case of plate having x=3.5D length and 0 point height

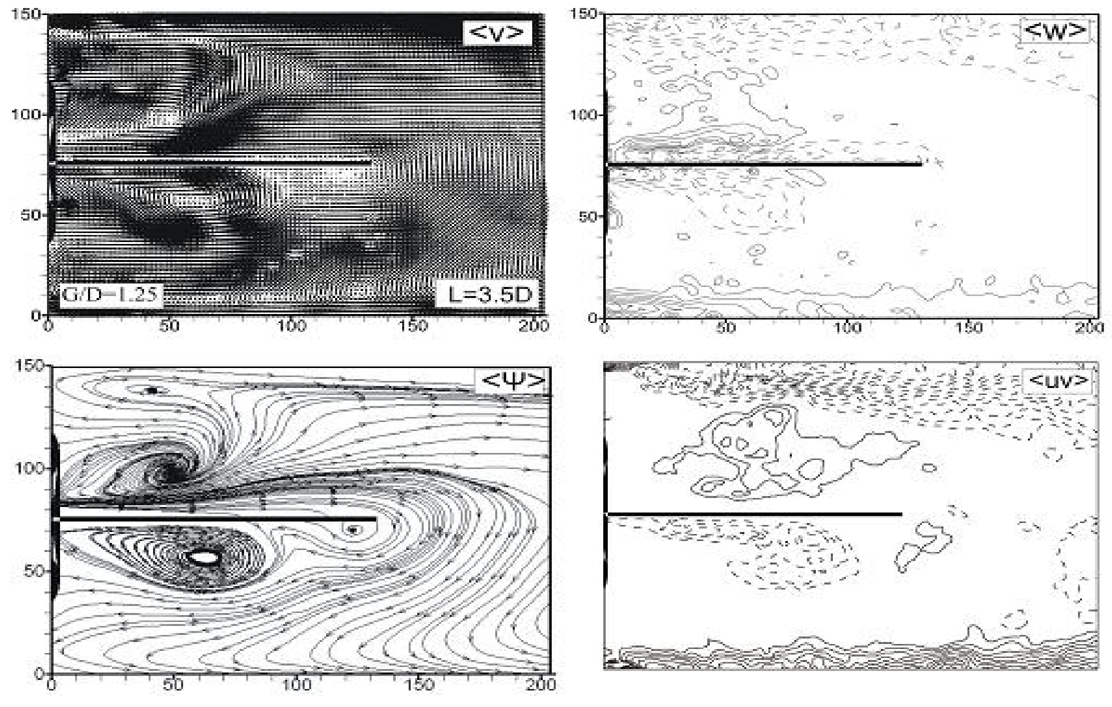

Figure 4.49. Flow characteristic which the case of plate having x=3.5D length and 5 mm height

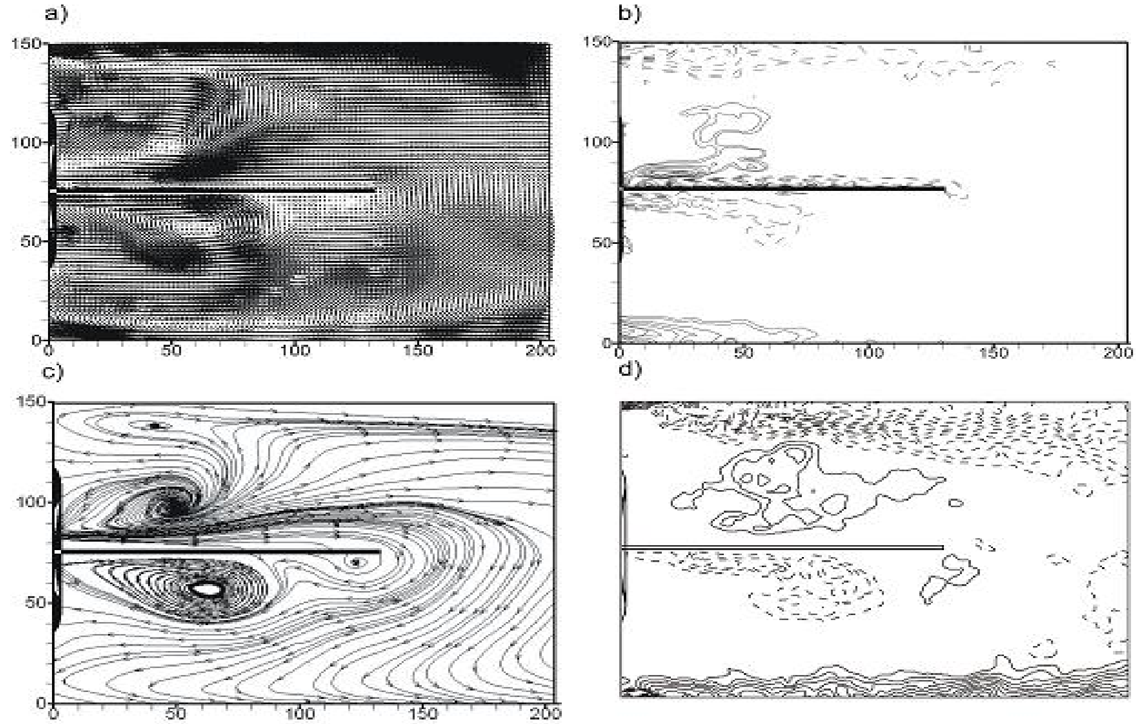

Figure 4.50. Flow characteristic which the case of plate having x=3.5D length and 10 mm height

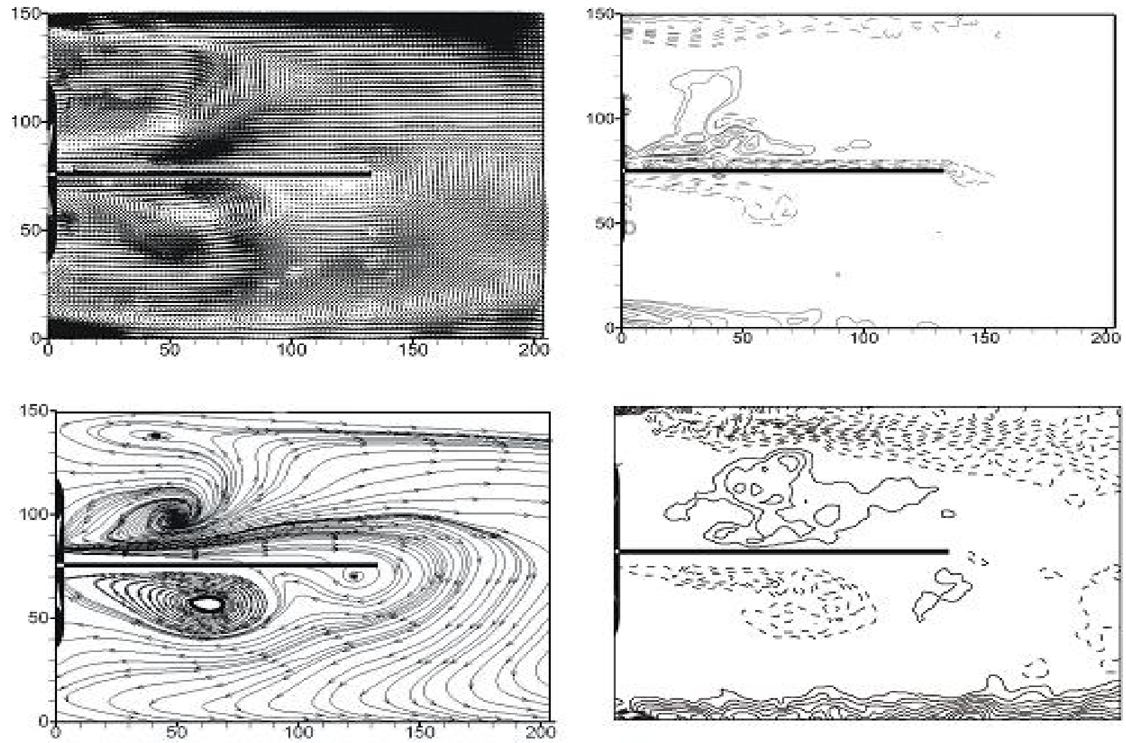

Figure 4.51. Flow characteristic which the case of plate having x=3.5D length and 12.5 mm height

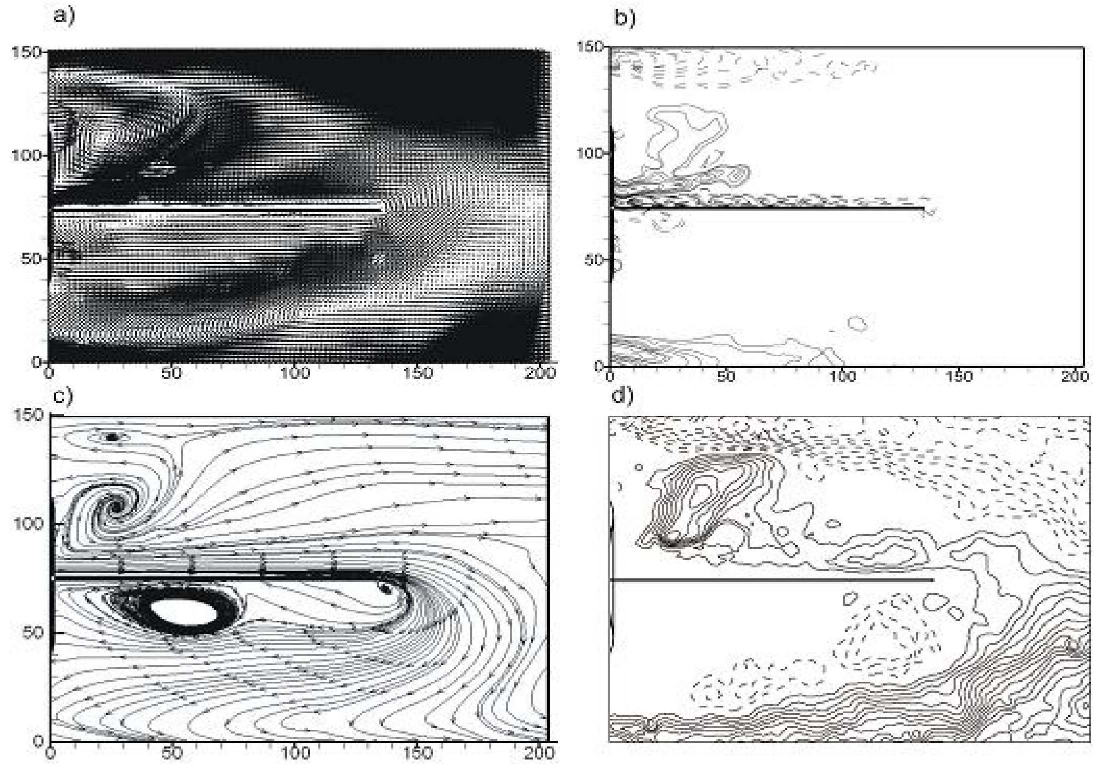

Figure 4.52. Flow characteristic which the case of plate having x=3.5D length and 17.5 mm height

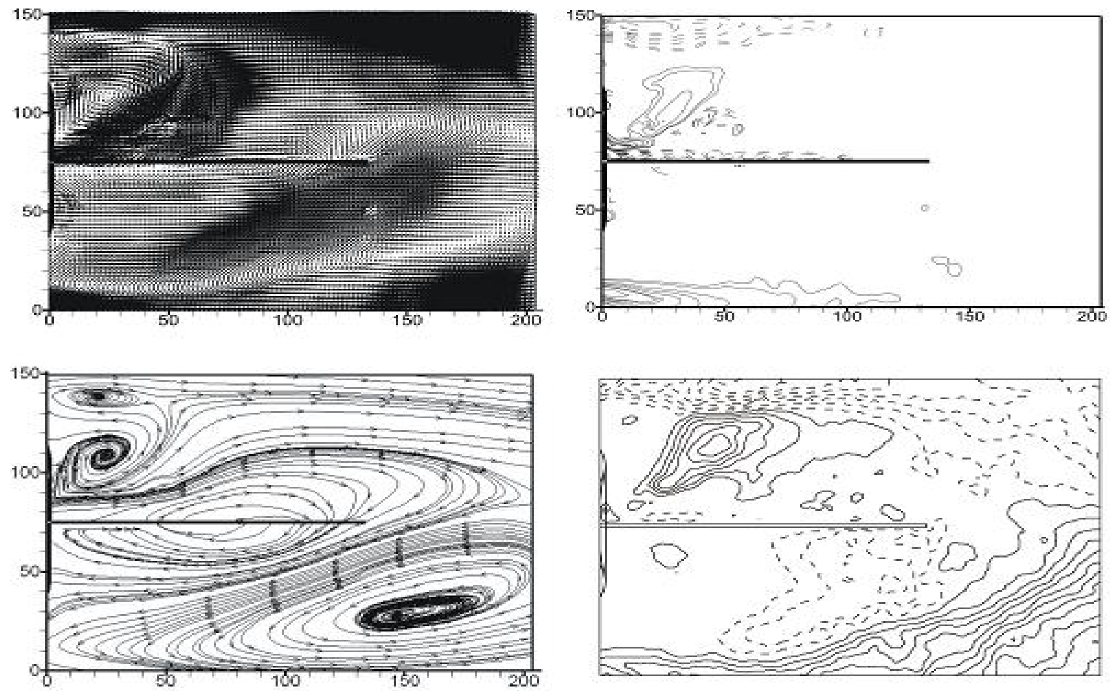

Figure 4.53. Flow characteristic which the case of plate having x=3.5D length and 22.5 mm height

4.3.5. Splitter Plate with 150 mm Length(x=3D)

The velocity vector field,(a), <v>, vorticity contours,(b), <ω>, streamline,(c),<ψ>, and normalized Reynolds stress contours,(d), <u'v'>, were shown between the figures 4.54 and 4.59. The figures between 4.54 and 4.59 it is shown that splitter plate having 150 mm length has very little effect on the flow characteristics.

It is seen that slight changes occur in the flow field until the plate length of x=3D. Here, further increase in splitter plate length, causes a decrease in the peak concentration of the Reynolds stress. Extra vorticity occurs very close to the trailing edge on both sides of the splitter plate. Afterwards, the peak concentration occurs approximately at the same location downstream of the cylinders.

At this splitter plate length, upper cylinder's positive Reynolds shear stress layer smaller than lower cylinder's negative Reynolds shear stress were in figures 4.54, 4.55, 4.56 and 4.57. After this plate height, symmetrical structure occurs.

When the distance between the bottom of the splitter plate and the table surface increases, it is seen that wake flow region, reynolds shear stress and streamline were reduced.

When length of the splitter plate is 3D, it is seen that the effect on the flow structure was controlled better than length of splitter plate D.

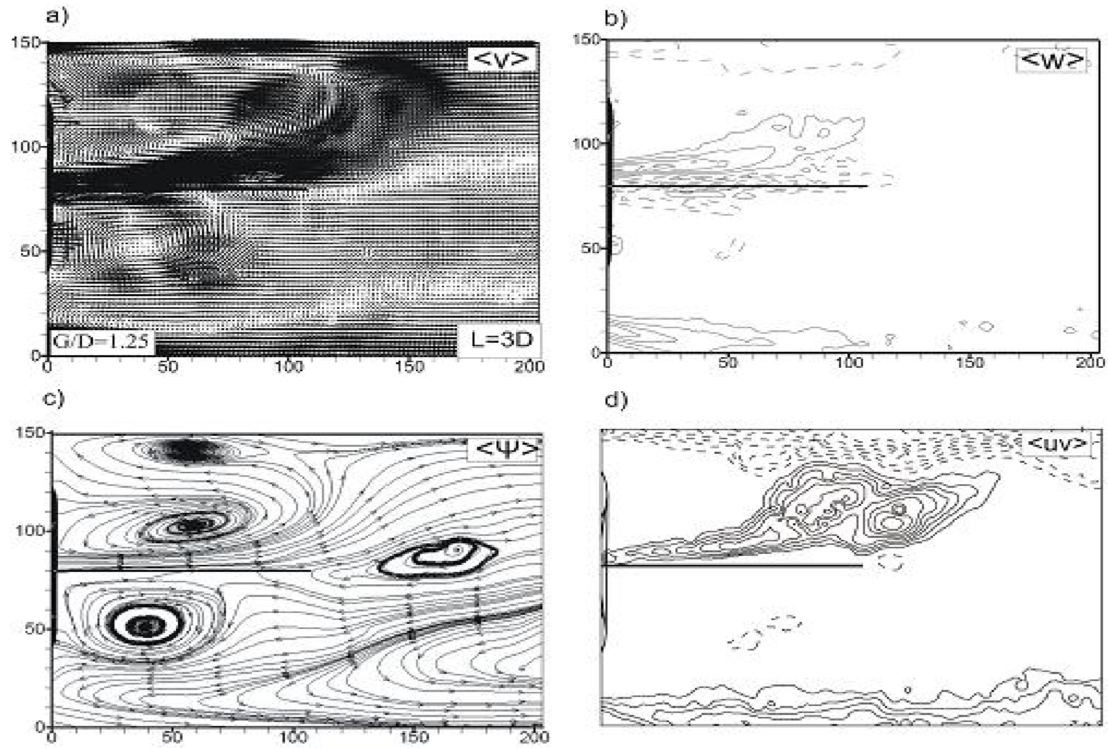

Figure 4.54. Flow characteristic which the case of plate having x=3D length and 0 point height

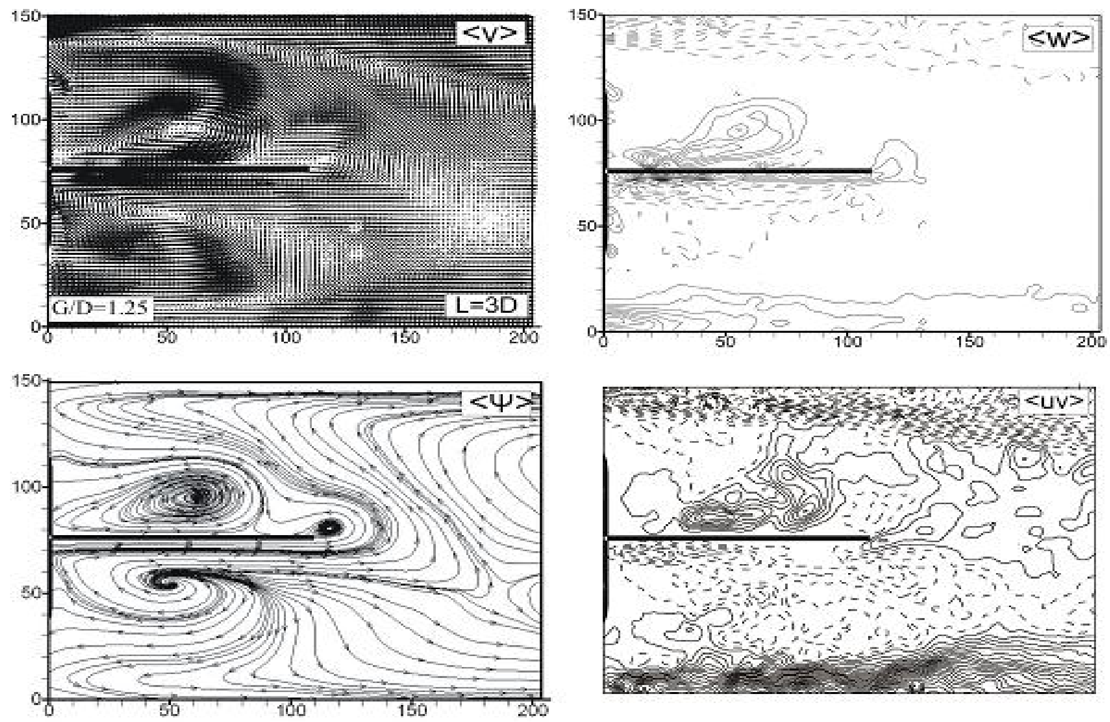

Figure 4.55. Flow characteristic which the case of plate having x=3D length and 5 mm height

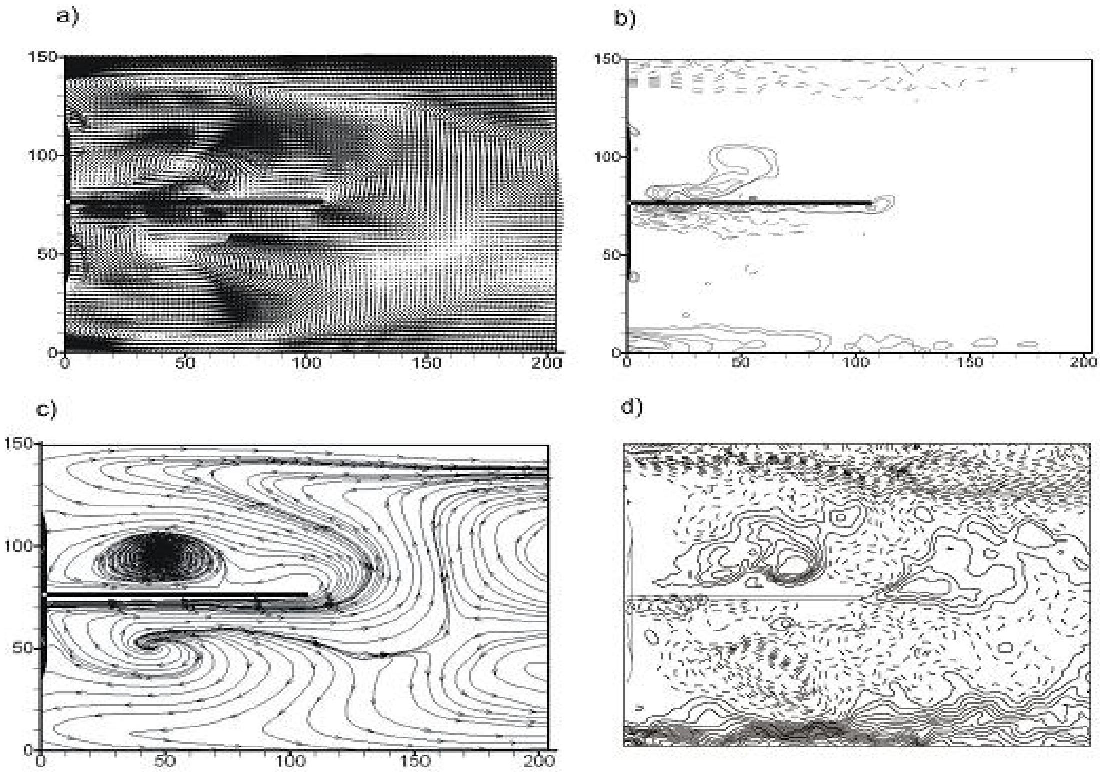

Figure 4.56. Flow characteristic which the case of plate having x=3D length and 10 mm height

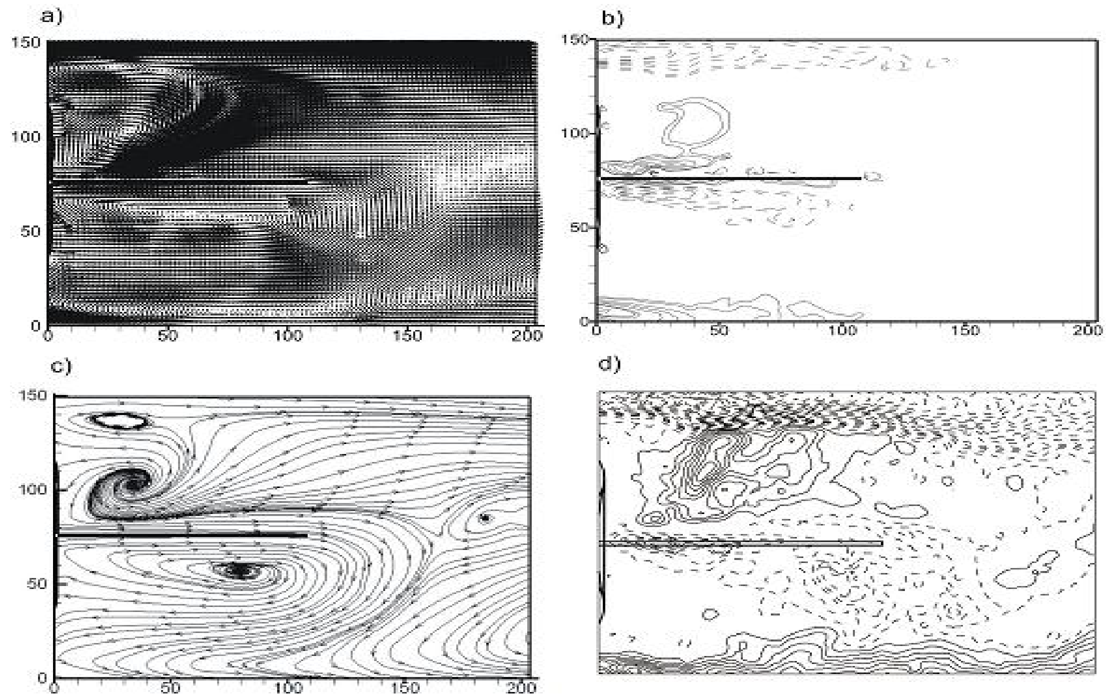

Figure 4.57. Flow characteristic which the case of plate having x=3D length and 12.5 mm height

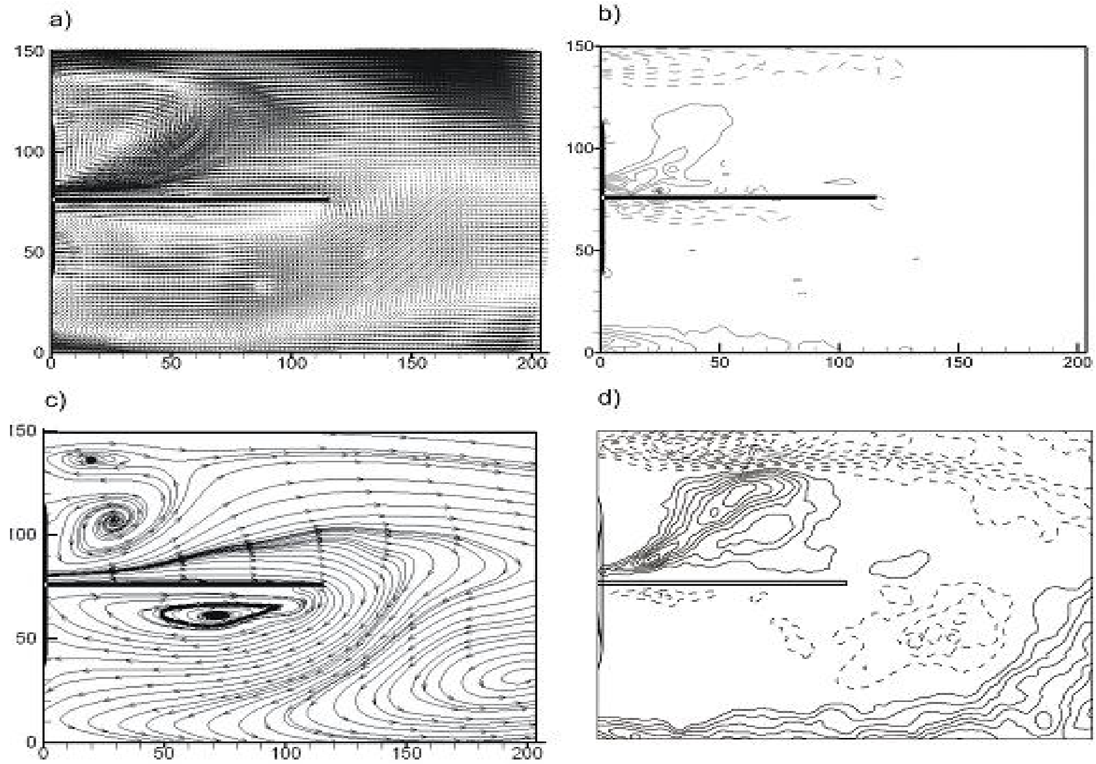

Figure 4.58. Flow characteristic which the case of plate having x=3D length and 17.5 mm height

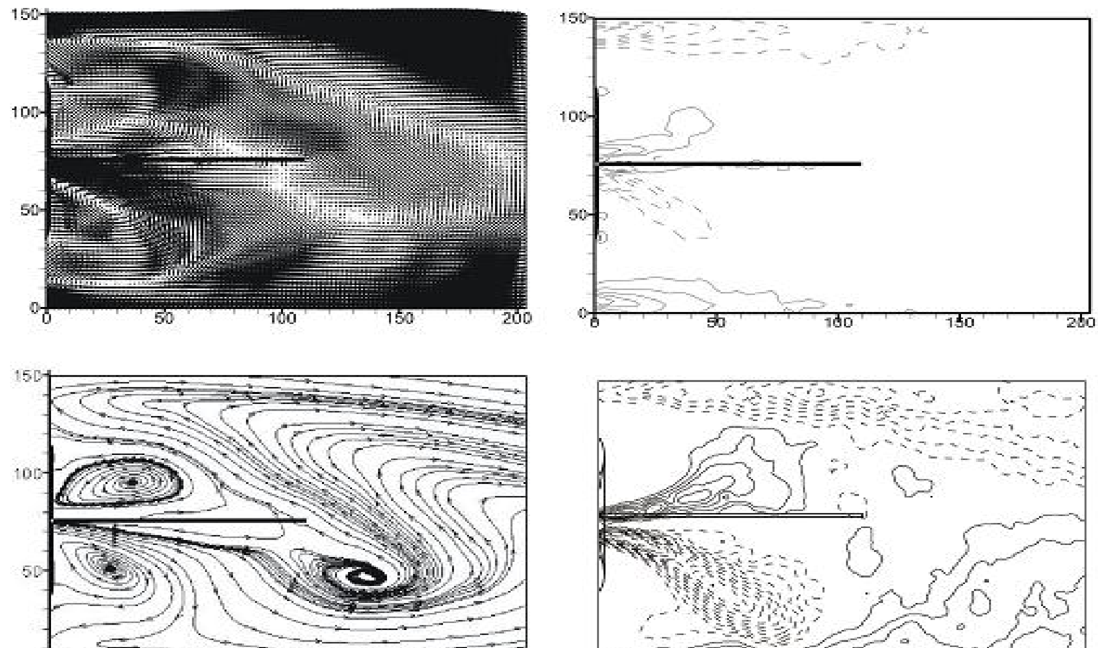

Figure 4.59. Flow characteristic which the case of plate having x=3D length and 22.5 mm height

4.3.6. Splitter Plate with 125 mm Length (x=2.5D)

The velocity vector field,(a), <v>, vorticity contours,(b), <ω>, streamline, (c), <ψ>, and normalized Reynolds stress contours, (d), <u'v'>, were shown between the figures 4.60 and 4.65. The figures between 4.60 and 4.65 that splitter plate having 125 mm length has effect on the flow characteristics.

Figure 4.60 depict the flow structures close to the bottom surface for the gap ratio of 1.25 as a function of splitter plate length. Slight changes occur in the flow field up to the plate length of x=2.5D. After this plate length, symmetrical structure occurs. Further increase in splitter plate length again causes a decrease in peak concentration of the Reynolds stress. Pair of extra vorticity occurs very close to the trailing edge of the splitter plate. The peak concentration occurs approximately at the same location downstream of the cylinders. **Figure 4.60** shows the flow characteristic for G/D=1.25 close to the free-surface elevation as a function of splitter plate lengths compared to the results obtained at the other five elevations. However, similar flow structures were obtained. Symmetrical and optimum flow structure was obtained after the plate length of x=2.5D.

At this splitter plate length, upper cylinder’s positive Reynolds shear stress layer was smaller than lower cylinder’s negative Reynolds shear stress shown in figure 4.60. After this plate height, symmetrical structure occurs.

Briefly, when the distance between the bottom of the splitter plate and the table surface increases, wake flow region, reynolds shear stress and streamlines are reduced.

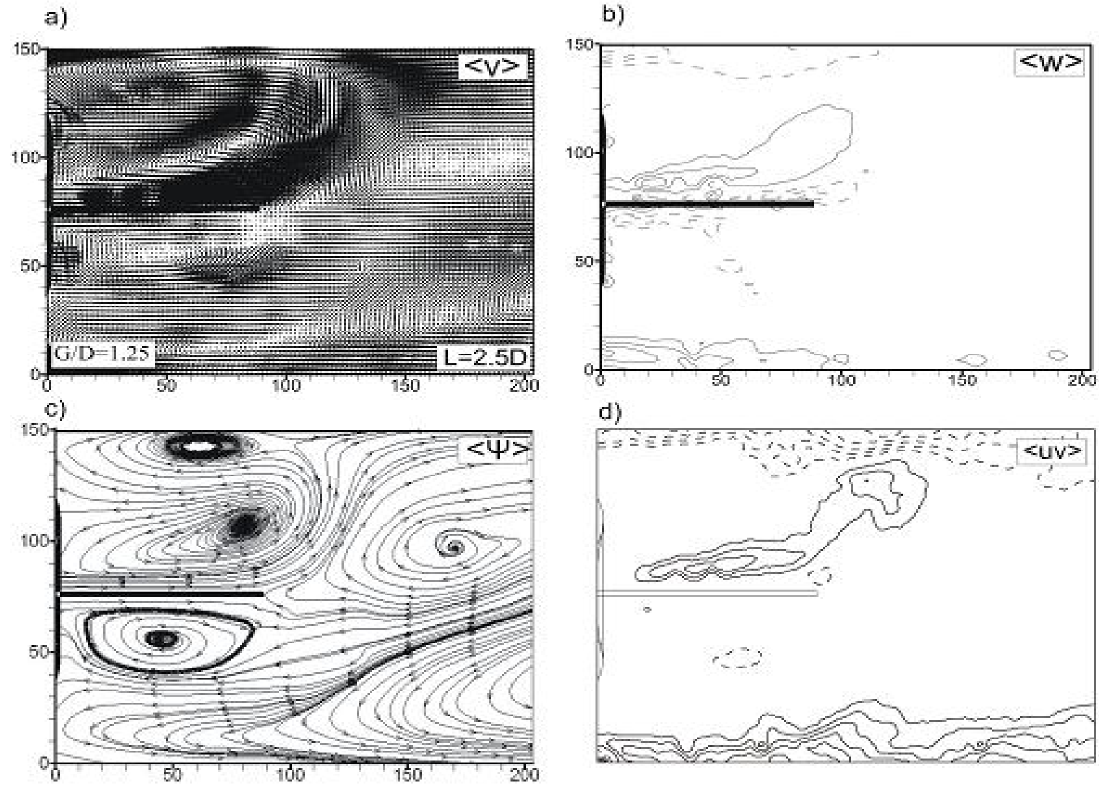

Figure 4.60. Flow characteristic which the case of plate having x=2.5D length and 0 point height

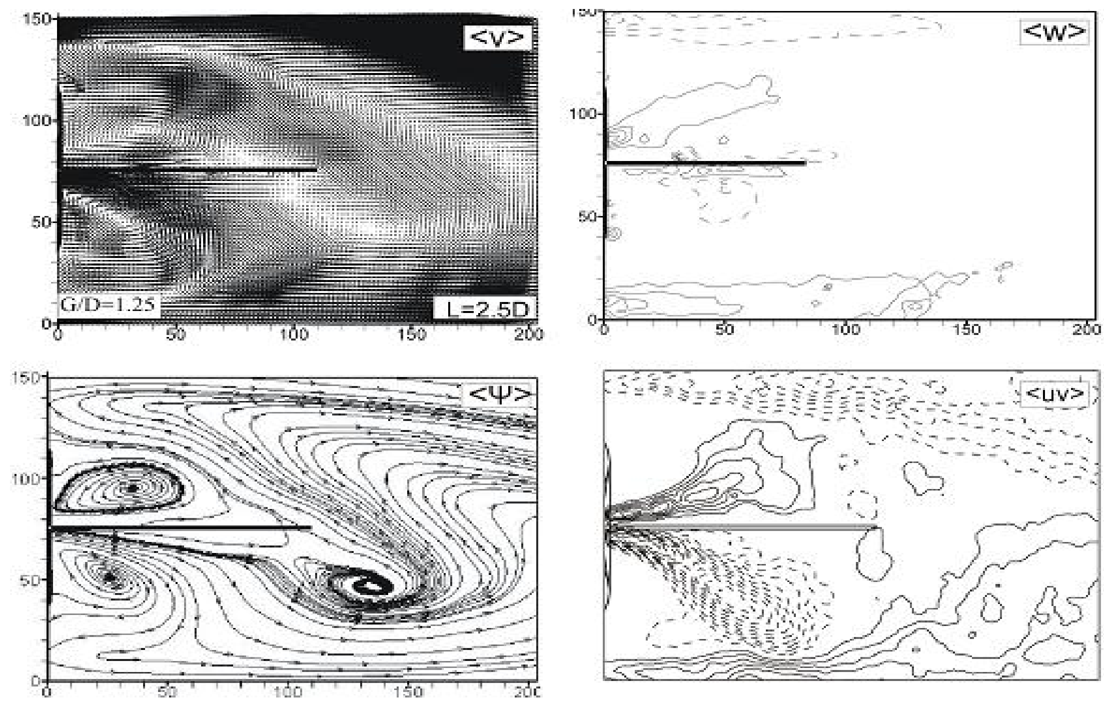

Figure 4.61. Flow characteristic which the case of plate having x=2.5D length and 5 mm height

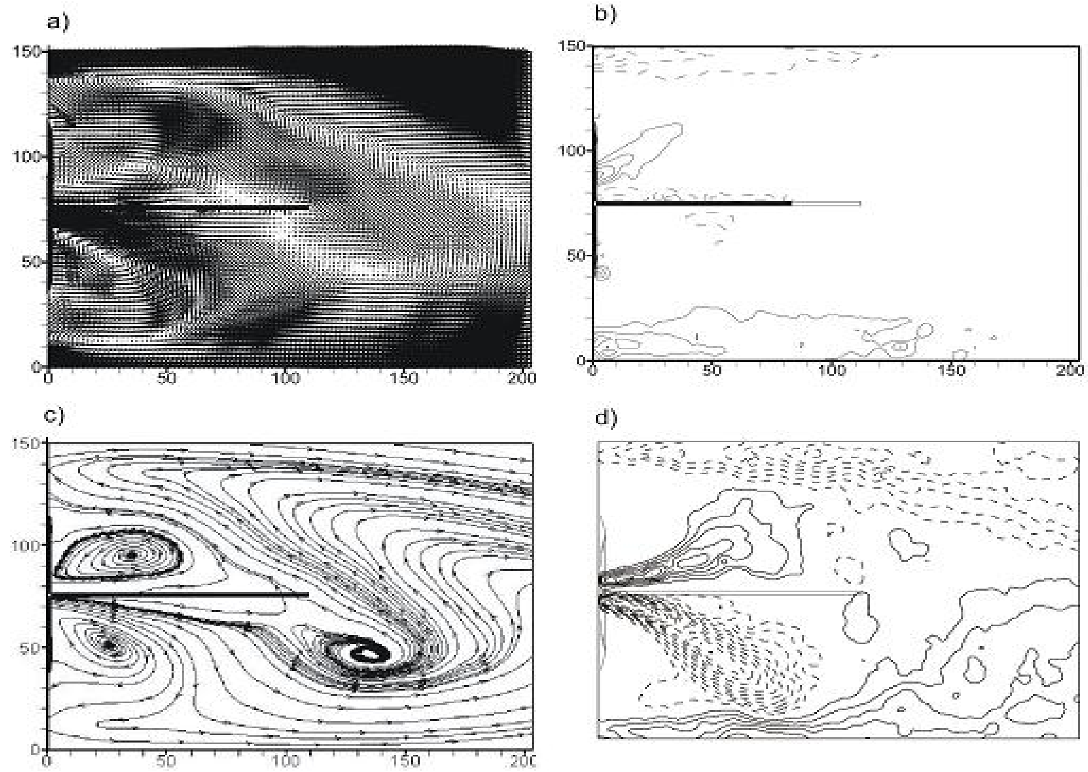

Figure 4.62. Flow characteristic which the case of plate having x=2.5D length and 10 mm height

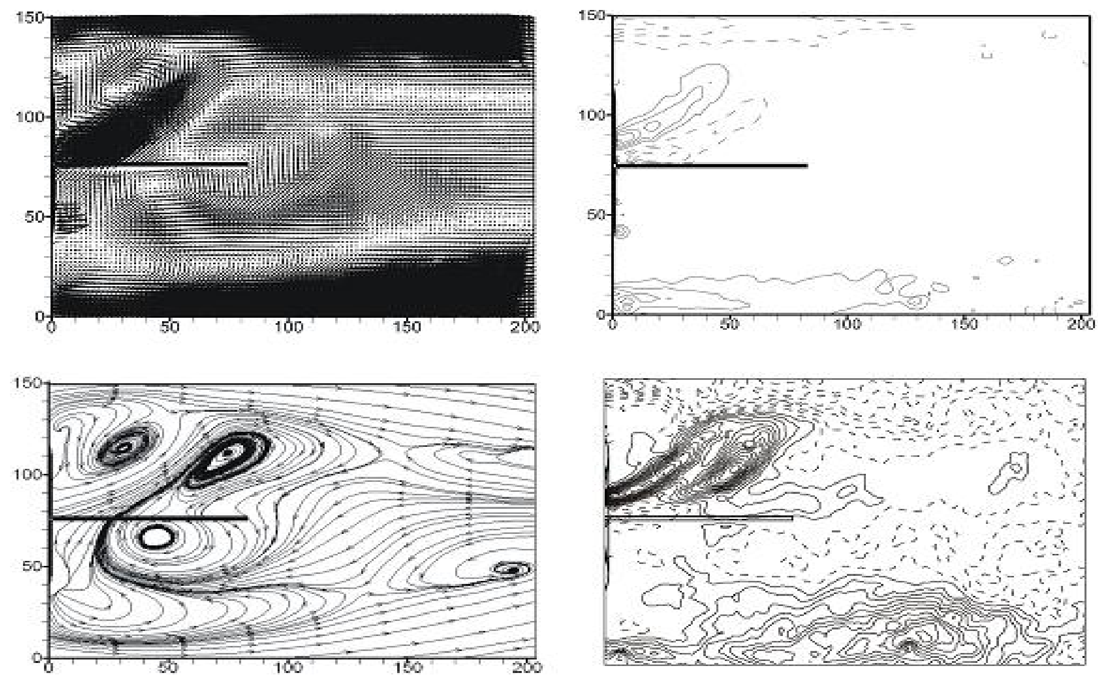

Figure 4.63. Flow characteristic which the case of plate having x=2.5D length and 12.5 mm height

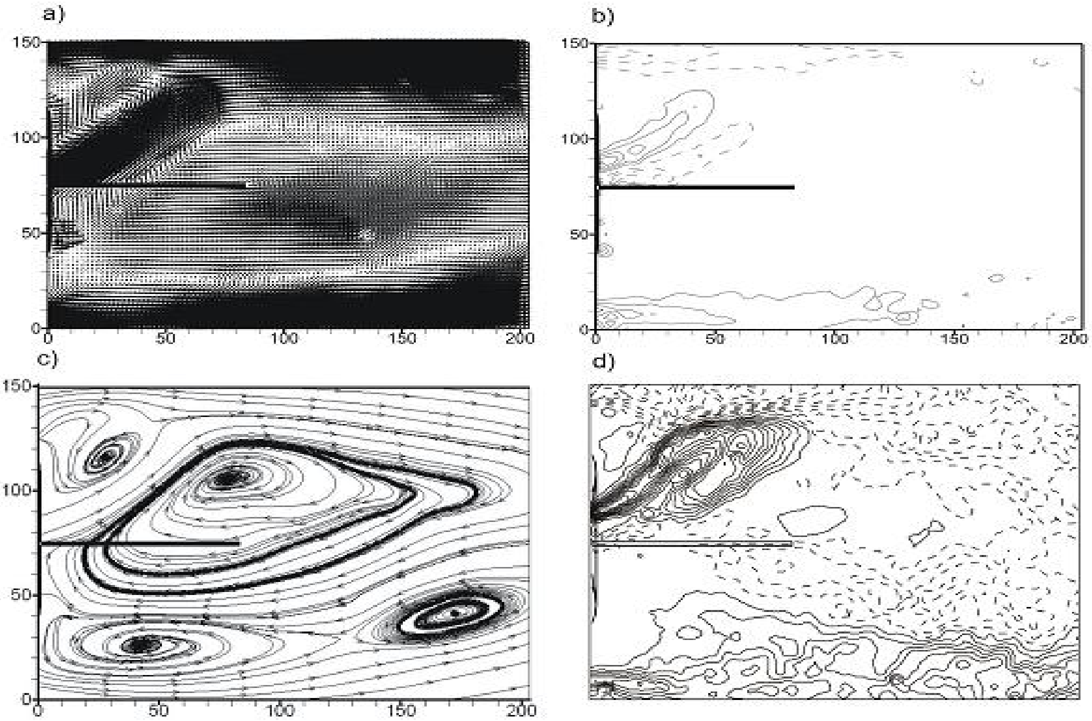

Figure 4.64. Flow characteristic which the case of plate having x=2.5D length and 17.5 mm height

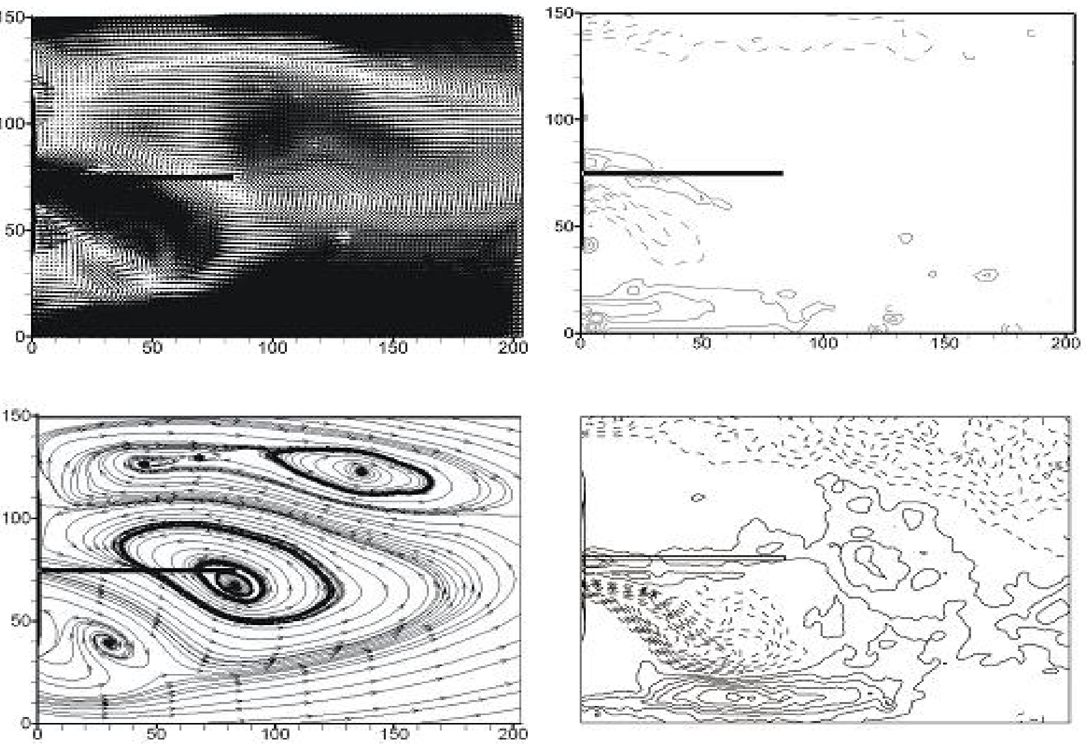

Figure 4.65. Flow characteristic which the case of plate having x=2.5D length and 22.5 mm height

4.3.7. Splitter Plate with 100 mm Length (x=2D)

The vorticity contours and Reynolds shear stress concentrations obtained for this case present strong similarities compared with the results obtained for no splitter plate case. Briefly, it can be concluded that splitter plate which has the length of 100 mm, has very little effect on the flow structure. Peak concentration decreases slightly compared to the peak value of Reynolds shear stress obtained for x=2D case.

Almost symmetrical flow structure is obtained downstream of the side-by-side circular cylinders. Jet flow was not deflected towards any cylinder's side. Compared to the no-plate case and x=D and 2D cases, the peak concentration of Reynolds stress decreases considerably. Especially, two Reynolds shear stress clusters between shear layers loose their strengths with the presence of splitter plate.

Compared to the results obtained, when the distance between the bottom of the splitter plate and the table surface increases, vorticity contours and streamlines reduce. It is seen that Reynolds shear stress reduces in Figure 4.66, Reynolds shear stress was symmetrical in Figures 4.67, 4.68, 4.69, 4.70 and 4.71, too.

Reynolds stress concentrations get smaller significantly compared to the no-plate case. The intensity of the Reynolds stress concentrations decreases as well as the location of peak point. Reynolds stress concentrations were approximately near the trailing edge of the plate.

The length of the wake region was nearly the same compared to the no-plate case and the length of the wake region is approximately one cylinder diameter. The negative and positive layers incline towards each other after the cylinder. The transverse spatial extent of each layer remains relatively narrow. Small scale vorticity layers occur both sides of the plate. Because of the Karman vortex street to the leading edge of the plate.

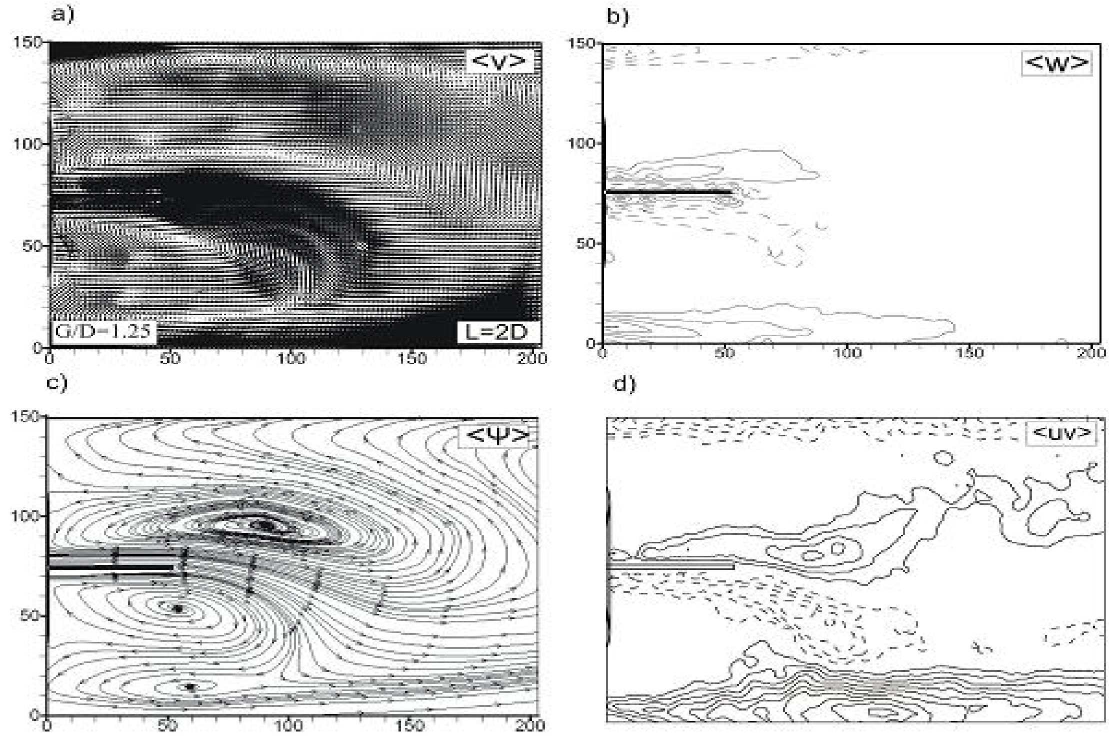

Figure 4.66. Flow characteristic which the case of plate having x=2D length and 0 point height

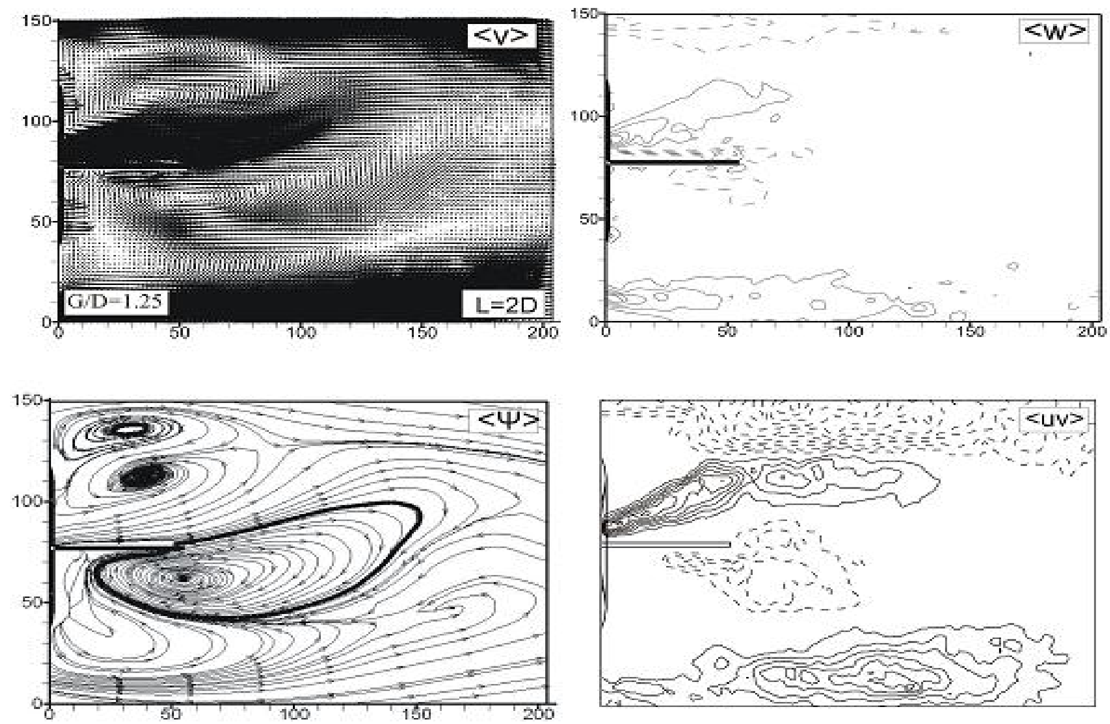

Figure 4.67. Flow characteristic which the case of plate having x=2D length and 5 mm height

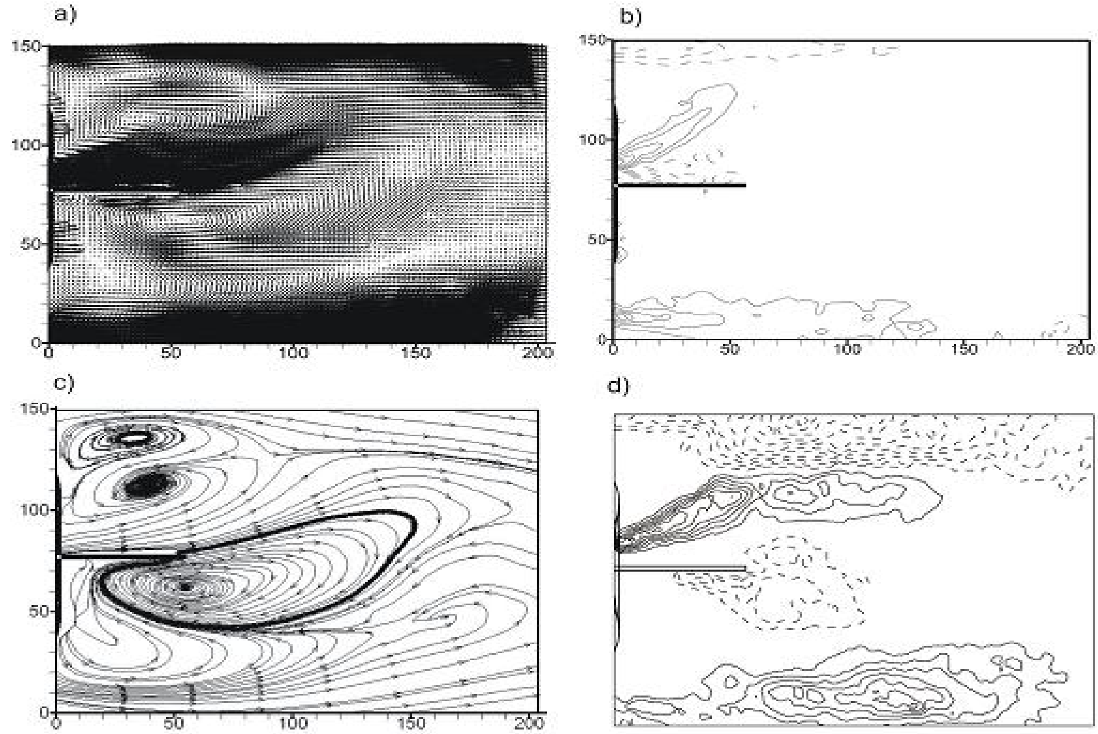

Figure 4.68. Flow characteristic which the case of plate having x=2D length and 10 mm height

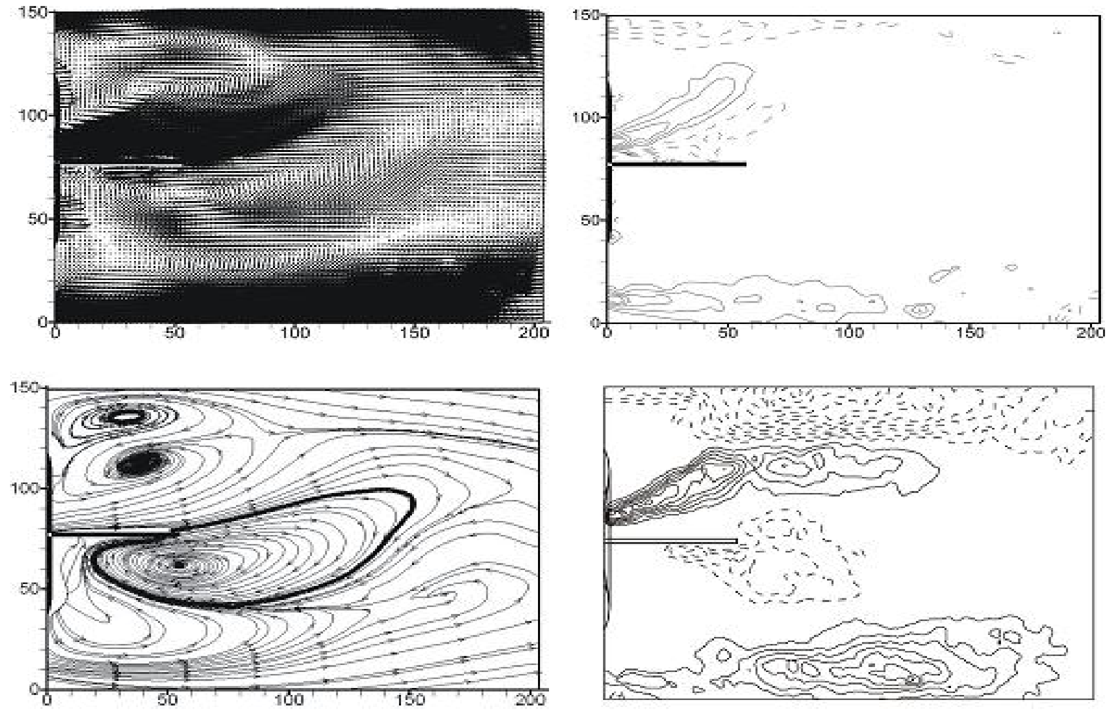

Figure 4.69. Flow characteristic which the case of plate having x=2D length and 12.5 mm height

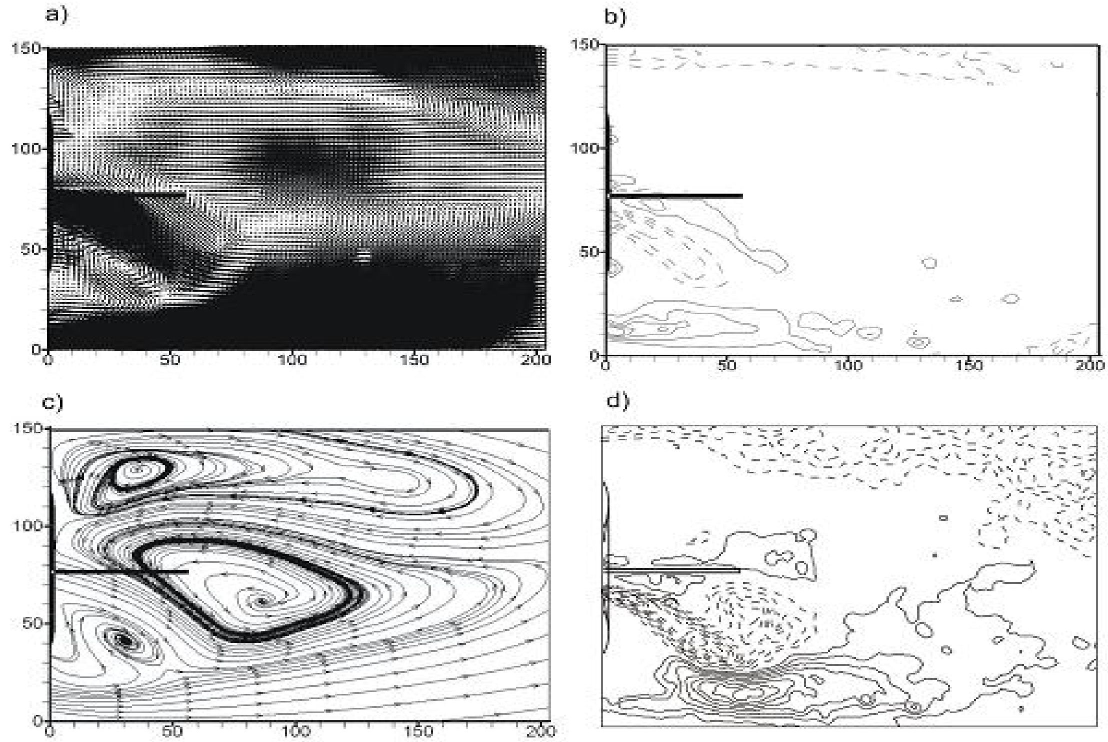

Figure 4.70. Flow characteristic which the case of plate having x=2D length and 17.5 mm height

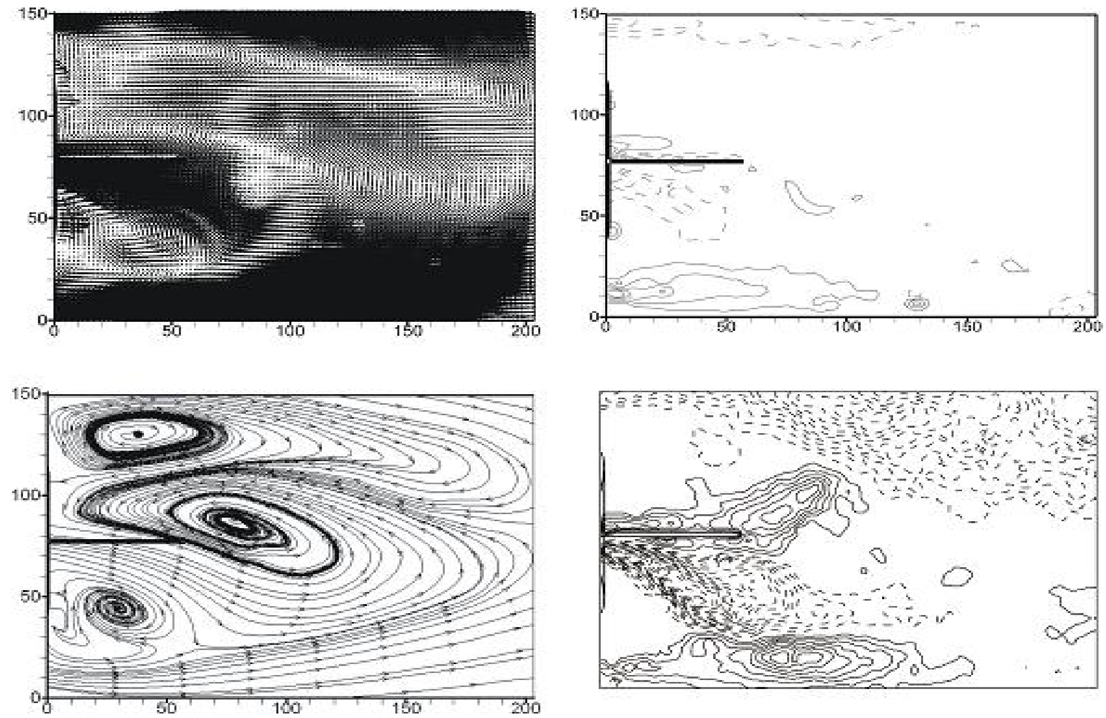

Figure 4.71. Flow characteristic which the case of plate having x=2D length and 22.5 mm height

4.3.8. Splitter Plate with 75 mm Length (x=1.5D)

The velocity vector field,(a), <v>, while second represent vorticity contours,(b), <ω>, streamline, (c), <ψ>, and normalized Reynolds stress contours,(d), <u'v'>, were shown between the figures 4.72 and 4.77. Splitter plate has 75mm (L=1.5D) length. At these experiments the distances between the bottom of the splitter plate and the table surface are taken as 0 mm, 5 mm, 10 mm, 12.5 mm, 17.5 mm and 22.5 mm.

The vorticity contours and Reynolds shear stress concentrations obtained for this case present strong similarities compared with the results obtained for no splitter plate case. Briefly, it can be concluded that splitter plate which has the length of 75mm, has effect on the flow structure. Peak concentration decreases slightly compared to the peak value of Reynolds shear stress obtained for x=1.5D case.

When the distance between the bottom of the splitter plate and the table surface increases, it is seen that streamline and vector field are reduced and the effect on the flow structure is controlled better for the splitter plate length of D.

For these cases, the vorticity contours are horizontal and they extend along the streamwise direction. For G/D=1.25 case the negative and positive vorticity layers get closer to each other for the heights of 10 mm, 12.5 mm and 17.5mm. And the Reynolds stress concentrations decreases compared to the no plate case. When the images at 0 mm, 5 mm and 22.5 mm the distance between the bottom of the splitter plate and the table surface cases are inspected, it is seen that the flow structure is similar with no-plate case. Full control of vortex shedding behind the cylinder is seen clearly for all cases. The wake region gets longer along the downstream. The negative and positive vorticity layers are horizontal and they do not incline towards each other. They extend causes to the elongation of streamline at the streamwise direction. The Reynolds stress concentrations decrease significantly compared to the no-plate case.

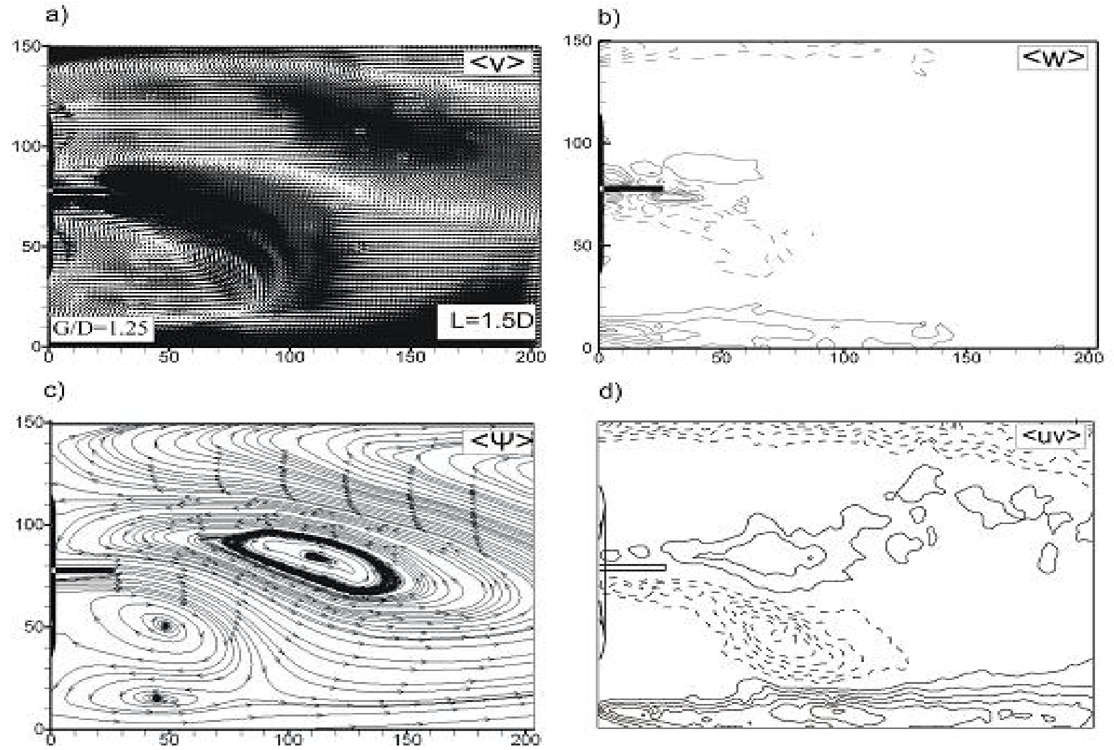

Figure 4.72. Flow characteristic which the case of plate having x=1.5D length and 0 point height

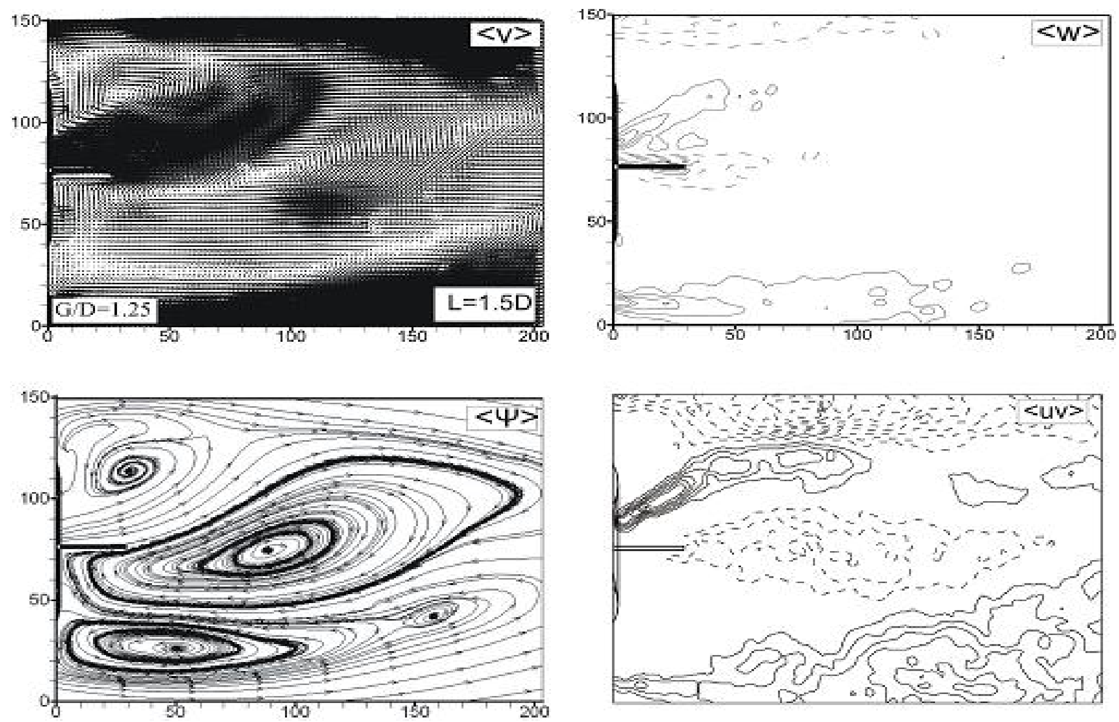

Figure 4.73. Flow characteristic which the case of plate having x=1.5D length and 5 mm height

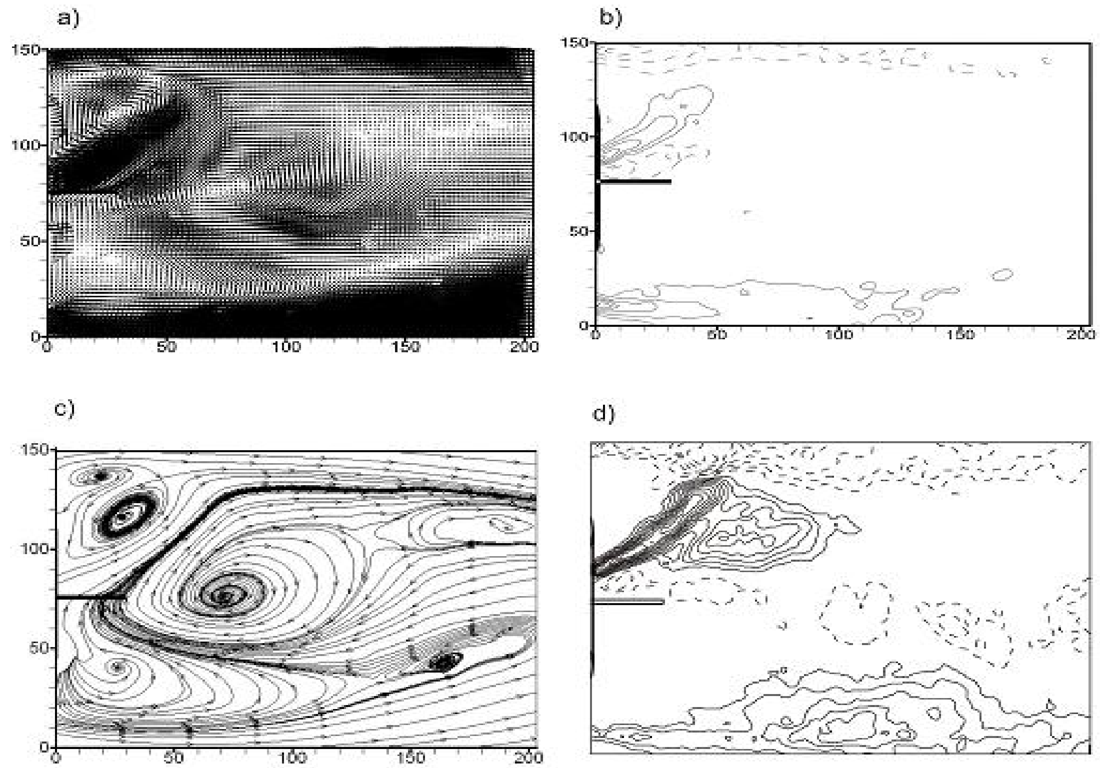

Figure 4.74. Flow characteristic which the case of plate having x=1.5D length and 10 mm height

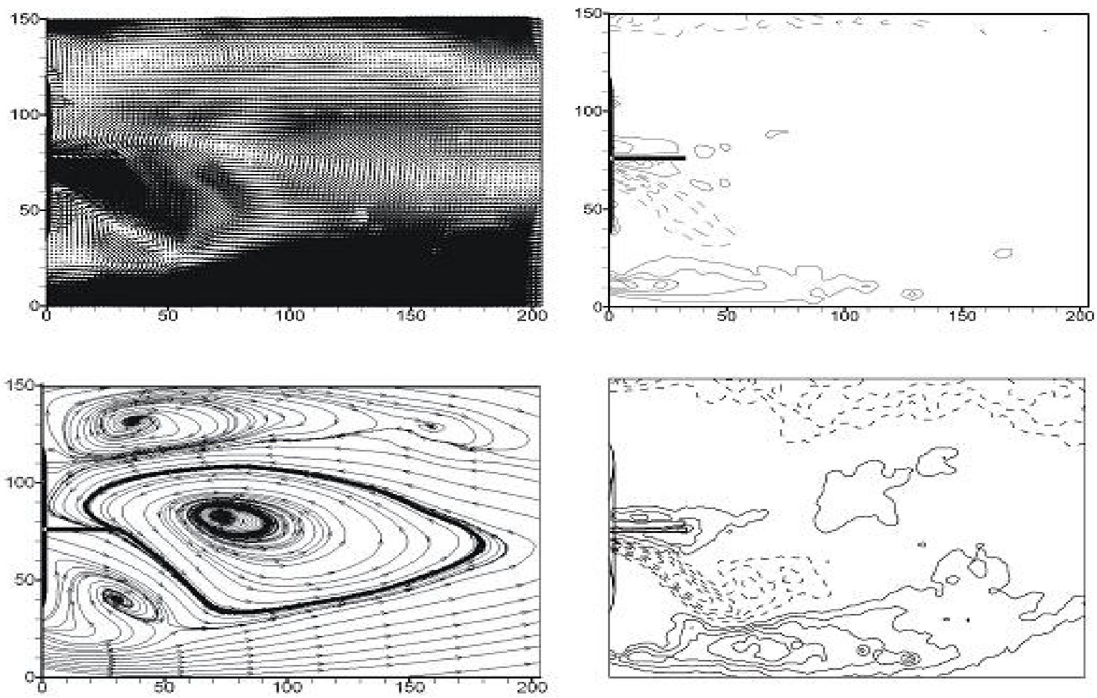

Figure 4.75. Flow characteristic which the case of plate having x=1.5D length and 12.5 mm height

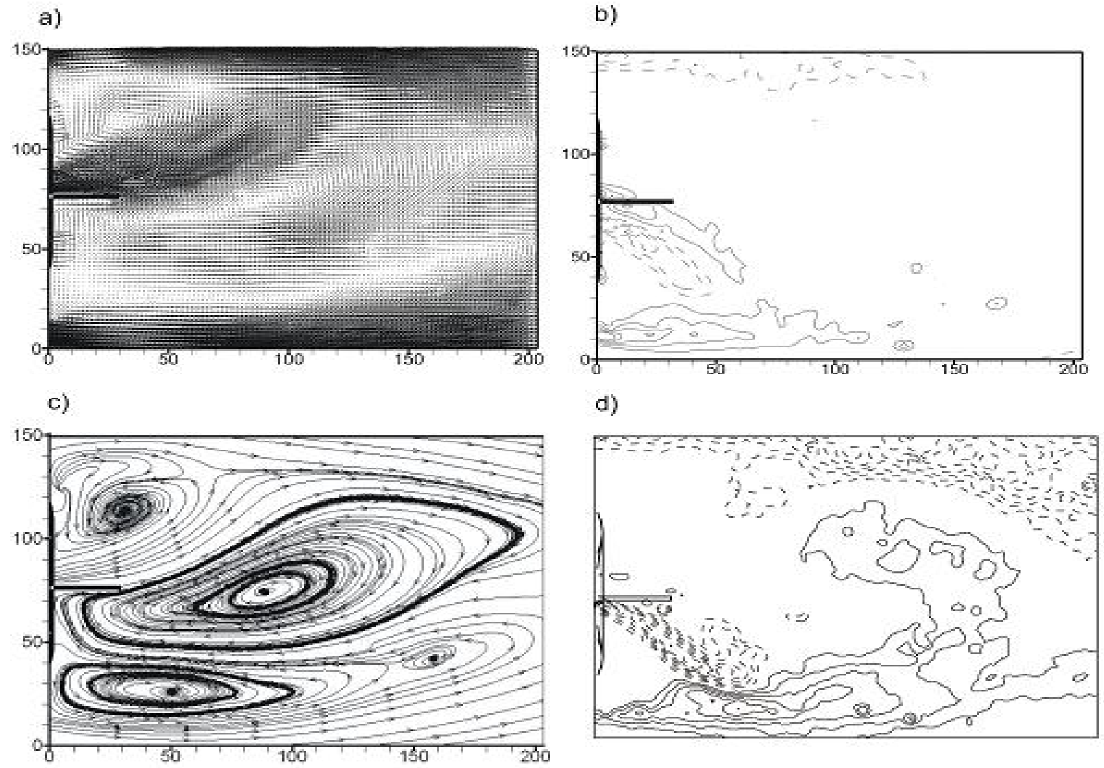

Figure 4.76. Flow characteristic which the case of plate having x=1.5D length and 17.5 mm height

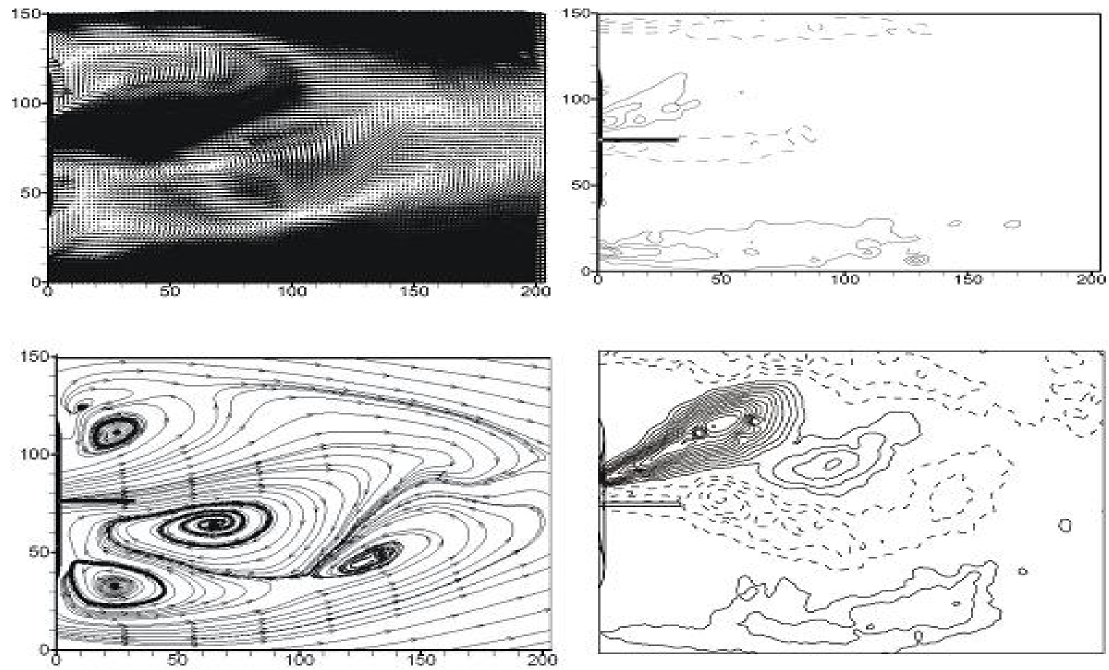

Figure 4.77. Flow characteristic which the case of plate having x=1.5D length and 22.5 mm height

4.3.9. Splitter Plate with 50 mm Length (x=D)

The velocity vector field, <v>, vorticity contours, <ω>, streamline,<ψ>, and normalized Reynolds stress contours, <u'v'>, were shown between the **figures 4.78, 4.79, 4.80, 4.81, 4.82 and 4.83**. The figures between 4.78 and 4.83, splitter plate having 50 mm (one cylinder diameter) length has very little effect on the flow characteristics. Deflection of the jet flow towards lower cylinder occurs and provides a wider wake downstream of the upper cylinder and a narrow wake downstream of the lower cylinder.

Figures 4.79, 4.80, 4.81, 4.82 and 4.83 show the effect of the splitter plate, it can be said that the splitter plate controls the vortex shedding behind the cylinder. The wake region gets longer and the plate remains in the wake region. The vorticity contours elongate to the streamwise direction. The negative and positive layers are symmetrical and horizontal. The Reynolds stress concentrations decrease significantly compared to the no-plate case. **Figure 4.80** shows the minimum Reynolds stress concentrations. In all cases the vorticity contour is symmetrical. They extend along the streamwise direction.

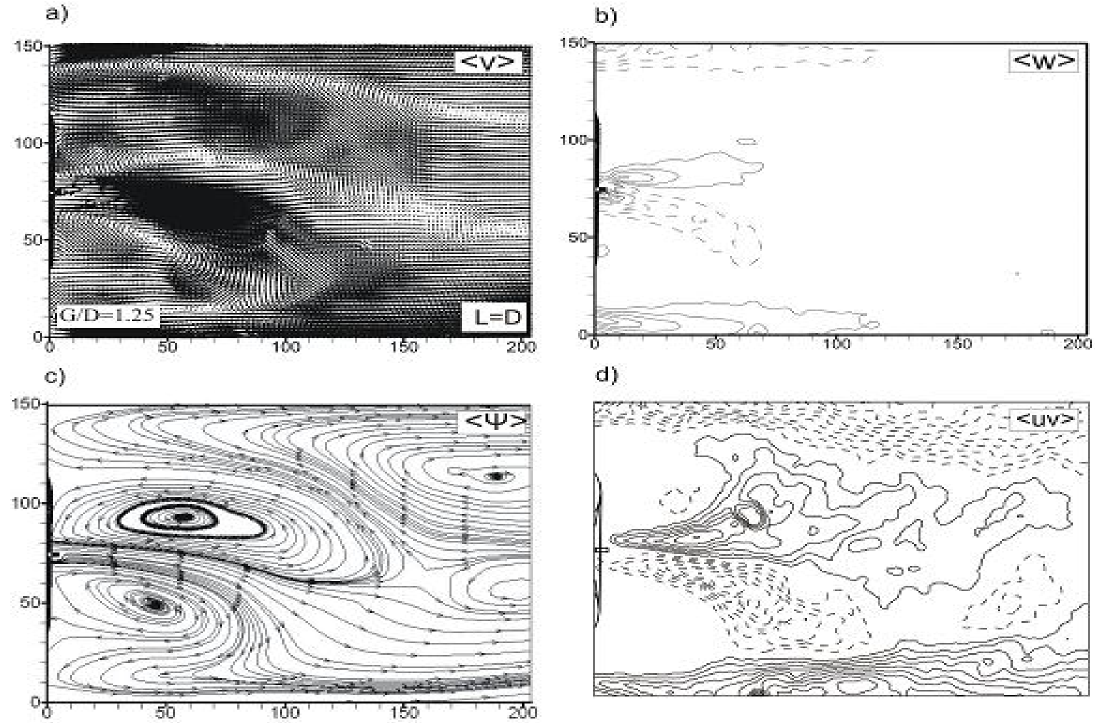

Figure 4.78. Flow characteristic which the case of plate having x=1D length and 0 point height

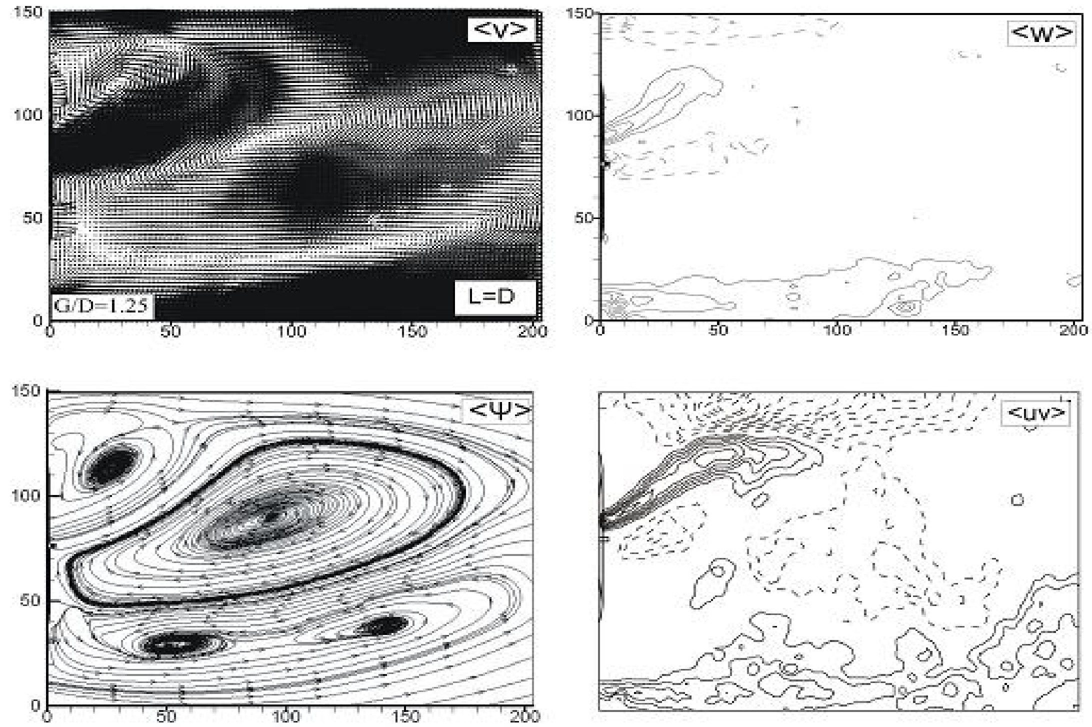

Figure 4.79. Flow characteristic which the case of plate having x=1D length and 5 mm height

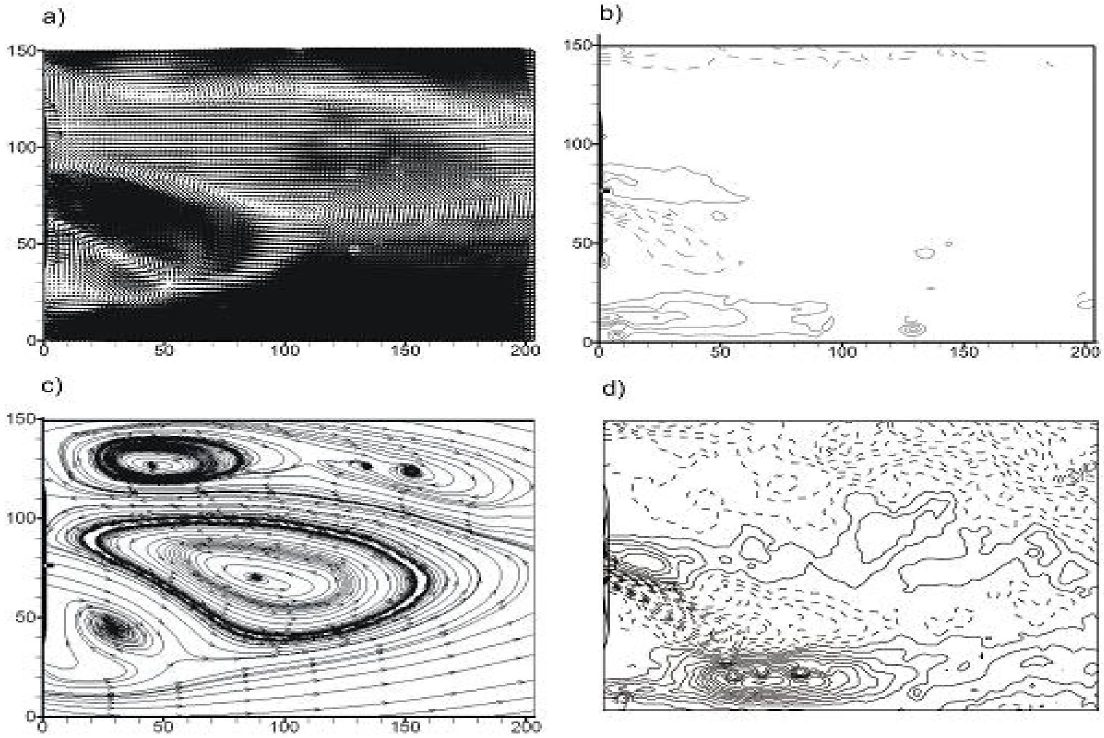

Figure 4.80. Flow characteristic which the case of plate having x=1D length and 10 mm height

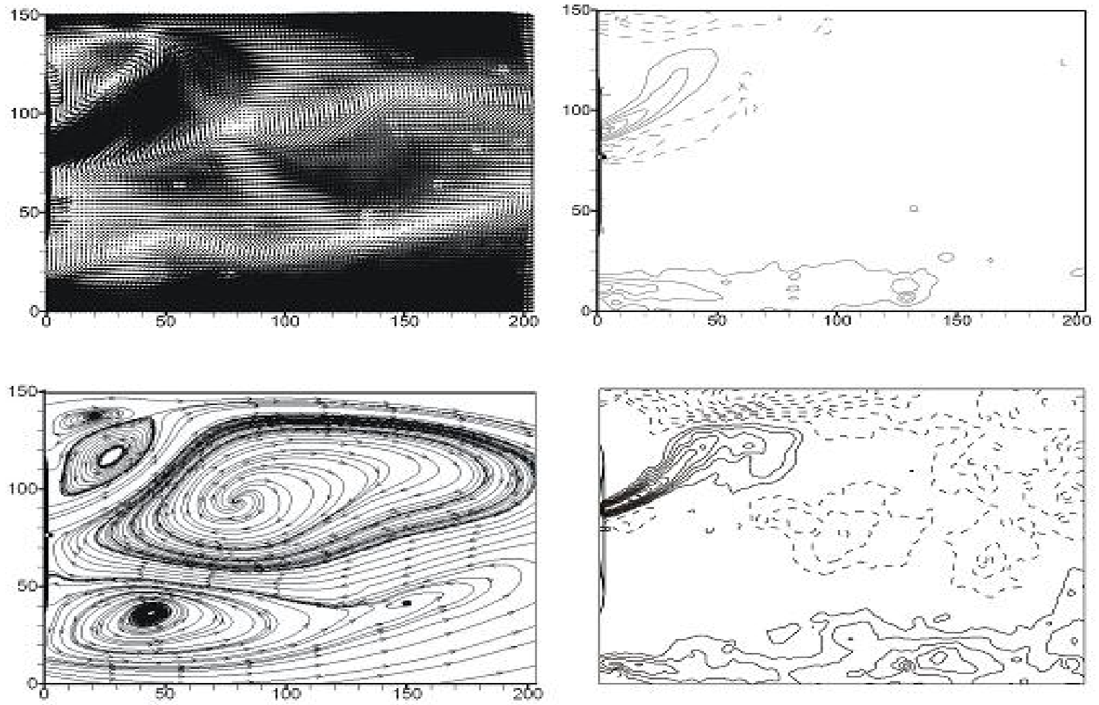

Figure 4.81. Flow characteristic which the case of plate having x=1D length and 12.5 mm height

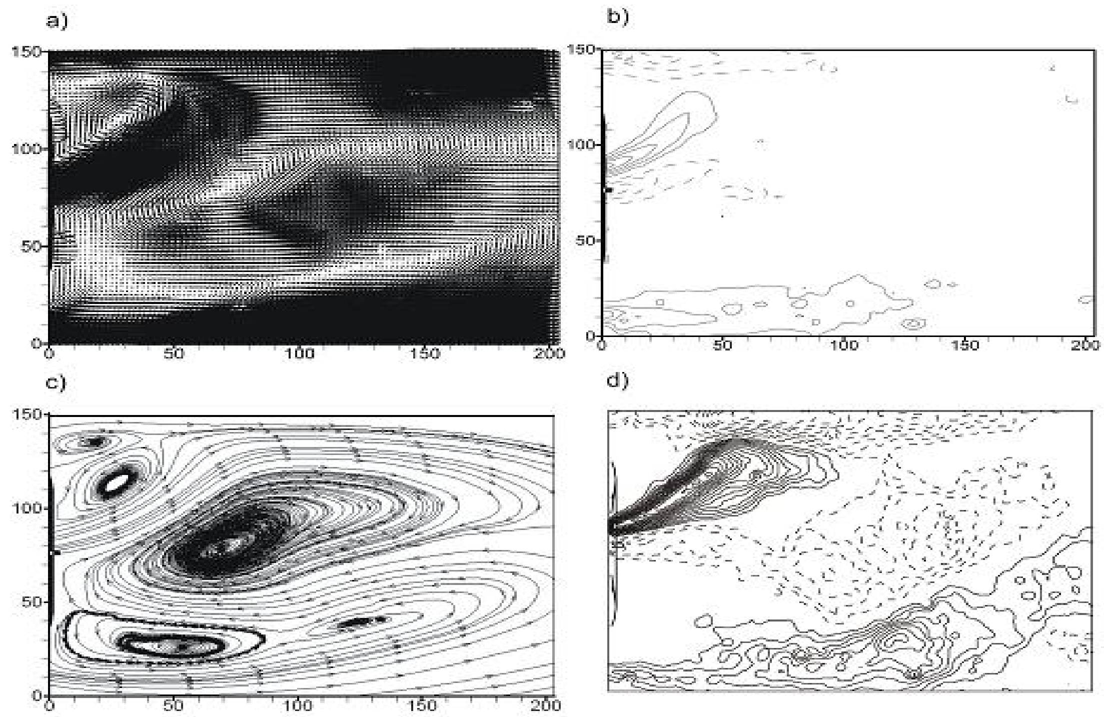

Figure 4.82. Flow characteristic which the case of plate having x=1D length and 17.5 mm height

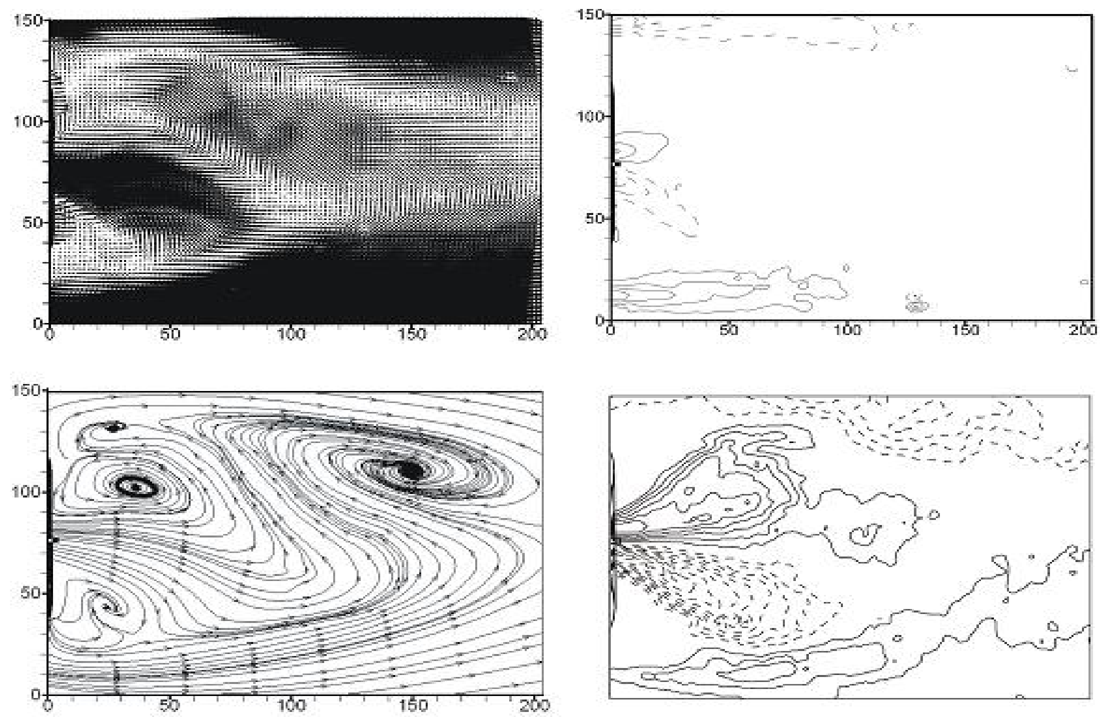

Figure 4.83. Flow characteristic which the case of plate having x=1D length and 22.5 mm height

4.3.10. Splitter Plate with 25 mm Length (x=0.5D)

Depicts the velocity vector field, <v>, vorticity contours,<ω> , streamline,<ψ>, and Reynolds stress concentrations,<u'v'>, for the length 25 mm (L=0.5D), for the distance between the bottom of the splitter plate and the table surface 0 mm, 5 mm, 10 mm, 12.5 mm, 17.5 mm and 22.5 mm are depicted.

As shown in Figure 4.85, splitter plate having 25 mm length has very little effect on the flow characteristics. For this case, the flow structure is similar with the no-plate case. Symmetrical flow structures can easily be seen at the distance between the bottom of the splitter plate and the table surface 5 mm, 10 mm, 12.5 mm and 17.5 mm. And the difference of the Reynolds stress concentration existence of positive layers at the side of negative layers. There was very little effect on control of the vortex shedding.

Similarly, the parallelism preserving vorticity contours were extended even further. Splitter plate was remained completely in the wake flow region. Also, the wake flow region of the momentum transfer can not occur in the region between plate and cylinder vorticity contours formation. The vorticity contours lengthen and the magnitude of the Reynolds stress concentrations decreases compared to the no-plate case.

Figure 4.86, 4.87 and 4.89, the wake flow region gets longer in streamwise direction. The region was symmetrical on both sides of the plate. The splitter plate stays in the wake region. The negative and positive vorticity layers stretch along streamwise direction. These vorticity layers were horizontal and symmetrical. The Reynolds stress concentrations were less than no-plate case.

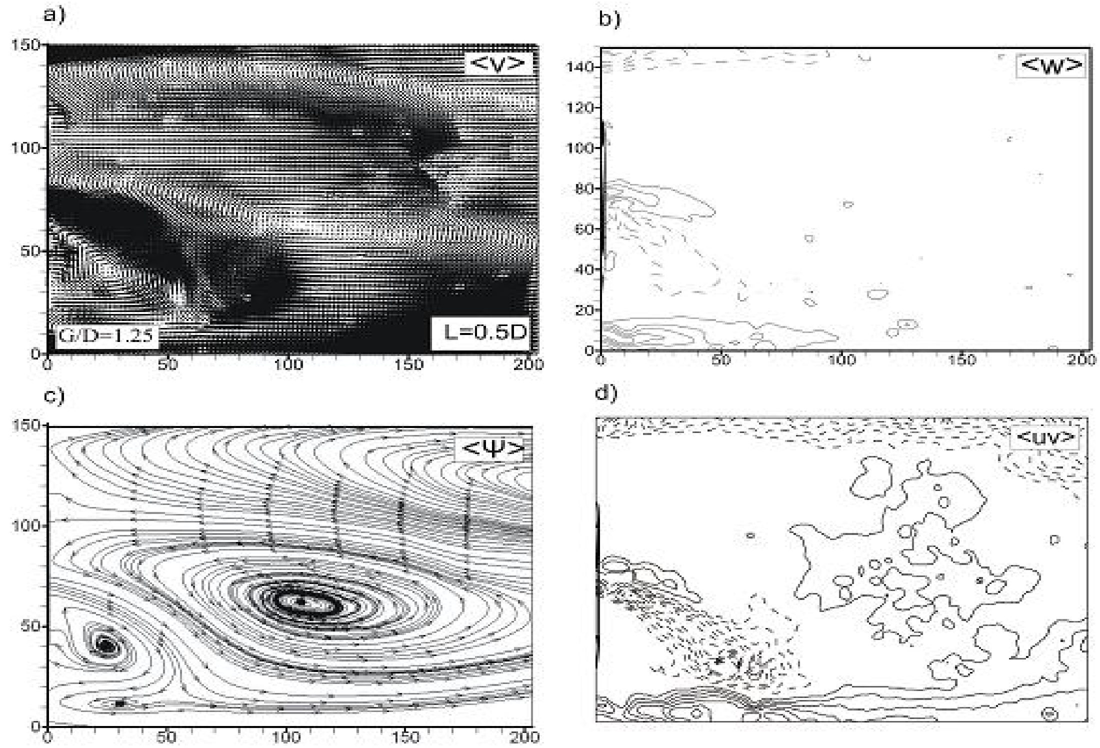

Figure 4.84. Flow characteristic which the case of plate having x=0.5D length and 0 point height

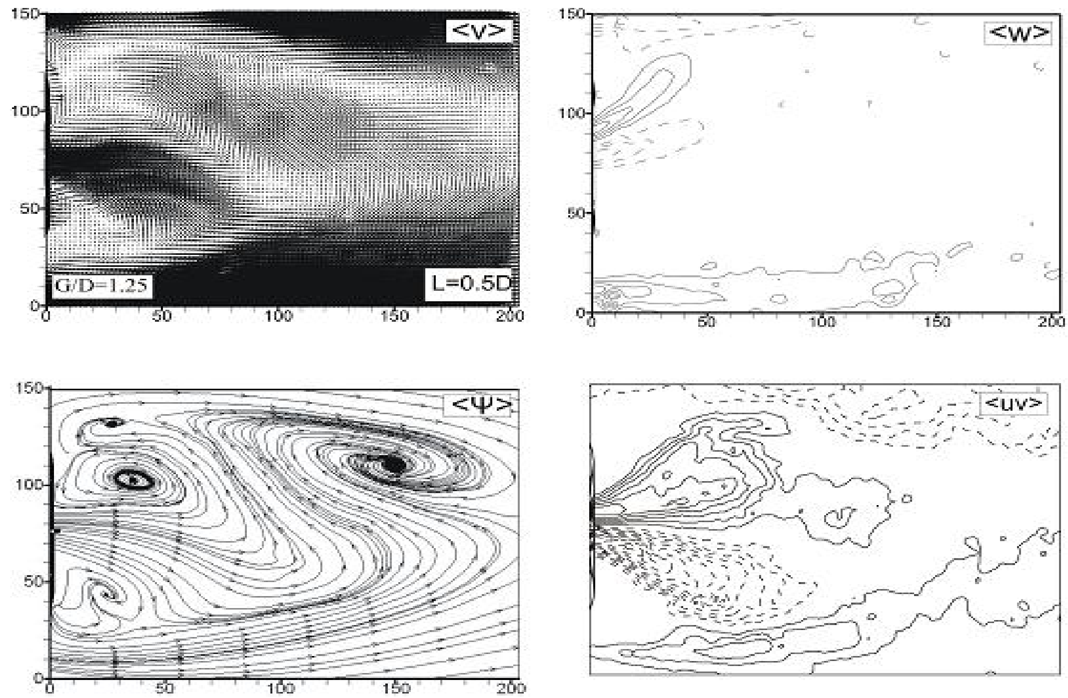

Figure 4.85. Flow characteristic which the case of plate having x=0.5D length and 5 mm height

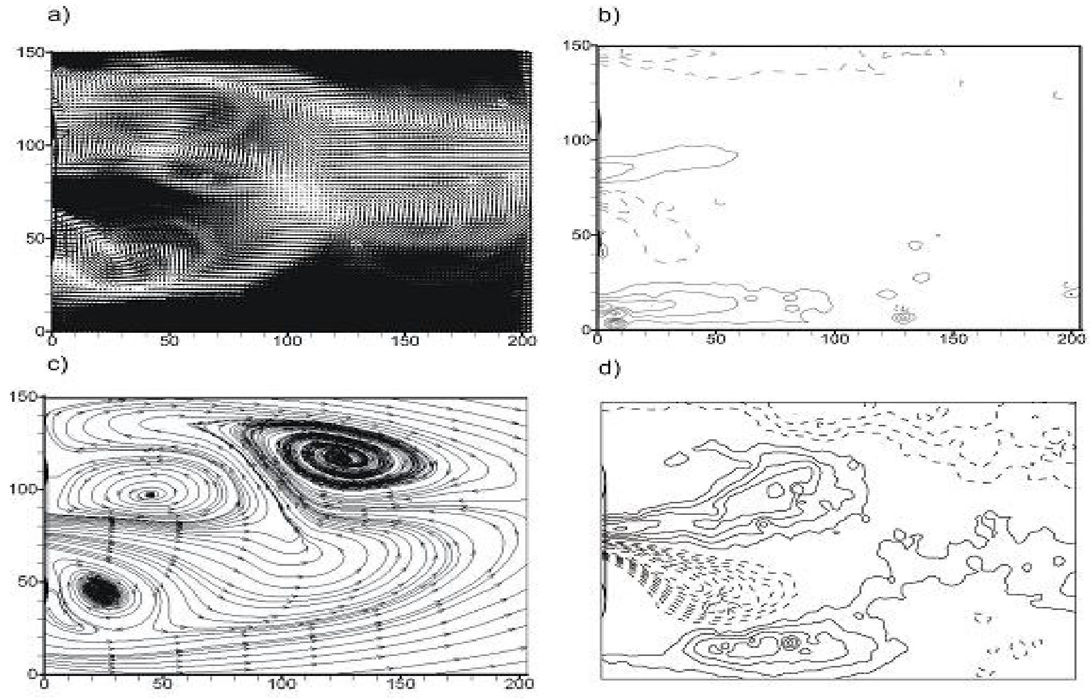

Figure 4.86. Flow characteristic which the case of plate having x=0.5D length and 10 mm height

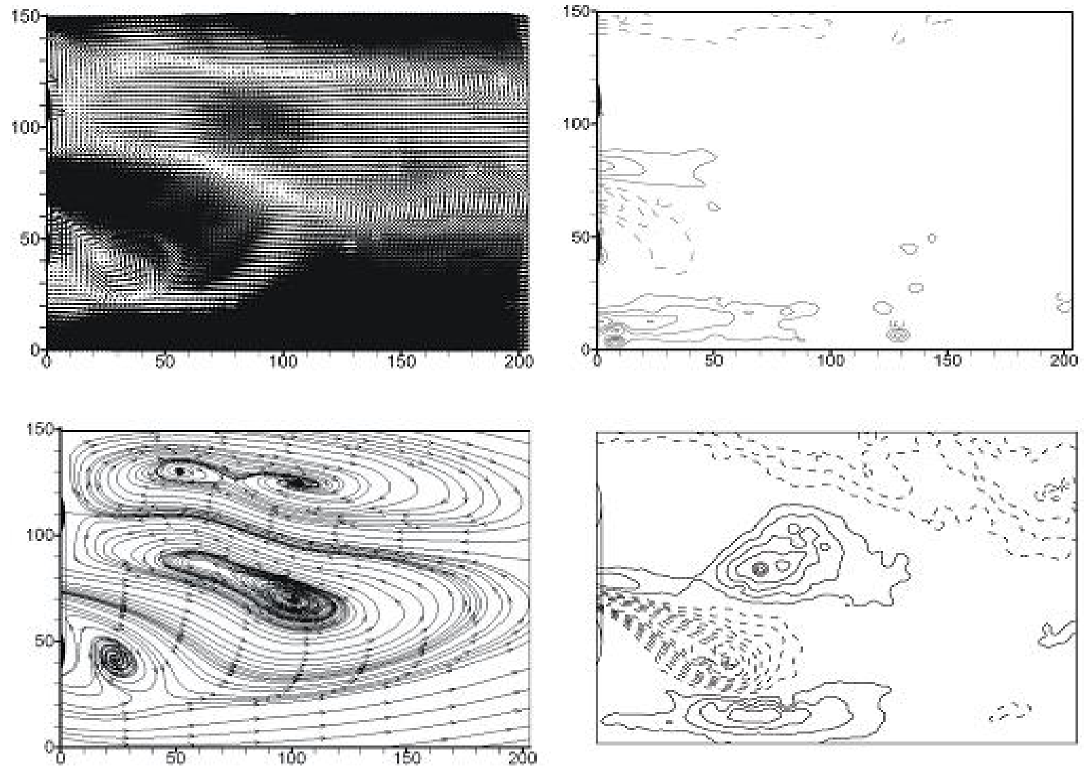

Figure 4.87. Flow characteristic which the case of plate having x=0.5D length and 12.5 mm height

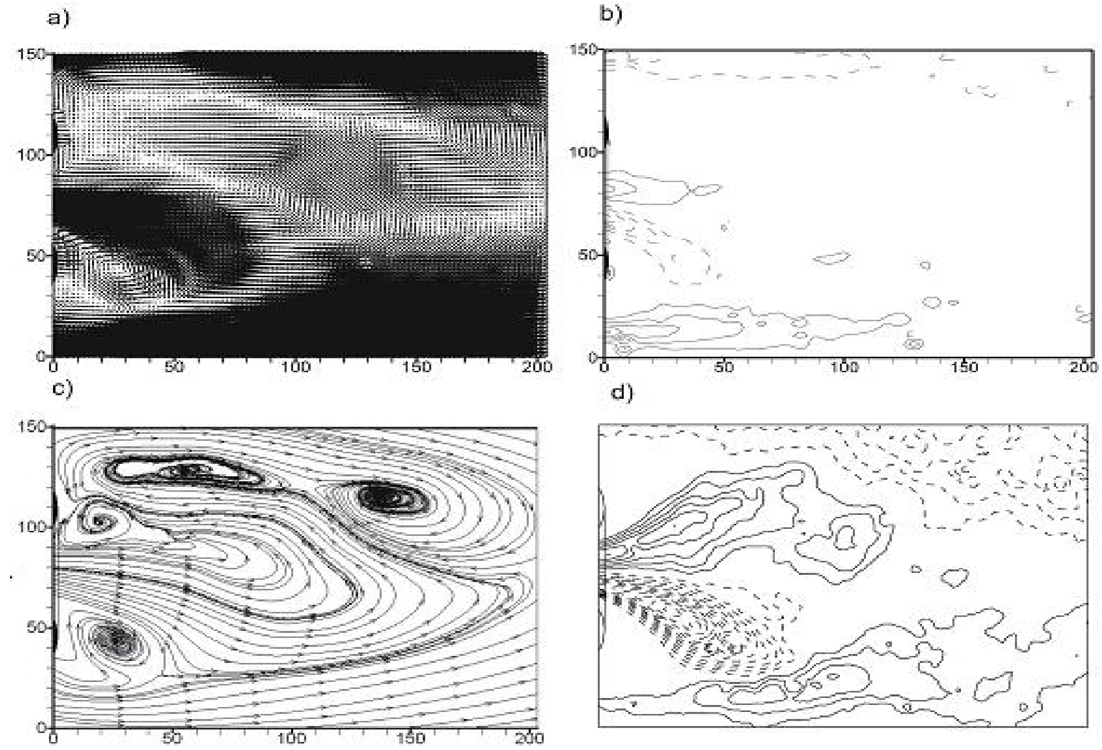

Figure 4.88. Flow characteristic which the case of plate having x=0.5D length and 17.5 mm height

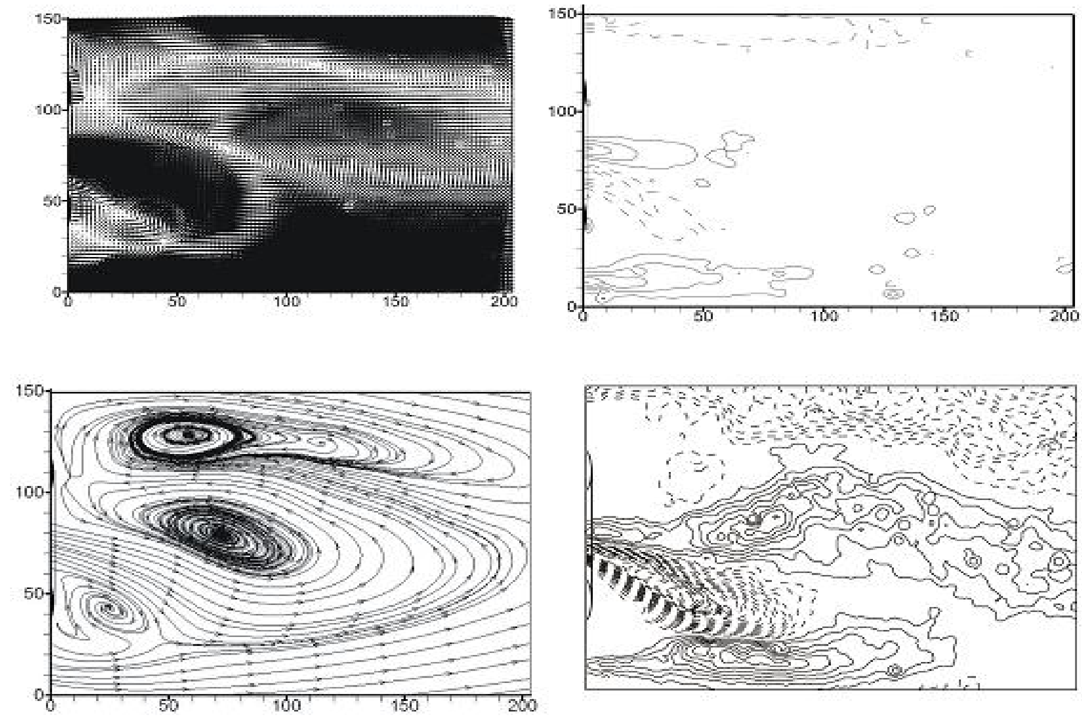

Figure 4.89. Flow characteristic which the case of plate having x=0.5D length and 22.5 mm height

4.3.11. Splitter Plate with Start Point Length

The velocity vector field,(a), <v>, represent vorticity contours,(b), <ω>, streamline,(c),<ψ>, and normalized Reynolds stress contours,(d), <u'v'>, were shown between Figures 4.90 and 4.95 are depicted.

As the distance between the bottom of the splitter plate and the table surface increases, the control of flow increases in **Figures 4.90, 4.91, 4.92, 4.93, 4.94 and 4.95.** For these cases, the flow structure was smilar with no-plate case. When the distance between the bottom of the splitter plate and the table surface increases, it is seen that wake flow region elogate, on the other hand, Reynolds shear stress, streamline and vorticity contours reduce. Positive and negative layers were formed for different Reynolds stress concentrations.

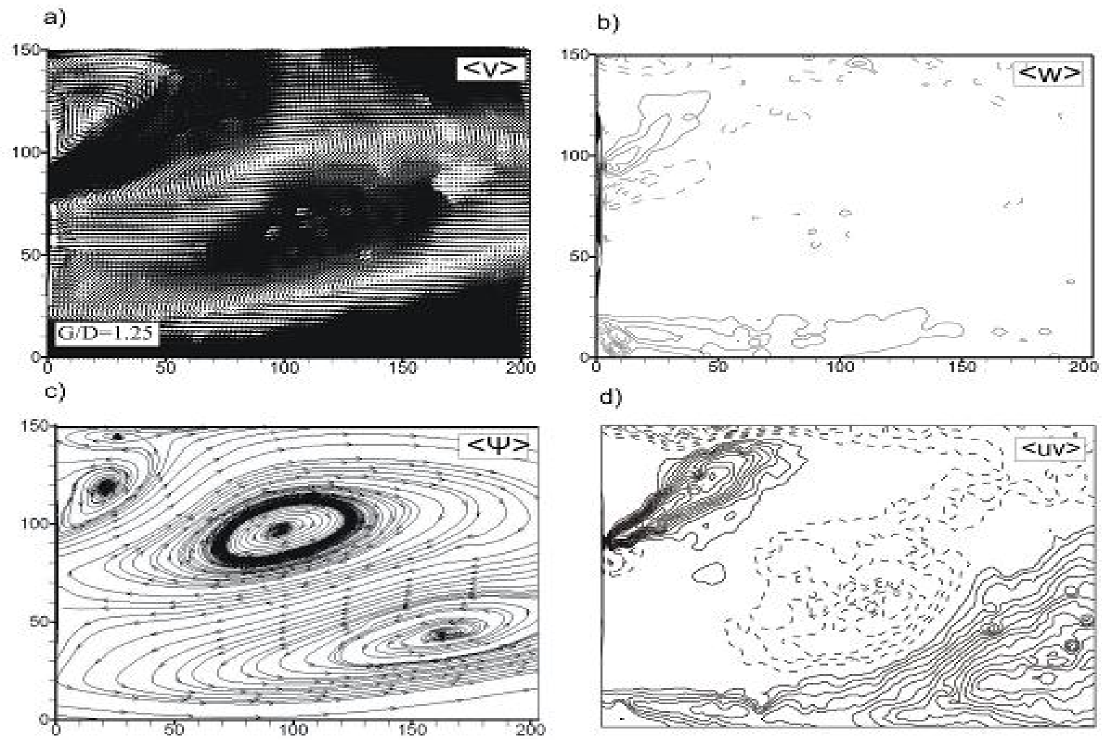

Figure 4.90. Flow characteristic which the case of plate having 0 point length and 0 point height

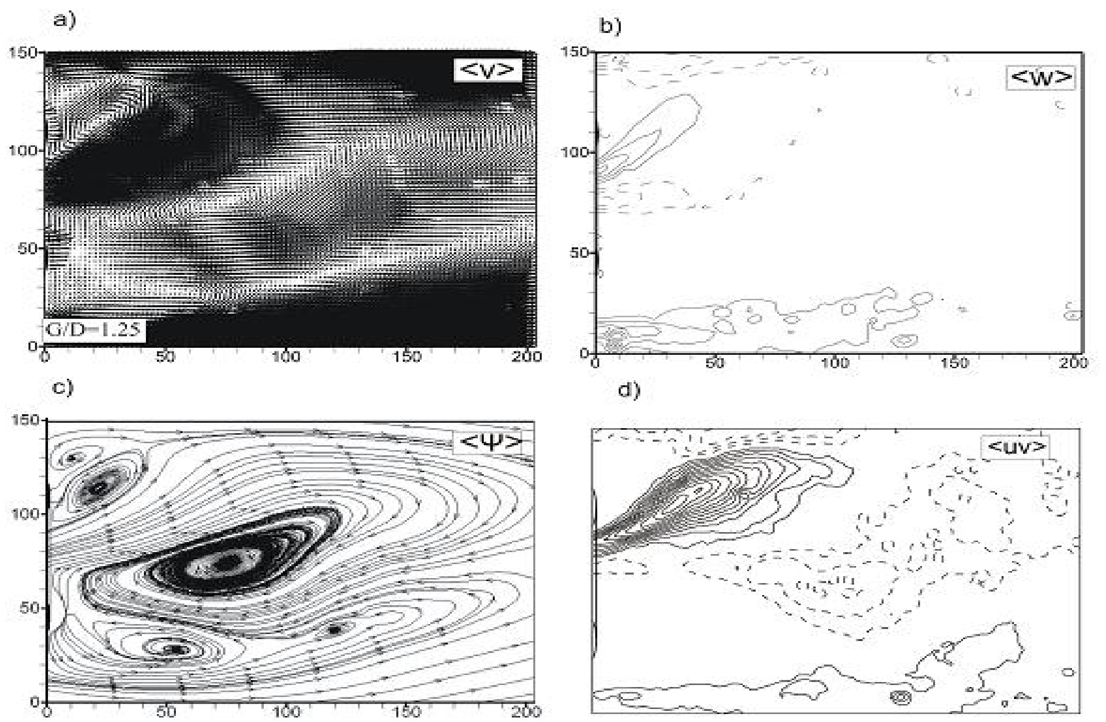

Figure 4.91. Flow characteristic which the case of plate having 0 point length and 5 mm height

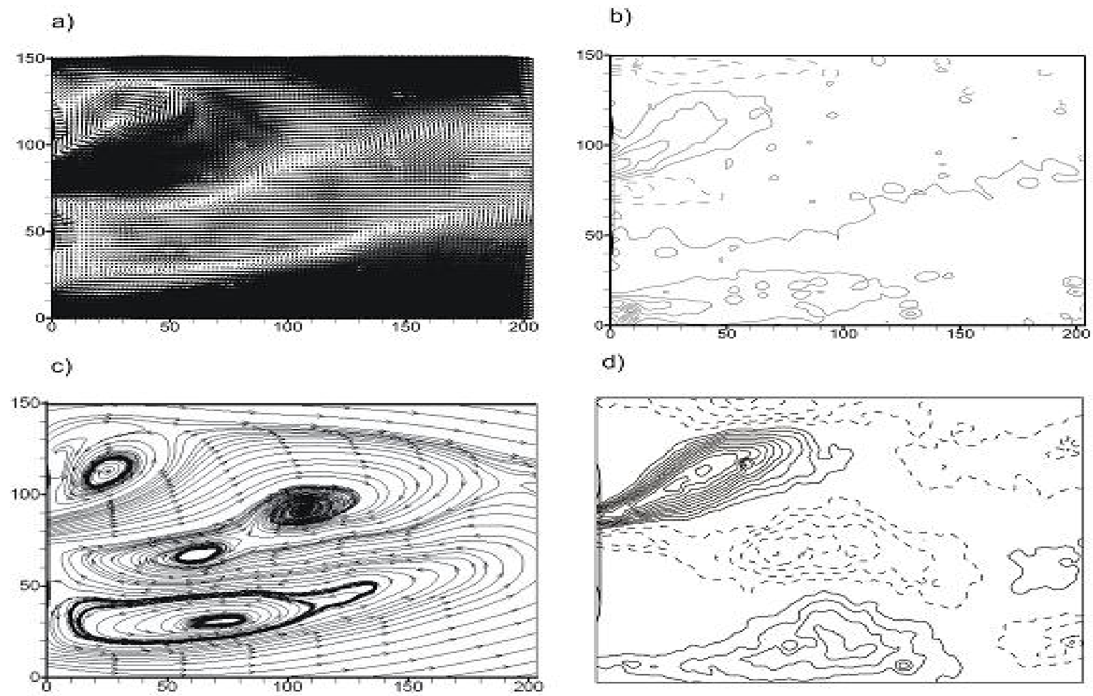

Figure 4.92. Flow characteristic which the case of plate having 0 point length and 10 mm height

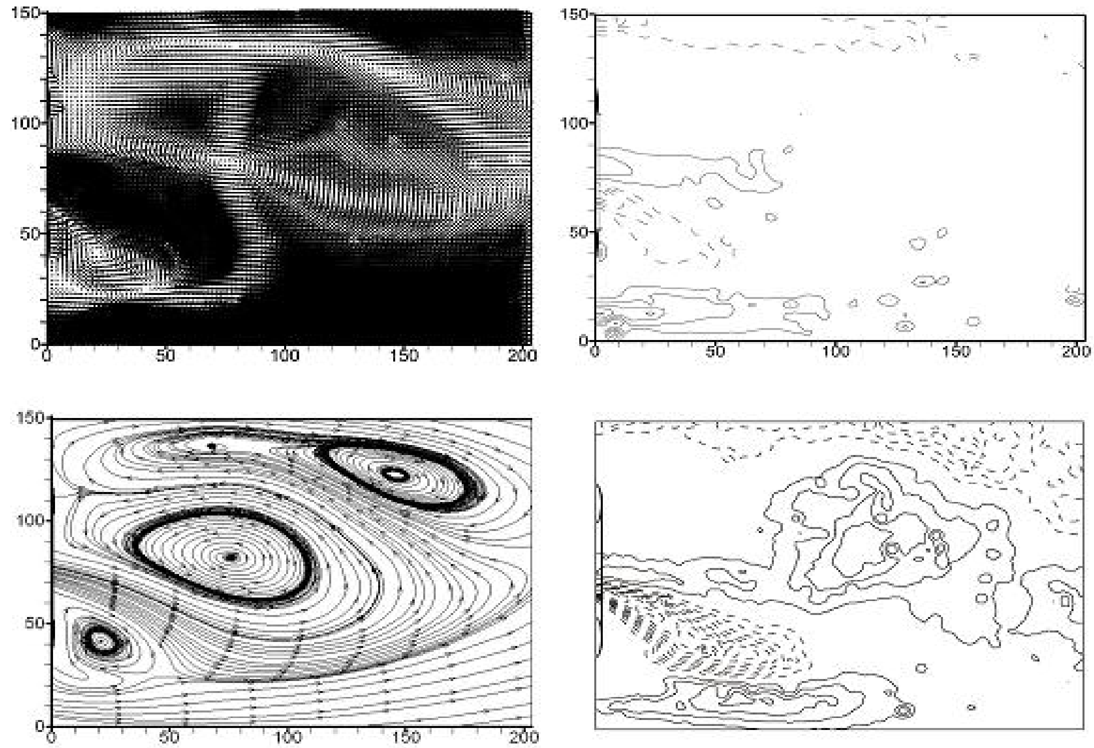

Figure 4.93. Flow characteristic which the case of plate having 0 point length and 12.5 mm height

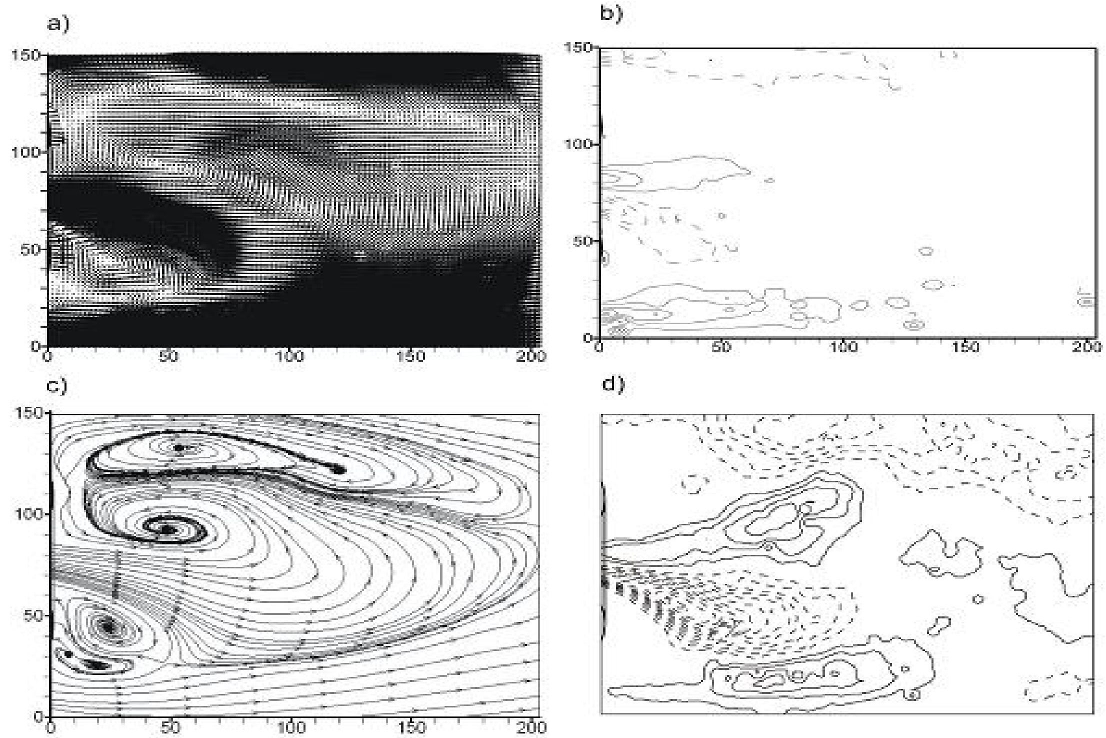

Figure 4.94. Flow characteristic which the case of plate having 0 point length and 17.5 mm height

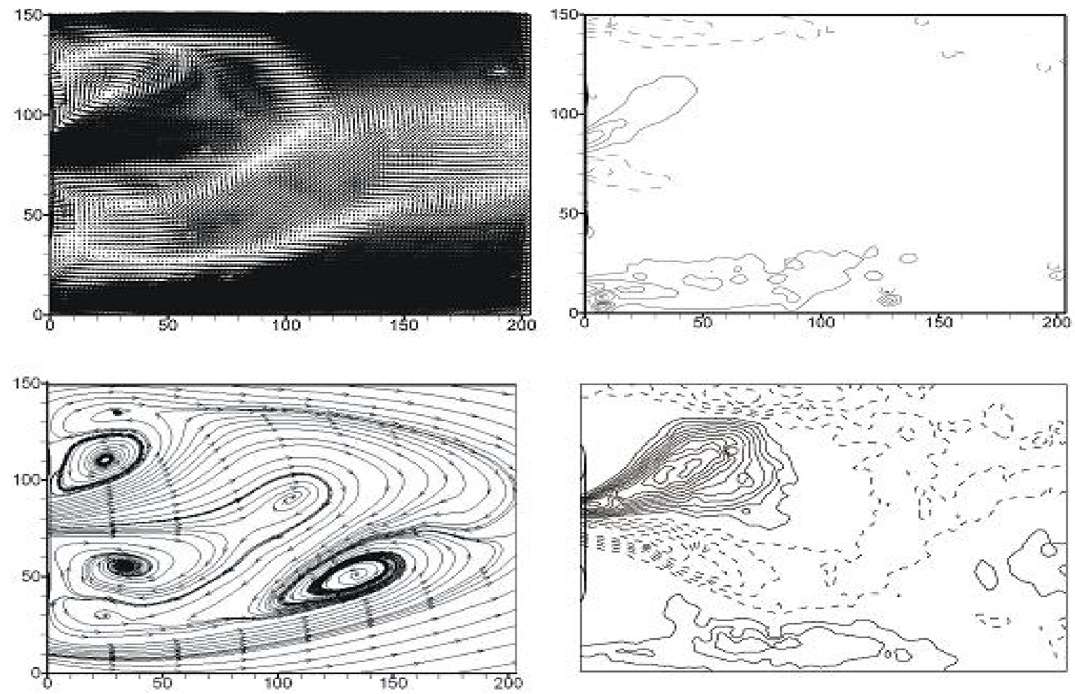

Figure 4.95. Flow characteristic which the case of plate having 0 point length and 22.5 mm height

5. CONCLUSIONS

In this study, the effect of splitter plates having various height and lengths on the control of vortex shedding behind two circular cylinders placed side-by-side in shallow water was investigated experimentally by using Particle Image Velocimetry Technique (PIV). Experiments were only carried out for the gap ratio of G/D=1.25. Morever, splitter plates were placed in two different directions. Firstly, experiments showed that the length of the splitter plate was an important parameter effecting the flow structure behind the cylinder. Thus for the final experiments, various splitter plates having the lengths between 0 mm and 250 mm with an increment of 25 mm were used. The effect of splitter plate thickness was 2mm. Secondly, splitter plate heights were taken as 0 mm, 5 mm, 10 mm, 12.5 mm, 17.5 mm and 22.5mm. The height of the used splitter plate was 20 mm. Reynolds number based on the cylinder diameter was Re=5000.

The velocity vector field, vorticity contours, streamline topology and reynolds stress concentrations were calculated using 350 instantaneous images.

The splitter plate which has 25mm length (x=0.5D) and 22.5 mm height, does not have any effect on the control of vortex shedding behind the circular cylinder.

All the cases of splitter plate which has 75 mm (x=1.5D) length control the vortex shedding behind the cylinder better than the splitter plate lengths of 25mm (x=0.5D) and 50 mm (x=D). The controlling vortex shedding behind the cylinder for the cases of 0 mm and 5 mm was same with the heights 17.5 mm and 22.5 mm cases.

The splitter plate, the flow starts to oscillate with smaller frequency compared to the natural frequency of the bare cylinder. When the splitter plate was located at both 2.5D and 3D locations, no effect of splitter plate was observed.

Splitter plate has very little effect on the flow characteristics at the mid-plane (for splitter plate having 3D and 2.5D length, 10 mm and 12.5 mm the distance between the bottom of the splitter plate and the table surface) and deflection of the jet flow towards lower cylinder occurs that provides a wider wake downstream of the upper cylinder and a narrow wake downstream of the lower cylinder. After this splitter plate length, symmetrical flow structure was obtained downstream of the side-by-side circular cylinders. Jet flow was not deflected towards any cylinder's side and the peak concentration of Reynolds stress highly decreases with the increasing splitter plate length. This location of the peak concentration slightly moves on downstream direction. A pair of vorticity contour appeared on both sides of the splitter plate. Increasing splitter plate length also caused vorticity contours to elongate in streamwise direction. For the free-surfaces (for splitter plate having 3D and 2.5D lenght, 22.5 mm the distance between the bottom of the splitter plate and the table surface), similar results were obtained at these elevations compared to the flow characteristics obtained at mid-plane (for splitter plate having 3D and 2.5D length, 10 mm and 12.5 mm the distance between the bottom of the splitter plate and the table surface) elevation.

The flow structures at the elevations for two cylinders cases showed that splitter plate length does not change the flow characteristics significantly. Biased flow and deflected flow were not prevented even for the longer splitter plate cases (x= 4D and 5D). Nonetheless, splitter plates have effect on normalized Reynolds shear stress concentrations slightly. Maximum Reynolds stress concentrations generally occur along the shear layers (for splitter plate having 5D length, 22.5 mm the distance between the bottom of the splitter plate and the table surface).

In addition to these results, to investigate the flow characteristics, the distance between the bottom of the splitter plate and the table surface increases, better control of the flow was achieved in 1D.

The general conclusion is; the splitter plate lengths of 50 mm, 75 mm, 100 mm, 175 mm, 200 mm, 225 mm and 250 mm have full effect on control of vortex shedding. For the cases which the splitter plate is placed on to the platform except the case of the splitter plate height of start point, the splitter plates have important effect on the suppression of vortex shedding. For the cases which the splitter was not located on the platform, the maximum control of the vortex shedding is obtained for 22.5 mm cases and minimum effect on the suppression of vortex shedding is 5 mm cases.

REFERENCES

AdrIan,RJ.,1991.”Particle-imaging techniques for experimental fluid mechanics.” Annu Rev Fluid Mech, Vol.23,p.261–304.

AKILLI, H., AKAR, A., KARAKUŞ, C., 2004. “Flow characteristics of circular cylinders arranged side-by-side in shallow water’’, 15 (2004) 187-197

AKILLI, H., ŞAHİN, B., TUMEN, N., 2005. “Suppression of vortex shedding of circular cylinder in shallow water by a splitter plate ’’, 16 (2005) 211-219

AKILLI, H., ŞAHİN, B., GÖZMEN, B., 2007. “The effect of varıous-height plates on flow characteristics behind a cylinder’’, ISSN 1019-1011

AKILLI, H. and ROCKWELL, D., 2002. Vortex formation from a cylinder in shallow water. Physics of Fluids, Vol. 14, No. 9, pp. 2957-2967.

ACHENBACH, E., Vortex shedding from spheres, Journal of Fluid Mechanics, vol. 62, Part 2, Jan 23, 209-221, 1974.

BEARMAN, P.W., 1965. Investigation of flow behind a two-dimensional model with blunt trailing edge and fitted with splitter plates, J. Fluid Mech. 21 241–255.

GUO, XIAO-HUI, LIN, JIAN-ZHONG, TU CHENG-XU, WANG HAOL, 2009, “Flow past two rotating circular cylinders in a side-by-side arrangement’’ 21(2):143-151

LIU LIU SHI, YING ZHENG LIU, JIN JIN WAN, 2009, “Influence of wall proximity on characteristics of wake behind a square cylinder: PIV measurements and POD analysis’’

LIM HEE- CHANG, LEE SANG- JOON, 2004. Flow control of a circular cylinder with o-rings. Fluid Dynamics Research 35, 107-122.

CURRICULUM VITAE

Sevgi Kıraç was born on January 20, 1980 in Adana, Turkey. In 1998, she graduated from Adana Erkek High School, and enrolled in Mechanical Engineering Department of Fırat University. In 2003, she graduated in mechanical engineering from the Department of Mechanical Engineering. She began her MSc education at the Department of Mechanical Engineering of Çukurova University.